ATMOSPHERIC TECHNOLOGY

NATIONAL CENTER FOR ATMOSPHERIC RESEARCH NUMBER 8 SPRING 1976

INSTRUMENTATION IN CLOUD MICROPHYSICS

ATMOSPHERIC TECHNOLOGY NUMBER 8 – SPRING 1976

INSTRUMENTATION IN CLOUD MICROPHYSICS

CONTRIBUTORS

Theodore W. Cannon
Nicholas J. Carrera
Harvey E. Dytch
A. J. Heymsfield
Peter V. Hobbs
James E. Jiusto
G. Garland Lala
Lawrence F. Radke
Robert E. Ruskin
W. David Rust
Paul Spyers-Duran
Francis M. Turner

ATMOSPHERIC TECHNOLOGY contains invited articles and brief, unsolicited articles that summarize the state of the art in instrumentation and techniques or describe specific new developments for probing the atmosphere. Contributions are semitechnical and provide timely information to a broad readership interested in the tools for atmospheric research. In some instances their contents will comprise summaries of papers that have been or will be submitted for publication in a primary journal. Articles are edited but not refereed or copyrighted, and their inclusion in *ATMOSPHERIC TECHNOLOGY* is not to be regarded as formal publication.

National Center for Atmospheric Research, Boulder, Colorado.

Contents

ATMOSPHERIC TECHNOLOGY is published semiannually for the **NCAR Atmospheric Technology Division**, Clifford J. Murino, Director. Facilities of the Atmospheric Technology Division and their heads are: **Research Aviation Facility**, Harry B. Vaughan; **National Scientific Balloon Facility**, Alfred Shipley; **Computing Facility**, G. S. Patterson Jr.; **Field Observing Facility**, Robert Serafin; **Research Systems Facility**, David W. Bargen.

Editor: Merry Maisel; **Editorial Staff**: Elmer Armstrong, K. Redman; **Production Editor**: Marie Boyko; **Art Director**: William Hemphill; **Designer**: Howard Crosslen; **Graphics Staff**: John Bazil, Lee Fortier, Wilbur Garcia, Justin Kitsutaka, Barbara Mericle, Michael Shibao; **Printing Staff**: Clarence Cook, Carl Edwards, Arthur Gray, Donald Green, Geraldine Morris, James Puhr.

The National Center for Atmospheric Research (NCAR) is operated by the nonprofit University Corporation for Atmospheric Research (UCAR) under the sponsorship of the National Science Foundation. NCAR is an equal opportunity employer.

UCAR Member Institutions: University of Alaska, University of Arizona, California Institute of Technology, University of California, Catholic University of America, University of Chicago, Colorado State University, University of Colorado, Cornell University, University of Denver, Drexel University, Florida State University, Harvard University, University of Hawaii, University of Illinois at Urbana-Champaign, Iowa State University, Johns Hopkins University, University of Maryland, Massachusetts Institute of Technology, McGill University, University of Miami, University of Michigan, University of Minnesota, University of Missouri, University of Nevada, New Mexico Institute of Mining and Technology, State University of New York at Albany, New York University, Ohio State University, University of Oklahoma, Oregon State University, Pennsylvania State University, Purdue University, Rice University, Saint Louis University, Stanford University, Texas A&M University, University of Texas, University of Toronto, Utah State University, University of Utah, University of Washington, University of Wisconsin, Woods Hole Oceanographic Institution.

Published by the National Center for Atmospheric Research, Post Office Box 3000, Boulder, Colorado 80303. Subscriptions free on request.

Introduction

The increase in our knowledge of cloud microphysical processes and meteorology in general has often been limited by a lack of instruments capable of giving us the desired observations. Cloud microphysics requires the measurement of concentrations and sizes ranging from $10^{10}/m^3$ for submicron Aitken nuclei, through $10^9/m^3$ for micron-sized cloud droplets and about $10^3/m^3$ for millimeter-sized particles, to less than $1/m^3$ for centimeter-sized hailstones. In addition to determining size and concentration, it is frequently necessary to be able to distinguish water from ice.

If we hope to obtain measurements over this entire range, a number of different instruments must be used. Moreover, the observations must be made in the cloud environment, which can sometimes be very hostile, and where extremes in humidity, temperature, turbulence, and hail can frequently be found. Also, the measurements are usually made from an airborne platform with the inherent problems of vibration and electrical noise. An instrument which may perform perfectly in the laboratory may be useless on an aircraft in a cloud. Reliability of operation in this environment must be an important consideration in the design and selection of instruments.

Because of their great beauty and variety, snow crystals were the object of many of the earliest observations in cloud physics. The first sketches of snow crystals are said to have been drawn by Olaus Magnus, the Archbishop of Uppsala, about 1550. The first scientific record of snow crystals was published by Descartes in 1635, and the invention of the microscope in the last half of the 17th century led to even closer examination. These early observations were primarily devoted to determining the different types of particles. Few studies were directed at understanding the physical processes until the 20th century, and in particular the last 40 years.

The airplane has played a major role in the development of cloud physics during this century. It not only made it possible to make observations directly in clouds, but also provided the motivation for investigating what conditions could be expected there. Pilots soon learned that the accretion of supercooled cloud droplets could lead to a buildup of ice on the wings, thereby greatly reducing the performance of the aircraft and making further flight quite hazardous. The need to determine when such conditions could be expected helped motivate many of the early aircraft observations.

In the beginning, measurements were made from open cockpits. Particles were either collected or impacted on objects such as rods covered with black velvet or glass slides coated with oil. After collection they were examined with a microscope directly in the aircraft. Later, improvements in sampling techniques made it possible to replicate the impacted particles so that they could be examined back in the laboratory.

Although much of our understanding of cloud microphysics has been gained using these impaction or collection techniques, the analysis process is tedious, time-consuming, and sometimes difficult to interpret. Within the past few years, a number of new instruments have appeared that can give automatic, continuous measurements of certain parameters. All of these new instruments hold promise of greatly increasing our understanding of the growth and development of particles within clouds, but, as in the past, interpretation and analysis of data remain tedious and ambiguous processes. There is no substitute for careful analysis.

In view of the new developments in cloud physics instruments, it seems particularly appropriate to devote an issue of *Atmospheric Technology* to this topic. Several of the articles in this issue (for example, those by H. Dytch and N. Carrera; A. Heymsfield; F. Turner, L. Radke, and P. Hobbs; and T. Cannon) discuss the newer instruments, some of which have not been described previously. Other articles (those by P. Spyers-Duran and R. Ruskin) describe more standard but still widely used techniques. In all of the articles we have attempted to present a balanced view of the principles of operation, advantages, limitations, and operational reliability of these instruments, and to give some examples of data from them. There are additional instruments in existence that have been used with varying degrees of success, but which, in the opinion of the editors, have serious shortcomings or are not in general use; therefore they have not been included in these articles.

In addition to the articles concerned with cloud particle measurements, there are two articles on techniques used in the measurement of cloud condensation nuclei (that by J. Jiusto) and ice nuclei (that by G. Lala). In the case of cloud condensation nuclei, we now have fairly reliable and proven methods of observation. But for ice nuclei the story is quite different. We are still in a very active stage of learning and experimentation, but, as the article shows, some understanding is beginning to emerge and some techniques have been developed which may give us the observations we so badly need for a more complete understanding of the role of ice-forming nuclei in clouds.

Last, but by no means least, there is an article (by W. Rust) on instruments currently being used for the measurement of electric field in and around clouds. Research in cloud electrification has largely been isolated from research in cloud microphysics, in spite of the fact that electrification probably does play a major role in the development of precipitation in large convective clouds. The merging of the fields of cloud physics

and cloud electrification is one of the frontiers in cloud physics research and measurement, and an area in which much more emphasis should be given to future instrument development and research.

Other areas in which continued development is likely to have considerable impact on cloud microphysics are those of remote-sensing techniques and computer analysis of data using pattern-recognition techniques. Although remote-sensing techniques are not routinely used at the present time, they are beginning to appear in special projects and have the potential of providing measurements in clouds from ground-based observations. Measurements from multiple-wavelength lidar have now reached the point that ice can be distinguished from water; quantitative measurements of size and concentration may soon follow. It soon should be possible to use dual-wavelength radars to detect the presence and location of hail and to determine liquid water contents and rainfall rates within thunderstorms. Dual-doppler radars are already giving measurements of air motion within precipitating clouds, from which precipitation particle trajectories can be inferred, and triple-doppler radars now being developed will give even better measurements, especially of the important vertical field of motion.

While remote-sensing techniques can provide valuable information, the need for direct measurements from aircraft will undoubtedly continue. Perhaps the largest present limitation of aircraft measurements is the need for human judgment in data reduction. We now have instruments that can give us images of cloud particles, from which concentration, size, and shape can be derived (e.g., the Cannon particle camera and the Particle Measuring Systems' two-dimensional optical spectrometer), but no way of rapidly analyzing the data. Automated data analysis is a necessity if we are to handle and interpret the enormous quantities of data which these instruments are capable of producing. Some work has already been started using pattern-recognition techniques and photo-densitometric scanning but much remains to be done.

Although this issue is concerned with instruments used in measuring microphysical properties of clouds, measurement of the temperature, pressure, humidity, and motion of the air (both horizontal and vertical) in and around a cloud is also essential for understanding its development and behavior. Instruments and techniques used in measuring these quantities have been discussed in previous issues of *Atmospheric Technology* and therefore have not been included here. The interested reader may refer to *Atmospheric Technology 4, 6,* and *7.*

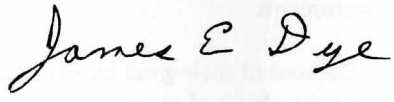

James E. Dye
January 1976

Measuring the Size, Concentration, and Structural Properties of Hydrometeors in Clouds with Impactor and Replicating Devices

Paul Spyers-Duran

Airborne investigations of clouds have been carried out by cloud physicists for more than 30 years. Determination of the sizes, concentrations, and shapes of hydrometeors (liquid or solid cloud particles) has been of central interest, requiring in situ observation of the development and growth of clouds and distinction among the various precipitation mechanisms.

At present, the size of clouds and their relatively short life cycle demand the use of an airplane as a sampling platform. Sampling hydrometeors using the direct methods described here involves carrying the probe into the cloud and capturing the particles on a suitably prepared and exposed surface. The high speed of the aircraft introduces difficulties and errors during sampling, and no single impactor or replicating instrument has been devised that is capable of sampling the entire range of particle sizes. The problems in sampling 10^9 cloud droplets ($<50\ \mu m$) per cubic meter are quite different from those in sampling ten precipitation-sized particles ($>200\ \mu m$) per cubic meter.

The accuracy of the measurements obtained from a given direct method is affected by the following:

- *Collection Efficiency of the Sampler*. Particles approaching the collector will tend to follow streamlines and will be deflected around the collector to a degree dependent on their size. Most collectors will discriminate more against the smallest cloud particles, and therefore it is necessary to correct the measured particle size distributions for the collection efficiency of the device. The collection efficiencies of different collector shapes have been calculated by Langmuir and Blodgett (1946) and by Ranz and Wong (1952). In addition, the shape of the probe and the sampling slit make the collection efficiency determination even more difficult.

- *Representativeness of the Sample*. The usefulness of the sample will depend on the size of the volume of air required for the sample relative to the size of the cloud and the rate of change of the droplet population.

- *Proper Exposure*. Coalescence of droplets can occur on overexposed slides if the covering fraction exceeds 0.1.

- *Calibration of the Impressions*. The collected droplets may diffuse into sampling media, such as oils, that are permeable to water, so immediate photography is a must. Also, accurate calibrations are needed in wind tunnels or with whirling arm facilities to relate the size of impressions to the original drop size, because particles deform upon impact with the collecting medium. The degree of distortion is dependent upon the nature of the surface coating and impaction speed (see Fig. 1).

- *Shattering*. Larger particles will shatter into many smaller particles upon hitting exposed surfaces at high speeds. This could make the sample very difficult to evaluate.

- *Icing*. Unheated leading edges will accrete ice in supercooled clouds, distorting the sampler configuration and changing the collection efficiency.

In all direct methods, a suitable exposed surface records the impressions or shapes of the particles. The data reduction is laborious and time-consuming. Often, human interpretation is necessary to evaluate the quality and representativeness of samples. In spite of these drawbacks, large amounts of data have been reduced, and our present understanding of cloud physics has come largely from these conceptually simple methods.

Author

Paul Spyers-Duran received a B.S. in meteorology from the University of Vienna in 1959. After graduate studies at the University of Chicago, he worked with the Cloud Physics Laboratory there for 13 years, developing and testing airborne cloud physics instrumentation. He joined the NCAR Research Aviation Facility in 1974.

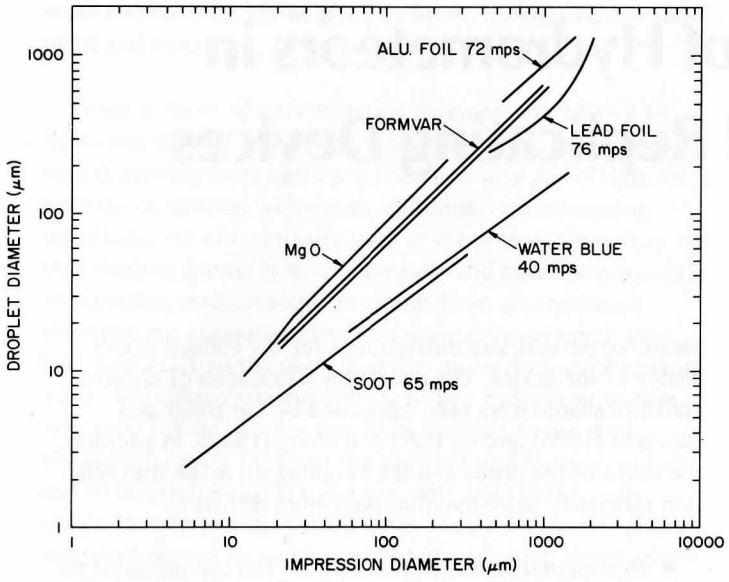

Fig. 1 Relation between droplet diameter and impression diameter for various sampling media.

Fig. 2 Drop impressions in soot layer. (Photo courtesy of J. Dye, NCAR.)

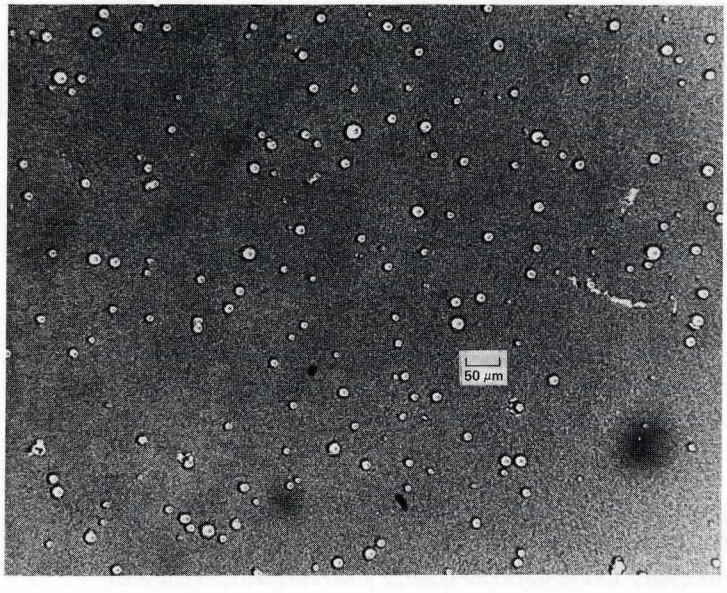

Slide Impactors

• *Oil-Coated Slides*. One of the earliest measurements of cloud droplet sizes was made by Fuchs and Petrjanoff (1937). A clean glass slide coated with a mixture of light mineral oil and petroleum jelly was used to capture cloud droplets and keep them submerged until they had been photographically recorded. The method was improved and used in an aircraft by Mazur (1943), who saturated the mineral oil with distilled water to prevent the droplets from diffusing into the oil.

Slides coated with castor oil were used in the first extensive set of measurements of droplet sizes in cumuliform clouds by Weickman and Aufm Kampe (1953). With this method it was possible to collect droplets as large as 200 μm in diameter with no apparent shattering if the impact velocity was less than 100 m/s.

A large amount of droplet data was obtained by an automated sampler designed by Brown and Willett (1955). In their sampler three slides coated with silicone oil moved in rapid succession through an airstream and were photographed under a microscope in a cold cabin. The results for mean droplet distributions in trade-wind and summertime U.S. continental cumuli were reported by Braham, Battan, and Byers (1957) and by Battan and Reitan (1957).

These methods gave us the first details of the droplet spectrum at different geographical locations. A disadvantage of using them is that the sample must be recorded immediately, a procedure which is difficult in turbulent air. It is also necessary to know the exact time that elapsed between sampling and recording in order to apply diffusion corrections.

• *Magnesium Oxide Method*. Another widely used method involves coating a clean glass slide with a thin film of magnesium oxide. Droplets impinging on the film leave round holes which are proportional to their size.

This technique was developed and calibrated by May (1950) for drop diameters between 10 and 240 μm. For droplets larger than 20 μm in diameter, the ratio of droplet diameter to impression diameter was found to be 0.86; it remains constant with droplet size. Data reduction requires the investigator to examine the slide surfaces by microscope with a strong transmitted light and record the images photographically. This method is not affected by drop diffusion and droplets cannot coalesce, so the samples can be preserved. One disadvantage is that this layer is rather fragile in texture and can break off because of buffeting by the airstream. Another is that drops below 8 μm in diameter cannot be sized with certainty because the texture and grain size of the magnesium oxide interfere. Squires and Gillespie (1952) used this technique in a gun-type sampler which could be reloaded in about 50 s during flights. They exposed ten rods 3 mm wide (yielding a high collection

efficiency) from a magazine every 3 s to study the droplet spectrum variation inside cumulus clouds.

• *Carbon Film*. The most widely used substrate is a carbon film, because its texture enables it to withstand buffeting by the airstream (see Fig. 2). Neiburger (1949), for example, coated small glass slides with a film of lampblack and exposed them through stratus clouds during flights in a blimp. He derived the drop determination from the size of the rings which were obtained in the soot layer. Squires (1958a, b, c) also used this method during his investigation of continental and maritime cumuli. His technique made possible one of the most significant advances so far in our understanding of differences between the behavior of continental and maritime cumulus clouds. Clague (1965) developed an automated sampler which could expose 18 slides 3 mm wide in rapid succession. Warner (1969) used this device extensively to study the microstructure of cumulus clouds over Australia.

• *Gelatin-Coated Slides*. This method of recording cloud droplet sizes uses a gelatin substrate, as in Fig. 3. Liddell and Wotten (1957) used glass slides coated with gelatin containing water-soluble dye. Cloud and fog droplets impinging upon the slide dissolve the gelatin, leaving a clear area with an intense ring caused by the concentration of dye. Jiusto (1965) first used the gelatin sampling technique in airborne cloud studies. Cloud droplets impacting on a gelatin-coated slide (without water-soluble dye) dissolve the hygroscopic gelatin and redeposit it in a characteristic "moon crater" manner. Pena et al. (1970) reported a continuous cloud sampler that used a 16 mm gelatin-coated film capable of sampling over a cloud path length of more than 30 km. Because of its collection efficiency, this sampler can only detect drops no smaller than 2.5 μm in diameter; it is limited to use in clouds with liquid water content less than 0.35 g/kg.

The highly sensitive gelatin method can resolve droplets 1 μm in diameter. It has a minimal problem with drop evaporation and coalescence, although the samples have to be protected from high humidity. Using a phase-contrast microscope during data analysis helps to enhance the images for sizing.

Foil Impactors

Droplets larger than 50 μm in diameter are found in low concentration in natural clouds. The "single shot" samplers fail to collect large droplets because of the small volume they sweep out during a short exposure (to meet the 0.1 covering factor requirements). Their substrates are not suitable for recording large droplets, because such droplets often shatter, giving erroneous counts as small droplets on other parts of the sample.

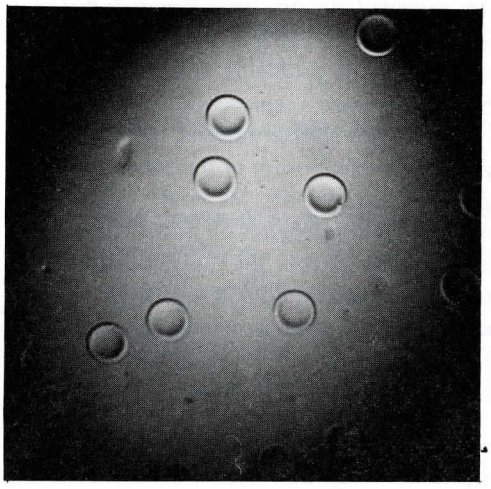

Fig. 3 Drop impressions in gelatin substrate. (Photo courtesy of J. Jiusto, State University of New York at Albany.)

Foil impactors were developed by various research groups as a means to measure precipitation-sized particles during cloud penetrations. Brown (1961) perfected a foil sampler which is capable of recording droplets larger than 250 μm in diameter while not recording the smaller sizes (see Fig. 4). His device consists of a lead foil mounted and supported on a continuous copper-mesh belt about 5 m long, which is driven past an aperture (1.24 X 1.59 cm) at a speed of 1.27 cm/s. The impinging drop creates an imprint which is a function of its size and the airspeed. The smallest imprint that can be recorded is that of a drop 250 μm in diameter at an airspeed of 76 m/s.

A similar device using aluminum foil 0.025 mm thick was reported by Duncan (1966). The foil is exposed over a ridged drum for 0.4 s by a shutter arrangement, then the exposed portion is wound past the aperture during the following 6.1 s. This exposure time was found to be the maximum possible in heavy rain (approximately 250 drops per cubic meter) without having the drop imprints overlap. The ratio of imprint diameter to drop diameter was found to be ~1.3 for drops of 0.75 - 3 mm; it increased to 1.5 for drops of 5 mm at an airspeed of 62 m/s.

A similar drop sampler is commercially available from Meteorology Research, Inc., Altadena, California. Schecter and Russ (1970) performed a detailed calibration between drop size and imprint diameter on this instrument at speeds of 72 and 118 m/s. They found that the ratios of imprint to drop diameter for drops from 0.5 to 5 mm in diameter range from 1.0 to 1.30. Unfortunately, their paper does not indicate what thickness or type of foil they used.

The foil impactors provided our first drop-size distributions for precipitation-sized particles (>250 μm in diameter) in natural clouds. Yet there are still problems with these devices. One is that it is difficult to obtain a representative sample of large drops if they occur in low concentrations. Increasing the sampling volume yields an overexposure of the smaller drops, resulting in overlapping of the imprints. Moreover, during icing conditions instrument reliability depends on how successfully deicing elements were employed. It is not always possible to make a clear distinction between liquid and solid hydrometeors from impressions obtained in a mixed-phase cloud. Calibration of imprints is not available for solid particles. Under all conditions, data handling and analysis are tedious and subjective.

Replicator Devices

Replicator devices have been widely used in cloud physics studies. They are mechanized sampling devices using the well known Formvar technique to capture and permanently encapsulate cloud particles (see MacCready and Todd, 1964; Spyers-Duran and Braham, 1967; Spyers-Duran, 1972a). They utilize a Mylar tape (usually a 16 mm polyester leader) which is coated with a solution of Formvar plastic and chloroform. (For airborne use, chloroform is preferred since it is nonflammable.) The continuously moving ribbon of Formvar is exposed in a cloud through a sampling slit several millimeters wide and then carried into a drying compartment where the plastic sets quickly. There, the encapsulated particles evaporate, leaving behind permanent replicas which can be sized and counted after suitable magnification. Since it is possible to obtain a continuous record through a cloud, the replicas can provide small-scale resolution of changes in cloud microstructure. Recently developed devices have the capability of viewing the replicas shortly after exposure so that tape speed and Formvar thickness can be adjusted in flight, as reported by Christensen, Keller, and Hallett (1974). Another major advantage of this method is that simultaneous recording of cloud droplets and ice crystals is possible (see Fig. 5).

Basically these devices are simple; however, they require a great deal of design compromise. In designs in which coatings

(a)

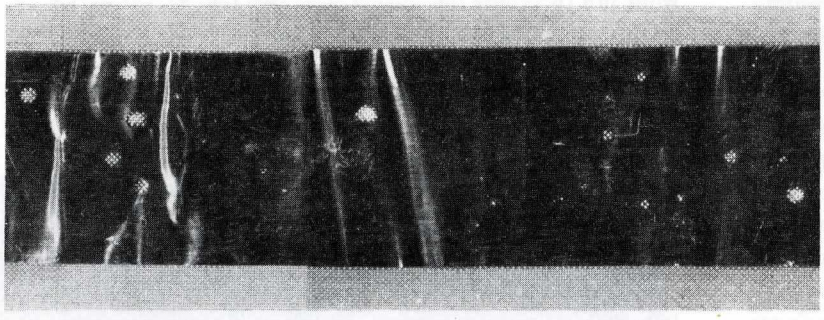

(b)

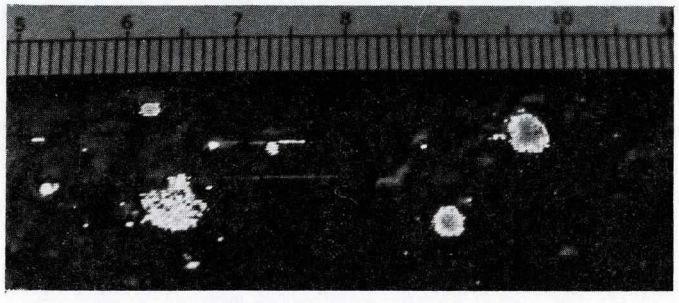

Fig. 4 Impressions of precipitation-sized particles in a lead foil exposed on the University of Chicago Lodestar aircraft (a), and in aluminum foil exposed on the South Dakota School of Mines and Technology T - 28 aircraft (b). Smallest diameter is 250 μm. (Sample a, courtesy of E. Brown, NCAR; sample b, courtesy of C. Knight, NCAR.)

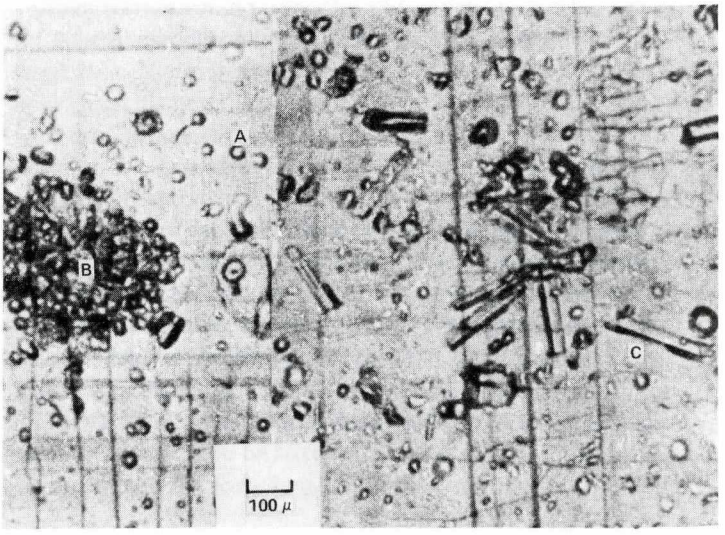

Fig. 5 Replicas of supercooled droplets (A), a snow pellet (B), and ice crystal columns (C).

are applied directly, they must be applied in the right thickness and viscosity to avoid being blown off; in designs for which the tape is precoated, enough time must be allotted for the Formvar to soften before exposure. Evaporation of the solvent cools the film to the point that ambient moisture may condense on it, causing blushing. With careful design, condensation can be eliminated by adding heat to the system, but excessive heat can melt ice crystals also. High airspeeds tend to make replication more difficult: the solution can blow off and particles can shatter during replication. Data analysis is laborious, and human interpretation is often necessary during data reduction to distinguish poor records from good ones and to determine areas where droplets are distorted. The large amounts of data generated during each flight are hard to manage.

In spite of all these drawbacks, replicating devices have become a very valuable tool in a number of cloud physics studies. Cloud droplet spectra have been measured in horizontal and vertical profiles of different types of clouds (Spyers-Duran, 1970, 1972a). A study of the onset of glaciation was made by MacCready and Takeuchi (1968); observations of ice crystals in a cumulus cloud seeded by silver iodide were obtained by Weinstein and Takeuchi (1970); and studies of ice content in clouds were undertaken by Mossop, Ono, and Heffernan (1967). Mossop and Ono (1969) have verified cirrus crystal survival in clear air, and Braham and Spyers-Duran (1967) have documented seeding of middle-level clouds. The replicating device has also made it possible to compare observed condensation and droplet growth with theory (Fitzgerald, 1972) and to measure the effect of pollution on cloud drop population in an urban atmosphere (Fitzgerald and Spyers-Duran, 1973; Spyers-Duran, 1972b; Eagan, Hobbs, and Radke, 1974a, b).

In the hands of a skillful operator, who can make proper adjustments to sample the variety of clouds studied at different geographical locations, the Formvar replicator method has several advantages. There is no problem with evaporation or drop coalescence. It is possible to obtain, from slow-flying aircraft or by the use of decelerators, ice crystal replicas in which the features and habit of the original crystal are recognizable.

Decelerators

Replicator devices would be an ideal way to study ice crystal habit, size, and concentrations in natural clouds if shattering of the delicate crystals during replication could be avoided. Experience shows that only the sturdier crystal forms——namely, small prisms, bullets, and hollow columns——survive impact and the replication process and that most crystals shatter into small fragments. To circumvent this problem, devices have been designed to lower the velocities of the particles in the air with respect to the aircraft by reducing the airflow past the sampler.

An ideal decelerator would meet the following design criteria:

- Gradual deceleration in order to achieve low turbulence during deceleration (Fragile crystals might break up during rapid oscillation.)
- Small divergent angle so the velocity profile remains symmetrical over the diameter with no flow separation at the walls
- Sufficient decelerator length to allow particles to be decelerated to an impaction speed of less than 15 m/s
- Known velocity at the sampling point
- Deicing of the leading edges and surfaces when flying through supercooled clouds.

Mossop et al. (1967) and Mossop and Ono (1969) designed and evaluated three different types of decelerators. The best results were reported from a sampling tube 3.7 m long, with a front diffuser section having an intake diameter of 4.1 cm and flared out at an angle of 6° to an internal diameter of 9.9 cm. With this device the velocity was reduced from 60 to 20 m/s and hexagonal plates, capped columns, and frail stellar crystals were successfully replicated.

Yamashita (1969) reports a decelerator that sets up a reverse airflow to reduce the velocity of the particles before replication.

In a detailed study, Hobbs, Farber, and Joppa (1973) reported a new approach to decelerators, one in which the deceleration occurs upstream of the entry duct. Two types of decelerators are discussed. One is a rectangular duct 23 cm long with a constant width of 12.7 cm. The area of the replication point is five times that of the exit point, thus the velocity produced at the replication point is one-fifth of the free airstream velocity. This device was used on a slow-flying aircraft.

The second decelerator was used on a faster flying B - 23 aircraft. In this device air deceleration is controlled over a longer length (91 cm). The device has a circular cross section with entrance and exit cones, and a velocity section 30 cm long to decelerate the particles to one-fifth of airstream velocity.

Both decelerators were tested in a wind tunnel where the velocity profile was determined. The authors do not give collection efficiencies of the decelerators for various types of

ice crystals, so accurate values of concentration cannot be determined. Their paper does include descriptions of several samples which were obtained from an aircraft, indicating that ice crystals larger than 1 mm in diameter can be collected without fragmentation.

Another decelerator was designed and tested by Davis and Veal (1974) for a 10:1 reduction in velocity; its straight section of 102 cm provides sufficient length to allow large dendrites and plates to be decelerated by at least a factor of five. The unit is 230 cm in length. The entrance cone with a semi-angle of 4° is 98 cm in length; the straight section has a diameter of 20 cm; and the exit cone is 30 cm long. This device was extensively tested in a wind tunnel to obtain its velocity profile and collection efficiencies. The collection efficiencies were found to exceed 0.9 for particles larger than 75 μm and were less than 0.06 for diameters smaller than about 15 μm. Samples obtained with this decelerator show the delicate structure of crystals preserved through replication.

Decelerators can also be used for direct capture of ice particles in subfreezing silicone oil. They can then be brought back to the laboratory for studies as reported by Schreck, Toutenhoofd, and Knight (1974).

Table 1 summarizes the practical limits within which drop samples can be obtained by the various measurement techniques. The lower limit depends on the collection efficiency of the sampling device, the upper limit on impaction speed and on drop breakup, which is also a function of substrate thickness.

Table 1
Size Range of Various Measurement Techniques

Substrate	Drop Size Diameter (μm)	Cloud Drops	Precipitation-Sized Drops
Oil	4 - 200	Yes	Drizzle size
Magnesium oxide	8 - 240	Yes	Drizzle size
Carbon	4 - 1,000	Yes	Drizzle size
Gelatin	2.5 - 50	Yes	No
Lead foil	250 - 5,000	No	Yes
Aluminum foil	500 - 5,000	No	Yes
Formvar	4 - 50	Yes	No

References

Battan, L. J., and C. H. Reitan, 1957: Droplet size measurements in convective clouds. In *Artificial Stimulation of Rain* (H. Weickmann and W. Smith, Eds.), Pergamon Press, Inc., Elmsford, N.Y., 184 - 191.

Braham, R. R. Jr., L. J. Battan, and H. R. Byers, 1975: Artificial nucleation of cumulus clouds. *Met. Monogr. 2 (11)*, 47 - 85.

———, and P. A. Spyers-Duran, 1967: Survival of cirrus crystals in clear air. *J. Appl. Met. 6*, 1053 - 1061.

Brown, E. N., 1961: A continuous-recording precipitation sampler. *J. Appl. Met. 18*, 815 - 818.

———, and J. W. Willett, 1955: A three-slide cloud droplet sampler. *Bull. Am. Met. Soc. 36*, 123 - 127.

Christensen, L., V. Keller, and J. Hallett, 1974: Ice particle concentration in prehail convective cloud in Colorado. In Preprint Vol., Conference on Cloud Physics, held 21 - 24 October, Tucson, Ariz.; American Meteorological Society, Boston, Mass., 191 - 194.

Clague, L. F., 1965: An improved device for obtaining cloud droplet samples. *J. Appl. Met. 4*, 549 - 551.

Davis, C. I., and D. L. Veal, 1974: *Interim Progress Report No. 9*, Department of Atmospheric Research, University of Wyoming, 10 pp.

Duncan, A. D., 1966: The measurement of shower rainfall using an airborne foil impactor. *J. Appl. Met. 5*, 198 - 204.

Eagan, R. C., P. V. Hobbs, and L. F. Radke, 1974a: Measurements of cloud condensation nuclei and cloud droplet size distributions in the vicinity of forest fires. *J. Appl. Met. 13*, 553 - 557.

———, ———, and ———, 1974b: Particle emissions from a large Kraft paper mill and their effects on the microstructure of warm clouds. *J. Appl. Met. 13*, 535 - 552.

Fitzgerald, J. W., 1972: *A Study of the Initial Phase of Cloud Droplet Growth by Condensation*. Technical Note No. 44, Cloud Physics Laboratory, University of Chicago, 144 pp. (Clearinghouse for Federal Science Information PB 211322).

———, and P. A Spyers-Duran, 1973: Changes in cloud nucleus concentration and cloud droplet size distribution associated with pollution from St. Louis. *J. Appl. Met. 12*, 511 - 516.

Fuchs, N., and I. Petrjanoff, 1937: Microscopic examination of fog and rain droplets. *Nature 139*, 111 - 112.

Hobbs, P. V., R. J. Farber, and R. G. Joppa, 1973: Collection of ice particles from aircraft using decelerators. *J. Appl. Met. 12*, 522 - 528.

Jiusto, J. E., 1965: *Cloud Particle Sampling.* Report No. 6, NSF G - 24850, Department of Meteorology, Pennsylvania State University, 19 pp.

Langmuir, I., and K. B. Blodgett, 1946: *A Mathematical Investigation of Water Droplet Trajectories*. Army Air Force Technical Report No. 5418, 65 pp. (National Technical Information Service PB - 27565). Available from XL Library of Congress Photoduplicating Service, Washington, D.C.

Liddell, H. F., and N. W. Wotten, 1957: The detection and measurement of water droplets. *Q. J. R. Met. Soc. 83*, 263 - 266.

MacCready, P. B. Jr., and C. J. Todd, 1964: Continuous particle sampler. *J. Appl. Met. 3*, 450 - 460.

———, and D. M. Takeuchi, 1968: Precipitation initiation mechanism and droplet characteristics of some convective cloud cores. *J. Appl. Met. 7*, 591 - 601.

May, K. R., 1950: Measurements of airborne droplets by magnesium oxide method. *J. Sci. Instrum. 27*, 128 - 130.

Mazur, J., 1943: *An Investigation on the Number and Size Distribution of Water Particles in Natural Clouds*. Meteorological Research Paper No. 109, Meteorological Office, London.

Mossop, S. C., and A. Ono, 1969: Measurements of ice crystal concentration in clouds. *J. Atmos. Sci. 26*, 130 - 137.

———, ———, and K. J. Heffernan, 1967: Studies of ice crystals in natural clouds. *J. Rech. Atmos. 3*, 45 - 64.

Neiburger, M., 1949: Reflection, absorption and transmission of isolation stratus cloud. *J. Met. 6*, 98 - 104.

Pena, J., R. de Pena, R. L. Lavoie, and J. Lease, 1970: A continuous cloud sampler. In Preprint Vol., Conference on Cloud Physics, held 24 - 27 August, Ft. Collins, Colo.; American Meteorological Society, Boston, Mass., 93 - 94.

Ranz, W. E., and J. B. Wong, 1952: Impaction of dust and smoke particles on surface and body collectors. *Ind. Engng. Chem. 44*, 1371.

Schecter, R. M., and R. G. Russ, 1970: The relation between imprint size and drop diameter from an airborne drop sampler. *J. Appl. Met. 9*, 123 - 126.

Schreck, R. I., V. Toutenhoofd, and C. A. Knight, 1974: A simple, airborne ice particle collector. *J. Appl. Met. 13*, 949 - 950.

Spyers-Duran, P. A., 1970: Observations of microstructure in two cumuli. In Preprint Vol., Conference on Cloud Physics, held 24 - 27 August, Ft. Collins, Colo.; American Meteorological Society, Boston, Mass., 173 - 174.

———, 1972a. *Systematic Measurements of Cloud Particle Spectra in Middle Level Clouds*. Technical Note No. 43, Cloud Physics Laboratory, University of Chicago, 54 pp. (Clearinghouse for Federal Science Information PB 211321).

———, 1972b: *Upwind and Downwind Cloud-Base Microstructure.* Technical Note No. 45, Cloud Physics Laboratory, University of Chicago, 98 pp. (Clearinghouse for Federal Science Information, PB 218678).

———, and R. R. Braham Jr., 1967: An airborne continuous cloud particle replicator. *J. Appl. Met. 6*, 1108 - 1113.

Squires, P., 1958a: The microstructure and colloidal stability of warm clouds. Part I. The relation between structure and stability. *Tellus 10*, 256 - 261.

———, 1958b: The microstructure and colloidal stability of warm clouds. Part II. The causes and variations in microstructure. *Tellus 10*, 262 - 271.

———, 1958c: The spatial variation of liquid water and droplet concentration in cumuli. *Tellus 10*, 372 - 380.

———, and C. A. Gillespie, 1952: A cloud droplet sampler for use on aircraft. *Q. J. R. Met. Soc. 78*, 387 - 393.

Warner, J., 1969: The microstructure of cumulus cloud. Part I. General features of the droplet spectrum. *J. Atmos. Sci. 26*, 1049 - 1059.

Weickmann, H. K., and H. J. Aufm Kampe, 1953: Physical properties of cumulus clouds. *J. Met. 10*, 204 - 211.

Weinstein, A. I., and D. M. Takeuchi, 1970: Observations of ice crystals in a cumulus cloud seeded by vertical-fall pyrotechnics. *J. Appl. Met. 9*, 265 - 268.

Yamashita, A., 1969: Methods of continuous particle sampling by aircraft. *J. Met. Soc. Japan 47*, 86 - 97.

Cloud Droplet Spectrometry by Means of Light-Scattering Techniques

Harvey E. Dytch and Nicholas J. Carrera, University of Chicago

The use of direct sampling techniques for the measurement of the concentration and size distribution of water droplets in clouds presents a number of difficulties. Sampling necessarily involves disturbing the airstream and is anisokinetic, with attendant collection efficiency problems; the technique is often discontinuous and provides data only through a few sections of a cloud; and analysis is a slow, tedious, post-flight process. Optical techniques offer an attractive method of circumventing many of these problems, and, for the small droplet size range, the use of the light-scattering properties of individual droplets to count and size cloud particles has been the basis of several recent designs.

General Theory: Advantages and Problems

The power scattered per unit solid angle by a homogeneous, dielectric sphere of radius r when illuminated by a plane-parallel beam of monochromatic light of wavelength λ can be computed as a function of scattering angle by the use of Mie theory. The scattering intensity is a complex function of the particle refractive index, absorption coefficient, size parameter ($\alpha = 2\pi r/\lambda$), and scattering angle, and can be completely specified only for spherical particles. However, for transparent spheres of known composition (e.g., water droplets), the scattered power integrated over a given solid angle by a collector at a particular scattering angle can be related to the size of the scattering particle if the intensity of the illuminating radiation is known. This is the basis of droplet sizing by means of light scattering.

If the scattered power as determined by Mie theory is integrated over a particular range of scattering angles and is examined as a function of particle size parameter (α) over a wide range of α, one notes a region of oscillation of the Mie intensity functions bounded by Rayleigh scattering (r^6 dependence) for small α and geometrical scattering (r^2 dependence) for large α. These oscillations are caused by the interference effects of refraction, internal reflection, and diffraction. The use of visible or near-infrared light sources [typically, helium-neon (He-Ne) lasers with $\lambda = 6328$ Å are employed for practical considerations] for the sizing of cloud droplets involves a range of α for which these effects may be significant. The amplitude of these oscillations and the range of α over which they occur are directly dependent upon the scattering angle and the solid angle chosen for light collection, making it increasingly difficult unambiguously to associate particle size with scattered light intensity at larger scattering angles. Moreover, at larger scattering angles, the relative intensity of the scattered radiation decreases with particle size. Thus, insofar as it is compatible with the restraints imposed by the sampling geometry, small scattering angles are desirable for keeping the scattered signal power high and as nearly monotonic a function of droplet size as possible.

The basic elements, then, common to most light-scattering droplet spectrometry schemes, are:

- A source of incident radiation
- A means of defining (optically or electronically) some portion of this illuminating beam as a sampling volume through which the sampled airstream passes
- Collecting optics and electronics to gather the radiation scattered at a given angle during droplet transit through this sampling volume and to convert it into an electronic signal
- A means of comparing the relative power of each

Authors

Harvey E. Dytch is a meteorologist for the Cloud Physics Laboratory of the University of Chicago, where he earned a bachelor's degree in geophysical sciences in 1971. His present field of interest, in connection with the Metropolitan Meteorological Experiment (METROMEX), is the influence of urban areas on warm cloud microstructure.

Nicholas J. Carrera, also currently engaged in METROMEX research, is a graduate of Harvard University and has received M.S. and Ph.D. degrees in physics from the University of Illinois, Urbana. He worked at the National Bureau of Standards and Brookhaven National Laboratory prior to joining the University of Chicago Cloud Physics Laboratory in 1973.

scattering event and associating it with a particular size of particle

- An associated data acquisition system.

One important advantage of a scattering technique lies in its nonmechanical definition of a sampling volume. This allows isokinetic sampling in the free airstream outside surface boundary layers without disturbing or modifying the cloud sample in the measurement process.

The definition of this sample volume, however, also presents one of the most severe basic limitations to scattering spectrometry. In order to clarify this, let us define the "static sampling volume" as simply the working volume under illumination within which valid scattering events can occur, defined optically when the instrument is at rest with respect to the airstream. When the probe is in motion, the "dynamic sampling volume" is then defined as the product of the area of the static volume orthogonal to the airstream through which droplets pass (the sampling area), the relative velocity of the airstream, and the response time of the instrument, as limited by the photodetection or electronic processing methods employed. In general, this dynamic volume is far larger than the static volume, and it is the dynamic volume that is here called the sampling volume. The sampling rate of the instrument is just the product of the sampling area and the relative airstream velocity.

A basic limitation in scattering technique, then, is the incompatibility of maximizing the sampling rate in order to achieve satisfactory sampling statistics (particularly for the larger droplets) and minimizing the sampling volume in order to ensure that scattering occurs at a unique scattering angle and that the droplets are individually sized and counted. If a high sampling rate is achieved at the cost of a large sampling volume, significant coincidence error can arise from multiple scattering events when more than one droplet is present in the sampling volume.

If the average number of droplets in the sampling volume is small, the probability of coincidence errors may be determined by Poisson statistics. If $P(n)$ is the probability of the presence of n droplets, N is the total concentration of droplets per unit volume, V is the sampling volume, and μ is the average number of droplets in the sampling volume, then $\mu = NV$ and

$$P(n) = \frac{\mu^n e^{-\mu}}{n!}$$

The ratio of multiple scattering events, P_m, to valid single scattering occurrences, P_s, is then

$$\frac{P_m}{P_s} = \frac{1 - e^{-\mu}(1 + \mu)}{\mu e^{-\mu}} \approx \frac{\mu}{2}$$

for $\mu \ll 1$, i.e., approximately the ratio of doublet to singlet events for small μ. Thus, for example, concentrations of 100 and 1,000 droplets per cubic centimeter require dynamic sampling volumes of less than about 2×10^{-4} and 2×10^{-5} cm^3, respectively, to obtain only 1% as many coincidence errors as valid measurements. So small a sampling volume as 2×10^{-4} cm^3, for example, provides very poor sampling statistics for the larger, less numerous cloud droplets. While concentrations of droplets smaller than 10 μm in diameter may be in the hundreds per cubic centimeter, concentration falls off rapidly with size, and droplets larger than about 50 μm may number only a few per cubic centimeter or two orders of magnitude lower in concentration. Therefore, a scattering instrument, if it is designed to operate over a size range encompassing the abundant smaller droplets in natural clouds, is necessarily restricted in spatial resolution for the larger cloud particles because of sampling statistics. The sampling volume can be increased somewhat to obtain better sampling statistics, with resultant increase in coincidence errors, but this may be acceptable.

To take some figures typical of droplet spectrometers currently in use, for a sampling area of 4×10^{-3} cm^2, an airspeed of 100 m/s, and an effective instrument response time of 10 μs (particles detected at a rate of 100 kHz would be seen as single scattering events), the sampling volume is 4×10^{-4} cm^3. For concentrations of $N = 100$ and $N = 1{,}000$ drops per cubic centimeter, this gives 2% and 23% probable coincidence errors, respectively. A total concentration of 1,000 drops per cubic centimeter is rather high for most clouds; perhaps a more typical figure would be 500 drops per cubic centimeter, which gives a 10% probable coincidence error. If greater accuracy is needed, it may be necessary to use multiple instruments, each restricted in droplet size range.

Within the static sampling volume itself, a field of illumination of perfectly uniform intensity is desirable, so that the scattering signal collected from a droplet of given size is independent of the path through the sampling volume. In practice, however, laser light sources emit nonuniform intensity profiles, varying from a Gaussian distribution for the lowest mode to higher order modes for which the probability that a particle transiting the beam will intersect a peak isophote is as high as 90%. This effect is most important as light intensity rolls off at the edge of the beam, since a droplet passing through near the edge will scatter less light. An additional problem derives from the shorter path length near the edge, shortening droplet transit times under flight conditions; because of electronics time constants, this may result in an effective reduction of the peak signal amplitudes of these shorter pulses. The combination of these effects results in "edge-effect errors": since droplets are not mechanically constrained to pass through the center of the illuminating beam, undersizing of droplets passing through the edges occurs. In the absence of circuitry designed to reject edge-

scattering events, errors of the first type, at least, may be corrected for theoretically, or through laboratory calibration with monodisperse droplets, by transforming the raw droplet size distributions obtained, once the probabilities of incorrect sizing are known.

Additional errors in light-scattering measurements, particularly for the smallest droplet sizes measured, may arise when the minimum detectable scattering signal amplitude is near the noise level of the instrument, both from light contamination of the collecting optics by background radiation and from slight fluctuations in the power output of the illuminating source. The use of high-power laser light sources, optical shielding and filtering of the collecting optics, and careful monitoring of laser power output can minimize these problems. Finally, precise laboratory determination of the dimensions of the instrument sampling area and in-flight determination of the true airspeed are necessary for accurate measurement of absolute droplet concentrations.

Calibration

The ideal calibration for any measuring instrument is to compare it with a standard and see what it reads. This should be done over the full range of the instrument and under actual or simulated conditions of use. Known input and measured response then determine a transfer function for the instrument which allows correction for all the instrument's errors. Such a calibration for the cloud droplet spectrometer would involve preparation of sized droplets in known concentrations, with these quantities to be varied over the entire measuring range of the instrument. These "standard clouds" would then be passed through the instrument at airspeeds to be used during field measurements. In fact, the calibration should really be done in situ, to take into account such things as vibration, disturbed flow over aircraft surfaces, electrical noise, and other disturbances that may not be foreseen in a laboratory calibration. At present such a thorough calibration is impractical or impossible. We attempt, then, to consider which parts of this ideal calibration are most important, and to arrive at some practical calibration procedures.

Single-droplet spectrometers make only two measurements: they size particles and they count them. The information that we desire, though, is size and concentration. To obtain concentration from counts, the sampling area and airspeed need to be known. Airspeed is normally measured by a separate instrument, which has its own calibration problems. We will consider here the calibration of sizing, counting, and sampling area. As we shall see, these determinations are not at all independent.

For size calibration, a monodisperse beam of particles is passed through the instrument and the response determined. Routine generation of individual water droplets is possible for diameters of 20 - 30 μm and larger, with size variations of only a few percent. Glass or plastic beads can be used for smaller diameters, and correction made for the difference in index of refraction. Very nearly monodisperse beads are commercially available (with, e.g., standard deviation less than 2% of nominal size), but less accurate sizes may be acceptable in view of other limits to the instrument resolution in the smaller size categories.

As discussed above, droplets which pass near the edge of the sampling area will be in a less intense portion of the light beam, and will be sized as smaller particles. For a Gaussian laser mode, as many as half of the droplets may be undersized (most of them by only one size category). This distribution into smaller size categories should be determined during the calibration by measuring the response for known particle sizes as particles pass through different parts of the sampling area.

The question of edge effects and undersizing is closely connected with the problem of defining and measuring the sample area. The effective sample area——the area within which a droplet will be correctly sized——differs with droplet size. For droplet sizes approaching the beam width, the passage of a droplet center too far from the beam center line results in scattering by only part of the droplet, and consequent undersizing. In addition, we must remember that the falling off of light intensity near the edge of the beam means that even small droplets near the edge but within the geometrical limits of the beam will be undersized. It is convenient to take the sample area to be the same for all sizes of droplets and to be that area within which any particle scatters light above the noise level. Careful surveying of this area with sized droplets can then determine the fraction and degree of undersizing of a uniform concentration of droplets. This will normally vary with droplet size, and can be applied as a correction to the indicated size spectrum to correct both for intensity falloff and for partial droplet scattering near the edge.

Besides scattered light intensity, the other parameter measured by the instrument is counts per unit of time. Since the time base for electronic logic circuits may be controlled quite accurately, no errors will arise here as long as the sampling rate is low. When the airspeed and droplet concentration combine to create overlap or near-overlap of particle passage through the sample area, counts will be lost, as discussed above. When this occurs, size information will be lost as well. It may be possible to determine what percentage of counts is lost due to coincidence, but if coincidence errors are appreciable, the indicated spectrum cannot be corrected for the errors without making some assumptions about the true

size spectrum. Such assumptions may be inappropriate and misleading. Every attempt should be made to operate within the limitations imposed by the instrument design, and estimates of coincidence error should be quoted as a qualification to the interpretation of published data, rather than applied as a "correction" to obtain data which are then claimed to be more accurate.

Again, careful size calibration, sample area determination, and attention to the operating limits of the instrument are only an approach to the full-blown calibration over all sizes, all concentrations, and all airspeeds for which the droplet spectrometer will be used. In addition, errors may arise after installation on the aircraft from noise pickup, vibration, fatigue, turbulent flow, and so on. Post-installation checks on calibration might include sampling passes through similar clouds at different airspeeds to check on possible coincidence effects, and ground checks with a "standard" or at least reproducible droplet spray, to check on day-to-day consistency. Size calibration can also be checked in the field with sized water droplets or beads.

Field Problems

The normal problems of alignment and stability of optical systems are exacerbated in an airborne environment, with its high vibration levels and rapid pressure and temperature changes. A simple and rugged design can help minimize these problems, but some adjustment capability is necessary if alignment is affected by vibration or airframe flexing. Signal intensity may be affected by aging of the light source, voltage fluctuations, alignment changes, or dirt on optical surfaces. This can be monitored and partially compensated for by using a reference signal from the light source to compare with the scattered signal. Wetting of optical components where the beam enters and leaves the airstream may be a problem during passes through precipitation or heavy clouds. In practice, a slight recessing of these optical surfaces below the protective enclosure seems to keep them dry in all but the heaviest precipitation. Condensation on external optics may occur in flying from colder to warmer air, but is likely to be of short duration. In supercooled or mixed clouds, deicing of structural instrument parts will be necessary for prolonged flight. Under these conditions, disturbed airflow may occur through the sampling area, and optical alignment changes may result from increased strain on external members which are not deiced.

Electrical noise is a general problem with electronic instrumentation, and the usual attention to shielding, voltage regulation, separation from noise sources, and so on will help reduce noise pickup. A recent discussion of aircraft electrical noise affecting atmospheric measurements can be found in Ruskin and Scott (1974).

Optical Cloud Particle Spectrometer

The optical cloud particle spectrometer (Ryan et al., 1972) is manufactured by Environmental Research and Technology, Inc., of Concord, Massachusetts. Its present configuration

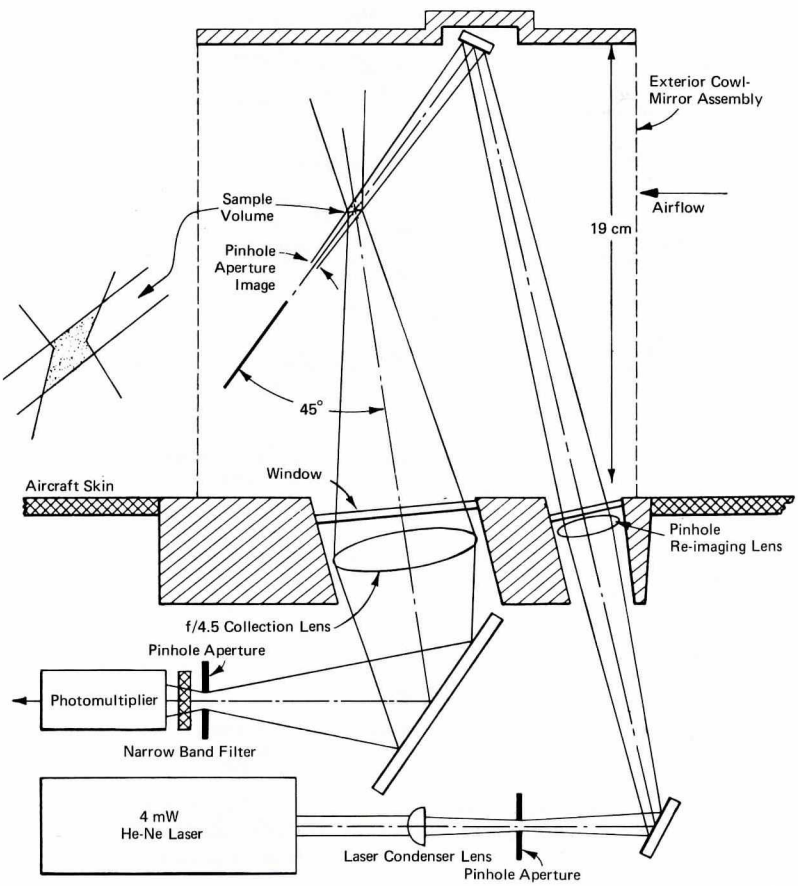

Fig. 1 Diagram of the cloud droplet spectrometer. (Courtesy of H. Blau, Environmental Research and Technology, Inc.)

(shown schematically in Fig. 1) uses a 4 mW He-Ne gas laser (6328 Å) mounted inside the aircraft as its light source. The laser output is focused through a beam-defining aperture and then reflected and re-imaged out of the aircraft onto a mirror mounted in an exterior cowl assembly. The scattering detector used is an S - 20 photomultiplier, in front of which are located a bandpass interference filter that is 100 Å wide (centered at 6328 Å) and a scattering detector aperture that is reflected and re-imaged outside the aircraft into the sample space. The intersection of this detector aperture image with the laser beam image at about 45° defines a 1.3×10^{-4} cm^3 static sample volume about 15 cm out from the aircraft skin, the sampling area of which is 0.4 mm^2, normal to the flight direction. Scattering signals from the photomultiplier are fed to a pulse-height analyzer, operating as a peak detector, which directs each scattering event into one of 12 channels corresponding to 12 droplet size ranges, covering diameters from 4.4 to 110 μm, varying in width from 1.5 to 32.0 μm. The use of an exterior cowl with blackened inner walls, together with the interference filter in front of the photomultiplier, minimizes the limiting effect of stray background radiation. The laser and detector windows and the exterior cowl-mounted mirror are recessed and canted at about 10° to the airflow to avoid wetting.

Fig. 2 Diagram of the axially scattering spectrometer probe. (Courtesy of R. Knollenberg, Particle Measuring Systems, Inc.)

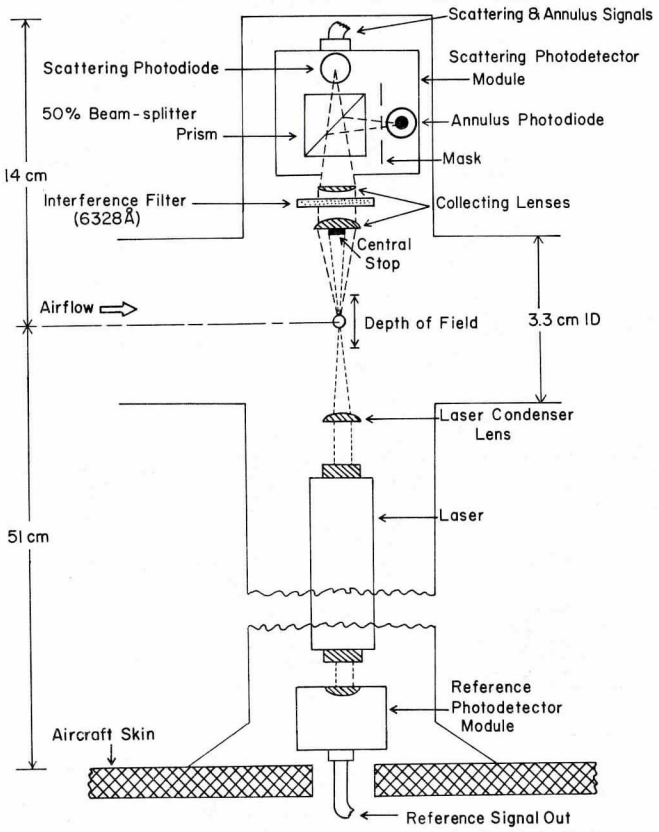

Ground calibration is accomplished by recording the response of the instrument to water droplets of selected size produced by applying a direct current potential to a hypodermic needle connected to a water reservoir. The droplet beam is directed through the sample volume and adjusted to give maximum scattered signal as recorded by an oscilloscope. Simultaneous photographs of the oscilloscope trace and photomicrographs of the sample volume itself are made by slaving a stroboscope that illuminates the sample volume to the scattering pulse. A calibration curve is then constructed from these photographs, relating droplet size to output voltage. Corrections for edge-effect errors are determined by scanning the generated monodisperse droplet beam at a constant speed through ten equal horizontal increments and recording the resultant droplet count. By performing this experiment for three droplet diameters near the low, middle, and upper size ranges for a given channel, correction factors are determined. Using this procedure, Ryan et al. (1972) determined that 50% of the droplets were properly sized, 25% were counted in the next lower channel, 8% in the next channel, and the remaining 17% almost evenly distributed in the next five channels, with no dependence of correction factor on droplet diameter for the 30 - 60 μm drops used. The sampling area is determined experimentally by placing a plane diffuser in the static sampling volume perpendicular to the flight direction and measuring its illuminated area; the error associated with this determination is estimated to be ±5%. Error in determining the size distribution, estimated by the

Fig. 3 Axially scattering spectrometer probe (black mast on left) mounted on University of Chicago Cloud Physics Laboratory airplane. Silver probe (to right of spectrometer) is an earlier, prototype scattering probe.

observed scatter in calibration measurements using monodisperse droplets, is thought to be ±15% of the reported value for each size interval.

Axially Scattering Spectrometer Probe

A 1 mW He-Ne laser (6328 Å), operating in a high-order multimode state, provides the source of illumination of the axially scattering spectrometer probe shown schematically in Fig. 2 and mounted on an aircraft in Fig. 3; the instrument is manufactured by Particle Measuring Systems, Inc., of Boulder, Colorado. The laser tube, mounted with the detector electronics and associated optics in a small external airfoil, projects a beam of light which is focused to approximately 200 μm in diameter in the center of a sampling aperture in the airfoil located about 51 cm from the aircraft skin. The scattered energy from droplets passing through the laser beam in the sampling aperture is collected by a pair of condensing lenses sandwiching a 6328 Å interference filter, while the unscattered laser beam is intercepted by a central stop on the first collecting lens. A 50% beam-splitter prism then divides the scattered light into a directly transmitted portion, which is focused on the scattering signal photodiode, and a reflected portion which passes through the 90° prism face. A central stop on this face defines an annular collecting field, allowing light transmission from droplet scattering only when the droplets are sufficiently displaced from the object plane in the center of the sampling aperture. By comparing the amplified signals from the scattering and annulus detectors, a given scattering event is rejected or accepted as valid, depending on whether it is within a 4 - 5 mm electronically determined depth of field. This depth-of-field limitation thus defines a static sampling volume of about 1×10^{-4} cm^3 in the center of the sampling aperture with a sampling area of approximately 7×10^{-3} cm^2.

The scattering signal from droplets within the proper depth of field is then passed to a pulse-height detector which compares the amplitude of the signal to a reference voltage derived by monitoring the laser output with a reference photodetector in back of the laser to cancel out changes in illuminating intensity. A square-weighted resistor array, measuring maximum pulse amplitude, and a string of voltage comparators associate each scattering event with one of 15 size classes 2 μm wide, covering droplet diameters from 2 to 30 μm. The instrument also has a range-switching option permitting the user to choose additional size ranges of 0.5 - 7.5, 1 - 15, or 3 - 45 μm; the size range limits are only properly linearized for the 2 - 30 and 3 - 45 μm size ranges, however. The prime instrument calibration, in the 2 - 30 μm range, is performed in the laboratory using water droplets and glass beads with a theoretical correction for refractive index.

Another option available is edge-effect reject circuitry that measures scattering pulse widths and compares the running mean particle transit time to the instantaneous transit time of each droplet. Only those scattering events with pulse widths long enough to have passed through the central 62% of the laser beam diameter are considered valid. With this optional circuitry, size errors are ±10% or ±2 μm, whichever is greater, while the static sampling volume is effectively reduced to about 4×10^{-5} cm^3 and the sampling area to 4×10^{-3} cm^2. The instrument is designed to function at airspeeds from 0.1 to 125.0 m/s and has a maximum particle rate of 100 kHz.

Particle Instrumentation by Laser Light Scattering

Custom-designed instruments for measuring water droplet spectra are made by Environmental Systems Corporation, Knoxville, Tennessee. While those made to date have been for power plant cooling-tower monitoring, the droplet sizes are in the natural cloud size range, and airborne operation of such instruments appears feasible. Solid-state lasers operating in the infrared have been used in a pulsed mode, with 200 ns pulses occurring at 300 Hz. Forward scattering and pulse-height detection are used to size individual drops. The laser, optics, and detector are compactly mounted in a cylindrical container (typical overall dimensions are about 60 cm by 7.6 cm in diameter). For one instrument, the static sampling volume was 5×10^{-3} cm^3 and the size range covered was 3 to 100 μm in diameter. Other models have been made for either larger or smaller droplet sizes and have ranged from 10^{-6} to 10 cm^3 in static sampling volume. Calibration is done with a droplet generator that produces individual monodisperse drops ranging from 30 to 900 μm in diameter, with standard deviations of 5%.

Early Cloud Droplet Spectrometers Developed in the USSR

Prior to the easy availability of small lasers, some interesting cloud spectrometer designs were developed in the USSR. They used incandescent light sources but were otherwise quite similar to the devices described above. Kazas, Konyshev, and Laktionov (1965) used a forward-scattering instrument that sized droplets over the range of 20 - 150 μm in diameter, using ten size categories. The problem of defining static sampling volume was treated mechanically, by using an inlet tube aligned with the airstream to direct droplets through the sampling area. A later instrument by Konyshev and Laktionov (1966) used 90° scattering and defined the sampling volume by the intersection of the light source beam and the detector acceptance beam, similar to the arrangement in the optical cloud particle spectrometer described above (Ryan et al., 1972). Konyshev's instrument is described as being usable over the range of 25 - 150 μm in diameter, with 20% coincidence errors and only 6% of the droplets incorrectly sized.

References

Kazas, V. I., Yu. V. Konyshev, and A. G. Laktionov, 1965: Airborne device for the continuous measurement of the dimensions and concentrations of large-scale cloud drops. *Izv. Atmos. Oceanic Phys. 1*, 710 - 712.

Konyshev, Yu. V., and A. G. Laktionov, 1966: An airborne photoelectric measurement device for cloud droplets. *Izv. Atmos. Oceanic Phys. 2*, 462 - 464.

Ruskin, R. E., and W. D. Scott, 1974: Weather modification instruments and their use. Chapter 4 in *Weather and Climate Modification* (W. N. Hess, Ed.), John Wiley and Sons, Inc., New York, N.Y., 136 - 205.

Ryan, R. T., H. H. Blau Jr., P. C. von Thüna, and M. L. Cohen, 1972: Cloud microstructure as determined by an optical cloud particle spectrometer. *J. Appl. Met. 11*, 149 - 156.

For Further Reading

Blau, H. H. Jr., D. J. McCleese, and D. Watson, 1970: Scattering by individual transparent spheres. *Appl. Opt. 9*, 2522 - 2528.

———, M. L. Cohen, L. B. Lapson, P. von Thüna, R. T. Ryan, and D. Watson, 1970: A prototype cloud physics laser nephelometer. *Appl. Opt. 9*, 1798 - 1803.

Hodkinson, R., 1966: Particle sizing by means of the forward scattering lobe. *Appl. Opt. 5*, 839 - 844.

Mie, G., 1908: Contributions to the optics of turbid media, especially colloidal metal solutions. *Ann. Physik 25*, 377 - 445.

Van de Hulst, H. C., 1957: *Light Scattering by Small Particles*. John Wiley and Sons, Inc., New York, N.Y., 420 pp.

Vonnegut, B., and J. Neubauer, 1952: Production of monodisperse liquid particles by electrical atomization. *J. Colloid Sci. 7*, 616 - 618.

For Further Information about Equipment

Sized Beads

Dow Corning Corporation
Bioproducts Department
Midland, Michigan 48640

Particle Information Services, Inc.
P.O. Box 702
Grants Pass, Oregon 97526
Telephone: (503) 476 - 9676

Droplet Spectrometers

Environmental Research and Technology, Inc.
696 Virginia Road
Concord, Massachusetts 01742
Telephone: (617) 369-8910

Environmental Systems Corp.
P.O. Box 2525
Knoxville, Tennessee 37901
Telephone: (615) 637 - 4741

Particle Measuring Systems, Inc.
1855 57th Court
Boulder, Colorado 80301
Telephone: (303) 443 - 7100

Particle Size Distribution Measurement: An Evaluation of the Knollenberg Optical Array Probes

A. J. Heymsfield, Meteorology Research, Inc.

To cloud physicists, cloud particle size distributions are information basic to the field. Particle size distributions can be used to obtain the cloud microphysical parameters of total water droplet or ice crystal number concentrations and of mean and maximum particle dimensions. The second, third, and sixth moments of the particle spectrum (visibility, water content, and radar reflectivity factor, respectively) can also be derived from these distributions.

From the particle size distribution, very important cloud-related meteorological and engineering problems can be solved. Among the meteorological problems is the need to assess the effect of weather modification attempts on cloud particle size distributions, number concentrations, and water contents. Another question is radar "calibration" of cloud parameters. Two examples of this are the calibration of radar-measured reflectivity factor, Z, with calculated precipitation rate, R, from aircraft-measured particle size distributions; and the calculation of vertical air motions in clouds from simultaneous doppler radar-measured particle fall velocity spectra (doppler spectra) and calculated doppler spectra from aircraft-measured size distributions. Still other applications involve problems related to engineering, such as establishing the cloud environment through a missile reentry corridor (Barnes, Nelson, and Metcalf, 1974), and establishing and documenting aircraft icing conditions to be used for aircraft certification.

Author

A. J. Heymsfield studied physics at the State University of New York, then specialized in meteorology at the University of Chicago, earning an M.S. in 1970 and a Ph.D. in 1973. Since then, as a research scientist for Meteorology Research, Inc., he has been involved in aircraft and doppler radar measurements and, most recently, in analysis of aircraft-doppler radar correlations.

Until recently, aircraft measurements of cloud particle spectra have relied on instruments which directly "capture" particles (see the article by Spyers-Duran in this issue); therefore a painstaking data-reduction process has been necessary. Foil, the continuous Formvar replicator, and oil-coated slides have been in use for years. Foil is limited by a minimum measurable diameter of about 200 μm, and is highly inaccurate for snow or ice particles; the replicator is limited by breakup of both large raindrops and ice crystals; and oil-coated slides are limited to the measurement of small particles. Now optical array devices have been developed (Knollenberg, 1970) to measure cloud and precipitation particle size spectra for particles larger than 20 μm by an "indirect" process, one which permits rapid reduction of data. It is the purpose of this article to describe Knollenberg's optical array devices, their reliability and operating conditions, and their accuracy in measuring particle size distributions.

Knollenberg optical array probes are now being manufactured by Particle Measuring Systems (PMS) of Boulder, Colorado. A photograph of one of the instruments, mounted on an aircraft, appears in Fig. 1. For a much more theoretical and detailed discussion, see Knollenberg's papers (1970, 1973) dealing with the subject.

Theory of Operation

A cloud particle in the free airstream which passes between the two arms of the optical array probe is illuminated by a 1.5 mW helium-neon (He-Ne) laser, and is imaged as a shadowgraph onto a linear photodiode array. The beam is vertical between sampling arms, and the focal plane is centered between the two sampling arms. The particle may shadow one or more of the photodiode elements. Each active element of the photodiode array contains its own amplifying and logic circuit called the photodiode circuit (PC). If the shadowing of an element causes at least a 50% reduction in light level to the PC (an electronic truncation of depth of field and minimum particle size), a flip-flop circuit is triggered. Two end photodiode elements are used in logic to reject particle shadows extending beyond the end of the active part of the photodiode array.

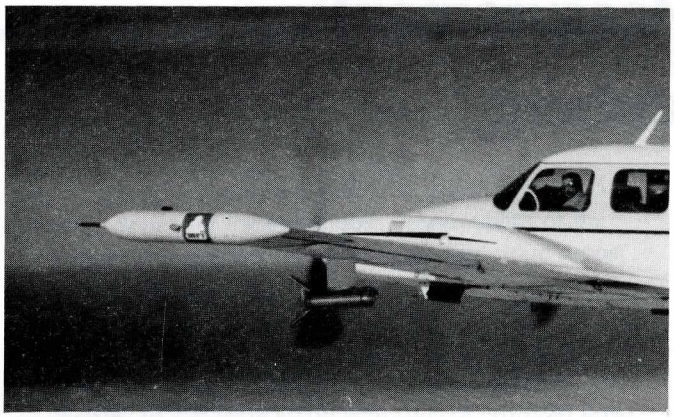

Fig. 1 Meteorology Research, Inc., Navajo aircraft with precipitation probe mounted on wing pod.

Information from each PC of the array is acquired in the instrument, and a particle is measured by accumulating the number of flip-flop circuits triggered. This information is acquired by a buffer memory system (BMS). The unit particle size results from a determination of the number of elements set, the size of each array element, and the magnification of the optical system. Each second of particle information collected by the BMS is dumped in proper form for recording on a nine-track incremental computer tape recorder.

Specifications

The systems now being built are equipped to size into 15 equal-sized channels. There are two basic size ranges currently in use: 20 - 300 μm for cloud probes, and generally 200 - 4,500 μm for precipitation. In the precipitation size range, some models size between 200 and 3,000 μm, and others between 300 and 4,500 μm, each divided into 15 equal-sized channels. Detailed specifications of these probes taken from PMS handbooks appear in Table 1.

The sampling volumes of these probes are of importance to users. Knollenberg (1970) used glass beads and opaque disks of various diameters placed on glass slides to determine their shadow size and light-intensity distribution in a parallel plane as a function of distance. Using coherent illumination, he found that the particle was in sharp focus at short distances and all of the decrease in light intensity was measured within a distance equal to the particle diameter. One would expect this effect from basic optics (Stone, 1963); for nonspherical solid particles, one would expect that at short distances all of the decrease in light intensity would be in an area equivalent to the cross-sectional area of the particle. At distances far from

Table 1
Specifications of PMS (Knollenberg) Optical Array Probes

	CLOUD PROBE	PRECIPITATION PROBE Range 1	Range 2
Power	115 V, 50-400 Hz or 60 Hz, 60 W Deice: 70 W/28 V or 100 W/115 V heaters supplied		
Dimensions	Cylinder: 71 cm long, 16 cm in diameter Optical Extensions (2): 25 cm long, 2.5 cm in diameter		
Separation between sampling arms	6.1 cm	6.1 cm	26.3 cm
Weight	12.6 kg		
Number of size channels	15	15	15
Size range	20-300 μm	200-3,000 μm	300-4,500 μm
Minimum detectable size	20 μm	200 μm	300 μm
Size resolution	20 μm	200 μm	300 μm
Maximum particle rate	100,000 Hz		
Coincidence errors	less than 0.1% with concentrations of $10^{-3}/cm^3$ (computed for 10 μm size)		
Maximum particle velocity	125 m/s		
Sampling volume (m^3/s) TAS is true airspeed, X is channel number	(for 20-160 μm particles) 2.0×10^{-8} (23-X)TAS (for 160-300 μm particles) 1.22×10^{-8} (23-X)TAS	1.22×10^{-5} (23-X)TAS	7.95×10^{-6} (23-X)TAS
Examples of sampling volume (m^3/s for 1 s of sampling at TAS of 100 m/s)			
Channel 1	(20 μm) 4.4×10^{-5}	(200 μm) 0.0269	(300 μm) 0.175
Channel 5	(100 μm) 9.0×10^{-4}	(1,000 μm) 0.022	(1,500 μm) 0.143
Channel 10	(200 μm) 1.59×10^{-3}	(2,000 μm) 0.016	(3,000 μm) 0.104
Channel 15	(300 μm) 9.76×10^{-4}	(3,000 μm) 0.010	(4,500 μm) 0.065

the particle diameter, the decrease in intensity was found to be distributed over a much greater distance than the particle diameter. For the measured shadow size to be within ±10% of the actual particle size (which corresponded to a 40% reduction in light intensity) the depth of field, *DF*, in nondimensional units was found to be $DF = \pm 3$. The detection threshold of a 50% reduction in light level before the circuits are triggered was derived from this criterion. The depth of field in dimensional units as a function of particle radius, r, and illumination wavelength, λ, is therefore $DF = \pm 3r^2/\lambda$. For a He-Ne laser with $\lambda = 0.6328$ μm, for a particle 0.2 mm in diameter $DF = 9.4$ cm, and for a particle 1.0 mm in diameter, $DF = 948$ cm. The depth of field in the sampling volume between arms of the probes is indicated nearly to scale in Fig. 2.

The sampling volume is the product of the depth of field, the effective array width (which is determined by the width of the array minus the diameter of the particle), and the true air speed. If the depth of field for a given particle diameter is wider than the separation between sampling arms, then the depth of field is equal to the arm width. This is true of the probes for diameters larger than 160 μm. The sampling volume for 1 s of sampling at a true air speed of 100 m/s is indicated in Table 1. For the 20 - 100 μm portion of the size range, the sampling volume is extremely small. A probe sizing in the range of 300 - 4,500 μm has a larger sampling volume than one sizing in the range of 200 - 3,000 μm because it has larger separation between arms. Diagrams showing the separation distance between arms of the three different probes are depicted nearly to scale, with the beam in its normal vertical orientation, in Fig. 2. By way of comparison with other instruments, the foil has a sampling volume of 0.14 m^3 at an aircraft speed of 100 m/s for 1 s, and under the same conditions the Formvar replicator has one 1.5×10^{-3} m^3.

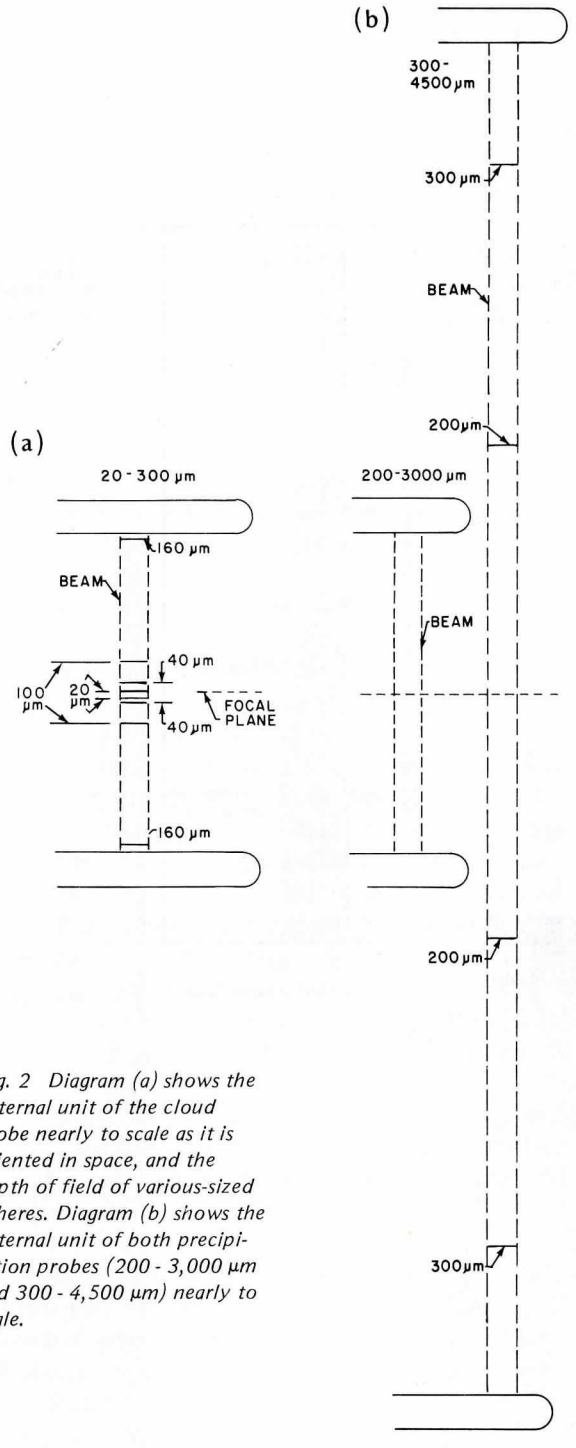

Fig. 2 Diagram (a) shows the external unit of the cloud probe nearly to scale as it is oriented in space, and the depth of field of various-sized spheres. Diagram (b) shows the external unit of both precipitation probes (200 - 3,000 μm and 300 - 4,500 μm) nearly to scale.

Mounting Locations

For unpressurized aircraft, the PMS probes can be mounted in the free airstream wherever most convenient. For pressurized aircraft, mounting is usually more difficult. PMS probes have been mounted on pressurized aircraft through an emergency exit door, above the aircraft, and below the wings in pods.

Operating Conditions and Reliability

Meteorology Research, Inc. (MRI), has instrumented and operated six PMS optical array probes on three aircraft during the past 18 months. The aircraft—a Navajo (shown in Fig. 1), a Cessna Citation jet, and a WB 57F jet—were operated throughout the United States; the latter two were also

Fig. 3 Average ice crystal spectra for a 2 min pass measured in a deep cyclonic storm system near Medford, Oregon. Solid lines represent measurements taken by the precipitation probe. The dashed line is the overlap of the cloud probe in the range from 110 to 300 μm. N_T is the total number concentration of particles >100 μm. The inset at upper left represents cloud probe measurements in the size range from 20 to 90 μm; these have been normalized to 200 μm size intervals for comparison with precipitation probe measurements.

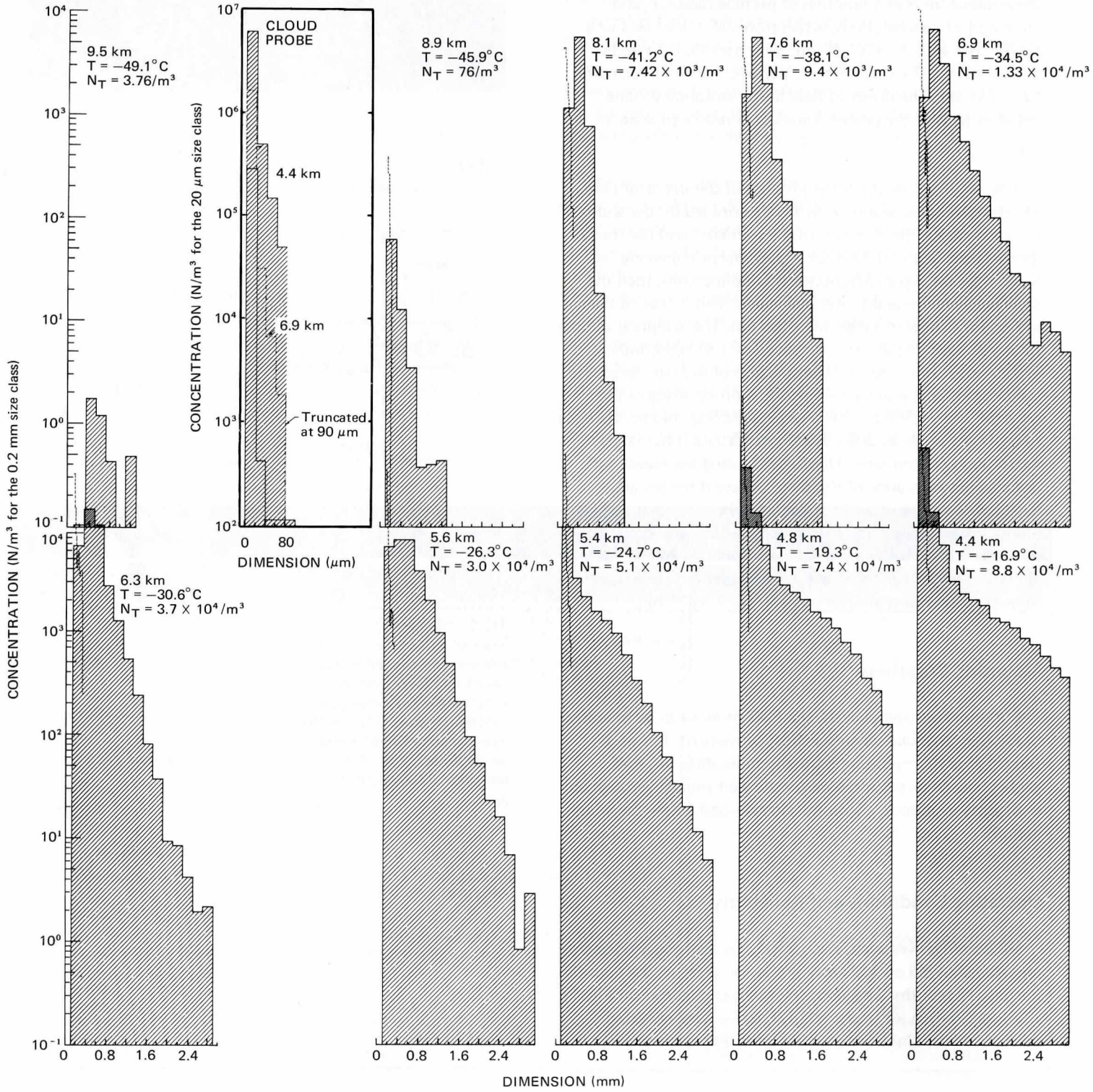

operated in the Marshall Islands in a wide variety of meteorological situations. A reasonably accurate estimate of the range of operating conditions and reliability of these PMS optical array probes can be obtained by looking through the records obtained for these six instruments.

• *Operating Conditions*. The probes were operated over a temperature range of +20 to −85°C. When the aircraft was ferried to its sampling location with the optical array probes not operating at temperatures lower than −60°C, the arrays cracked. However, when the instruments were in operation at these extremely low temperatures, we had no problems with the array cracking. In heavy rain or snow on level passes or ascents we had no difficulties with condensation or precipitation sedimenting on any of the lenses. In rapid descents of 305 - 610 m/min (1,000 - 2,000 ft/min), the heaters were apparently not sufficient to keep the lenses from fogging, with a consequent loss of data.

• *Reliability*. We have found that the probes are not maintenance-free and often require considerable effort to ensure accurate data acquisition. If careful maintenance is not performed, incorrect spectra may be obtained. The most common problem with the probes was misalignment of the laser beam. This caused "noise" on several channels, most of which could be filtered out through data processing. Other problems included failure of components on circuit boards, which generally caused loss of data from one channel (but which could be corrected for in the processing); occasionally, power supplies and lasers burned out, which caused complete loss of data. We had continual problems with one of the cloud probes which were never resolved.

Sample of Data Obtained with Probes

Figure 3 presents data obtained from the optical array probes by sampling with the Citation aircraft near Medford, Oregon, in a deep, intense storm system consisting of all ice crystals. Precipitation and cloud probe data are indicated in the figure. The distributions shift toward the right to larger sizes and the concentrations increase considerably from 9.5 to 4.4 km, indicating crystal growth downward. The distributions decrease exponentially with increasing size. The concentrations measured where the two probes overlap do not appear to have the same values. This could have been due to resolution problems caused by nonspherical particles in the first size class of the precipitation probe (which is discussed later in this article) and by the small sampling volume in the last few channels in the cloud probe.

Cloud probe data at selected levels in the size range from 20 to 90 μm appear in the upper left hand inset in Fig. 3. The distributions also decrease in concentration exponentially with increasing length.

Accuracy of Measurements

• *Calibration*. The three precipitation probes operated by MRI were not calibrated according to specifications at the time of delivery. A zoom lens, which is mounted inside the instrument to control the magnification of the particle image and therefore the calibration, had not been set correctly, but a relatively simple calibration brought the instruments to specifications. When the probes were delivered to us, they were calibrated for square photodiodes, but the photodiodes supplied were rectangular. The sizes of the first four classes had to be recalibrated. The original arrays have been replaced by arrays which have square photodiodes. From our experience it is desirable to calibrate the instrument before placing confidence in its accuracy.

• *Rain*. The probes were calibrated for spherical particles, and therefore, cloud droplets and raindrops should be sized and counted most accurately. Tracings of typically sized cloud droplets and raindrops, and their original dimensions, appear in Fig. 4, parts A and F, respectively.

The cloud probe seems to count and size cloud droplets very accurately. Let us then consider the precipitation probe accuracy in rain. An ideal way to estimate the accuracy of this probe is to sample rain clouds of different intensities, to measure size distributions, to calculate the radar reflectivity factor, Z (which is related to the sum of the sixth powers of the diameters), and simultaneously to measure the same parameter by radar in nearly the same volumes. This was done by Takeuchi, Peace, and Howard (1975), using the Navajo aircraft and the National Severe Storms Laboratory (NSSL) radar in Norman, Oklahoma. A comparison of the data appears in Fig. 5. Each point is a 1 km pass average, with 137 total points. The dashed line is the 45° line; all points should fall on this line. The solid line is fit in the form PMS = $A' + B'$ (radar), and fits very closely to a 45° line. The accuracy of the radar is ±3 dBZ, and therefore there is excellent agreement between the radar-measured and the probe-calculated radar reflectivity factor in rain.

There are some problems in evaluating large raindrop sizes, because they become more oblate as their diameters increase. When the water content and the radar reflectivity factor are calculated, the nonspherical nature of large drops must be considered.

• *Ice and Snow Particles*. Tracings of typical ice and snow particles as they would be seen when viewed from above or as they pass through the vertically oriented laser beam and their original dimensions appear in Fig. 4 (B-E and G-L). The depth-of-field calibrations of the probes were made for spherical particles. Let us consider the depth of field of typical cloud ice particles and any inaccuracies due to their nonspherical cross sections.

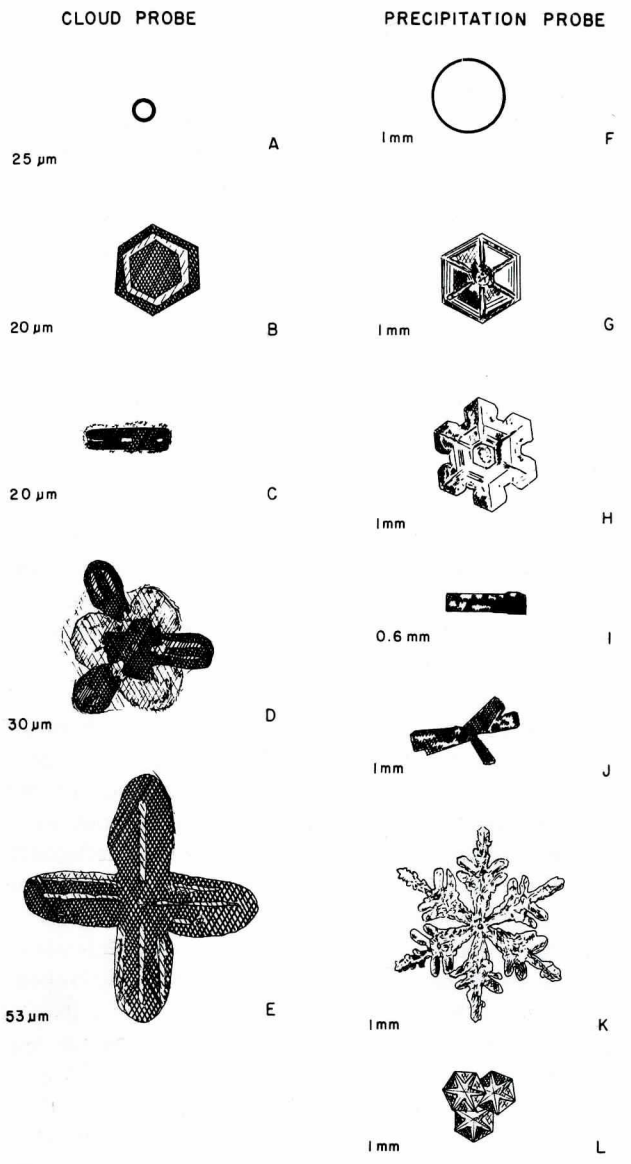

Fig. 4 Parts A - E are tracings of ice crystal microphotographs for sizes smaller than 100 μm as they would appear if viewed from above or focused on the optical array of the probe. Parts F - L are ice crystals larger than 300 μm as they would be focused on the optical array of the precipitation probe.

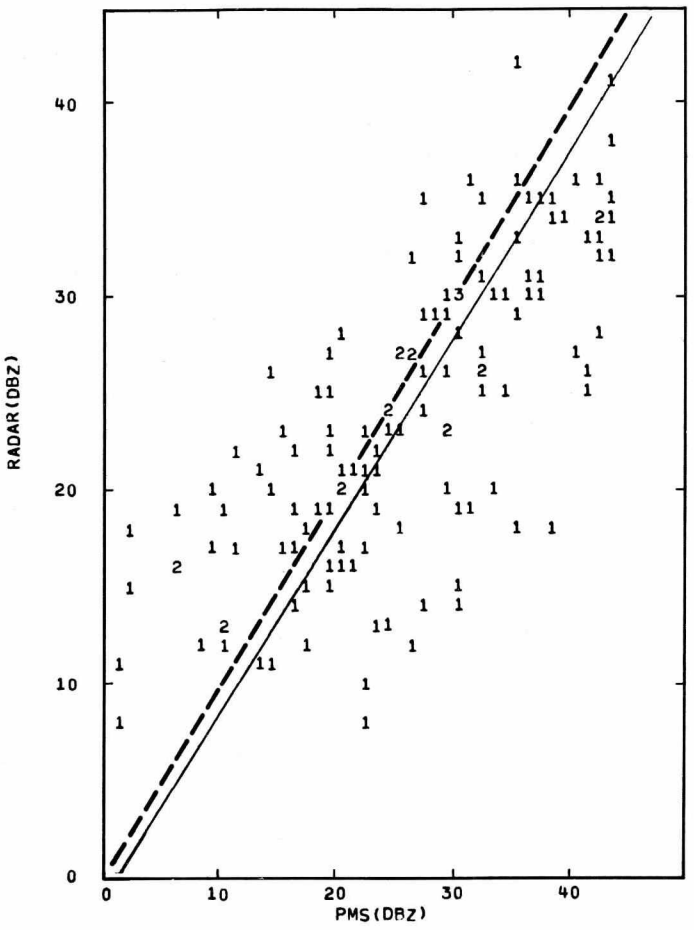

Fig. 5 Radar reflectivity factor measured by NSSL radar (dBZ = 10 log Z) and calculated from PMS precipitation probe in nearly the same region of the cloud. Each 1 point is a 1 km average, and a 2 point indicates two 1 km points on top of each other. The dashed line is at 45°, and the solid line is a least-squares curve through the data points.

Parts B-E of Fig. 4 show tracings of ice particles smaller than 100 μm in length, which one would expect to be sized by the cloud probe. The plate ice crystal (B) is generally oriented with its long axis horizontally aligned to the array, and its cross section is therefore read as nearly spherical. The depth of field will be the same as that for a sphere of equivalent diameter, it will be sized properly, and the calculated concentration will be correct. But consider the column in part C. Its long axis will be horizontal in the atmosphere, but its orientation will be random when it passes through the linear optical array. Therefore, it will be read at values ranging from its full length (20 μm) to its width (6 μm) when passing through the array. A 100 μm column with a similar length-to-width ratio may be sized anywhere from 100 μm to about 30 μm. The distributions can be "transformed" on the basis of this random columnar crystal orientation (Heymsfield and Knollenberg, 1972) if all the particles are columnar.

Other problems may be associated with measuring the columnar particle in part C. Assume that it passes through the array at its full length. Even if in perfect focus on the array, its cross-sectional area per channel will be $6 \times 20 = 120\ \mu m^2$, compared to the channel cross-sectional area of $20 \times 20 = 400\ \mu m^2$. Therefore, the reduction of light intensity will be 120/400 = 30%, not enough to trigger the flip-flop switch or to register a count as a particle. In addition, the

depth of field for this particle will be much smaller than that for a sphere of diameter equivalent to the length of the column, since the width of the column is only 6 μm. The depth of field will be more similar to that of a 6 μm sphere. The effective sampling volume for such particles is much less than the calibrations. Thus, columnar crystals will be undersized and undercounted.

Consider the bullet rosettes (D and E). The rosette in part D has a cross-sectional area equal to that of a sphere and, therefore, its measured size and concentration will be correct. There is no problem with underestimating the length of the bullet rosette in part E due to its orientation when passing through the array, since it is nearly spherical. However, it can present problems because of its nonspherical cross-sectional area and its depth of field. Each bullet has a width of about 12 μm. Therefore, a photodiode which has an equivalent cross section of 400 μm^2 will see a reduction in light of $12 \times 20 = 240\ \mu m^2$, or 60%. The rosette will probably be sized correctly if it is within the depth of field. However, the depth of field due to its 12 μm width will be nearly equivalent to that of a sphere 12 μm in diameter, and concentrations of such particles will be underestimated.

Parts G-L of Fig. 4 show tracings of ice particles larger than 300 μm in length which would be sized by the precipitation probe and which would cause problems similar to the crystals in parts B-E. The 1 mm plate in part G would be sized properly. The 1 mm sector plate in part H would probably be sized correctly, even though the extensions to its arms are quite narrow. The column in part I is 0.6 mm in length and 0.15 mm in width. The distributions obtained with such particles would have to be "transformed" for orientation. In addition, the 150 μm width of the particle will not be in focus throughout the distance between sampling arms of the 300 - 4,500 μm probe, but may be in focus through only 20% of the distance, leading to considerable undercounting of such particles and underestimation of their concentration. This problem was encountered when measuring cirrus ice crystals with the 300 - 4,500 μm probe, but not with the 200 - 3,000 μm probe. Consider columns less than 400 μm in length with a 4:1 length-to-width ratio. Even if the crystals are in focus throughout the distance between arms, they will not be sized since less than a 50% reduction in light level will result when the particles pass the photodiodes. Thus, small columns will be undersized and undercounted. The 1 mm bullet rosette in part J will present few sizing problems since it is a three-dimensional particle and the width of the arms will be sufficient to reduce the light level to less than 50%. There may be some depth-of-field problems with the 300 - 4,500 μm probe. The 1 mm dendrite in part K will present the most difficult sizing problems. Its arms are only about 80 μm in width, and they will cause only a 40% reduction in light to the 200 - 3,000 μm probe photodiodes and a 26% reduction in light to the 300 - 4,500 μm probe photodiodes. Therefore, it will not be counted by either probe. In addition, the arms of this particle in the beam will have a depth of field vastly reduced in comparison to a sphere 1 mm in diameter. The aggregate in part L will present few problems in sizing, since it has a nearly spherical cross section. In summary, plates, plates with extensions, bullet rosettes, and aggregates will be sized and concentrations counted nearly correctly; columns can be generally transformed but will be underestimated in concentration; and dendrites will be sized poorly. The 200 - 3,000 μm probe has much higher resolution for small ice crystals than the 300 - 4,500 μm probe.

- *Sampling Volume Analysis*. Because of the small sampling volume of the optical array probes, some particle distributions may imply considerable uncertainty in the predicted water content. Consider particles of 3,000 μm in maximum dimension; in an ice cloud such particles may be expected in concentrations of $100/m^3$ and in a rain cloud in concentrations of $10/m^3$. The probe will most probably sample (sampling volume channel 15, precipitation probe, range 1) $100/m^3 \times 0.01\ m^3 = 10$ particles per second in the ice cloud, and one particle per second in the water cloud. We might more generally expect to sample between eight and 12 particles in the ice cloud per second, which will not affect the water content calculation significantly, while in the water cloud we may expect to sample zero or two particles per second, which will drastically affect the water content calculation. Therefore, ice cloud size distributions that usually contain a large number of sampled particles per second in each size class yield a large sample population and confidence in the sample size in calculating water content, while water droplet distributions contain only a small sample population in each size class and imply uncertainty in the calculated water content. Let us estimate the uncertainty in the water content calculation due to the sample size from the distributions in Fig. 3 by using the method discussed by Nathan and Bennet (1966). Following their approach, using a Poisson-type size distribution, 95% of all samples will be within 2σ of the population's mean water content. Assuming bullet rosette ice crystals, the 2σ bounds for the distributions are as follows:

  - 4.4 km ± 12.5% of the calculated water content
  - 6.3 km ± 10.4%
  - 8.1 km ± 8.4%
  - 8.9 km > –100% to +150%

All but the 8.9 km distribution had a large sample number, which gives considerable confidence to the sample size in predicting water content.

- *Cutoff at Maximum Sampling Length*. Figure 3 shows particle spectra taken by the precipitation probe

(200 - 3,000 μm), which, at low altitudes, have large numbers of particles in the largest size class. Since, in general, the ice crystal mass will go as the second power and the radar reflectivity factor as the fourth power of length, the particles not counted are very important to the cloud microphysics, water content, and radar reflectivity factor. The 300 - 4,500 μm probe improves the maximum sampling length, but suffers from resolution problems at the low end of the spectrum. It would be advantageous to have a probe sizing to 2,000 μm in 200 μm steps, and then reduce the resolution for particles larger than 2,000 μm to 400 μm steps. Thus, the probe would size particles from 200 to 4,000 μm, with high resolution, possibly with the same electronics.

- *Radar Interference*. We attempted correlating the radar reflectivity factor calculated from the optical array probe spectra with that measured by a radar in nearly the same sampling volume. The WB 57F was flying in cloud, a tracking radar beam was fixed on the aircraft, and reflectivity was measured just ahead of the aircraft. There was complete contamination of the particle spectra measurements due to radar interference. By providing additional shielding of the probes and positioning the radar beam about 150 m ahead of the aircraft, the problem was eliminated. Such positioning of the beam resulted in only a 2 s time lag between radar and aircraft measurements, ensuring sampling of the same cloud microstructure.

Conclusions

The Knollenberg optical array probes provide a method by which large numbers of cloud particle spectra can be reduced rapidly and measurements can be made quite accurately. However, the probes require considerable care and attention to ensure accurate data acquisition. Accurate particle spectra measurements are obtained for raindrops; less accurate results are obtained in ice clouds. Particle spectra in clouds containing single plates, aggregates of crystals, and bullet rosettes can be measured accurately; in clouds containing columnar ice crystals, the number concentrations and sizes are underestimated and in clouds with dendritic crystals, the particles are undersized. The precipitation probe in the size range of 200 - 3,000 μm has a much higher resolution in clouds with small ice crystals than the 300 - 4,500 μm probe; however, the 300 - 4,500 μm probe has the advantage of a larger sizing capability, making it more useful in clouds containing large ice crystals.

Acknowledgments. The author wishes to thank L. Jahnsen, R. Davey, and D. Takeuchi for their thorough field testing and operation of these instruments; J. Foreman for drafting the figures; and H. Wilkinson for typing the manuscript.

References

Barnes, A. A., L. D. Nelson, and J. Metcalf, 1974: Weather documentation at Kwajalein Missile Range. In *Proc. Conference on Aerospace and Aeronautical Meteorology*, El Paso, Tex.; American Meteorological Society, Boston, Mass., 66 - 69.

Heymsfield, A. J., and R. G. Knollenberg, 1972: Properties of cirrus generating cells. *J. Atmos. Sci. 9*, 1358 - 1366.

Knollenberg, R. G., 1970: The optical array: An alternative to scattering or extinction for airborne particle size determination. *J. Appl. Met. 9 (1)*, 86 - 103.

———, 1973: Cirrus-contrail cloud spectra studies with the Sabreliner. *Atmos. Technol. 1*, 52 - 55.

Nathan, A. M., and L. Bennet, 1966: *Precipitation Water Content Meter*. Final Report No. 1,004, New York University, New York, 42 pp.

Stone, J. M., 1963: *Radiation and Optics*. McGraw-Hill Book Company, New York, 544 pp.

Takeuchi, D., R. Peace, and S. Howard, 1975: *Final Report to the Bureau of Reclamation*. Report No. MRI 75 FR-1294, Meteorology Research, Inc., Altadena, Calif., 407 pp.

For Further Reading

Wilmot, R. A., C. Cisneros, and F. Guiberson, 1974: High cloud measurements applicable to ballistic missile systems testing. In *Proc. Conference on Aerospace and Aeronautical Meteorology*, El Paso, Tex.; American Meteorological Society, Boston, Mass., 194 - 199.

For Further Information about Equipment

Meteorology Research, Inc.
464 West Woodbury Road
Altadena, California 91001

Particle Measuring Systems, Inc.
1855 57th Court
Boulder, Colorado 80301

NUMBER 8 – SPRING 1976

Optical Techniques for Counting Ice Particles in Mixed-Phase Clouds

Francis M. Turner, Lawrence F. Radke, and Peter V. Hobbs, University of Washington

One of the first attempts to distinguish ice particles from water drops in the atmosphere was made more than 30 years ago in the Thunderstorm Project (Byers and Braham, 1949), during which it was noted that ice particles and water drops produced different sounds when they impacted on the Plexiglas canopy of an aircraft. This simple method has the important advantage of providing real-time information, although its usefulness is probably confined to particles that have already reached precipitation sizes. Subsequently, attention was directed towards the development and use of various particle collection and impaction devices (e.g., Formvar replication techniques and metal foil impactors), which are discussed in the article by Spyers-Duran in this issue.

Authors

Francis M. Turner was affiliated with the University of Washington from 1968 to 1975, receiving B.S., M.S., and Ph.D. degrees in electrical engineering. He served as a teaching assistant and research associate there, and designed several instruments for studying air pollution and cloud microstructure. During the past few years, his interest has centered on the development of the University of Washington's optical ice particle counter.

Lawrence F. Radke, a research associate professor at the University of Washington since 1972, received all his academic training there. He earned an M.S. in 1966 and a Ph.D. in 1968, both in atmospheric sciences. He is presently engaged in airborne studies of cyclonic storm microstructure, industrial and natural sources of trace gases and particles, and inadvertent weather modification.

Peter V. Hobbs, founder and Director of the Cloud Physics Research Group at the University of Washington and a professor of atmospheric sciences since 1970, joined the university in 1963, after earning B.S. and Ph.D. degrees in physics from the Imperial College of Science, University of London. He has served as an associate editor of several publications and as a NATO visiting lecturer in Europe, has published a book on ice physics, and is currently collaborating on an introductory textbook in atmospheric science.

While these devices can provide valuable information on the types of particles in the air, determining the concentrations of ice particles is difficult: some of the ice particles fragment on impact when the Formvar replicator is used, and particles 250 μm in diameter are the smallest that can be measured when foil impactors are used. Moreover, these devices do not provide real-time data on ice particle concentrations and require much tedious postflight analysis to deduce concentrations.

In the past few years, two groups (the Cloud Physics Group at the University of Washington and Mee Industries, Inc., Rosemead, California) have worked independently on the development of optical devices for the detection and counting of ice particles in clouds in real time from aircraft. In this article we describe the most recent versions of these two devices and the methods that have been used to calibrate them, and present a few examples of results obtained in the field.

Description of the Instruments

Figure 1 shows a schematic representation of the latest version of the University of Washington's automatic ice particle counter (UW-IPC). This instrument uses a linearly polarized helium-neon laser to illuminate any particle that passes through the sample port. The primary purpose of the series of collimating disks is to keep outside ambient light from entering the detection system. A polarizing filter is placed at the end of the detection system and is set for maximum extinction of the incident, linearly polarized light. The main beam of the laser is absorbed in the light trap so that direct light is not detected by the photomultiplier tube. The forward-scattered light that enters the detection system is limited to forward-scattering angles of approximately 0.5 - 3.5°. An aperture on the photomultiplier-tube side of the polarizing filter limits the azimuthal angles of the forward-scattered light to ±5° on each side of the main planes of scattering. The light then passes through an interference filter (0.01 μm band-pass at 0.6328 μm wavelength) and is detected by the photomultiplier tube.

Figure 2 shows a schematic diagram of the Mee Industries Model 120 ice crystal counter (Mee-IPC). A projection lamp is used as a light source. The light passes through an optical

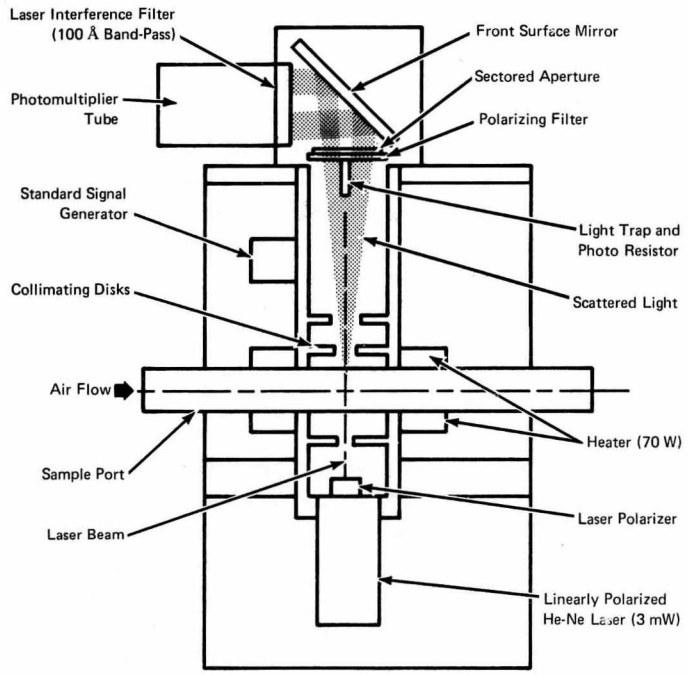

Fig. 1 Schematic representation of the University of Washington's automatic optical ice particle counter.

system so that linearly polarized infrared light is incident on particles passing through the sample pipe. The light sensor (a solid-state device) detects the infrared light that is scattered at an angle of 90° (actually a cone of light around a scattering angle of 90°) after the light passes through an optical system containing a polarizing filter set for maximum extinction.

It can be seen from the description of the two instruments that the UW-IPC detects forward-scattered light while the Mee-IPC detects light scattered at an angle of 90°. As we will see below, this difference becomes important in discussing the mechanisms for the detection of ice particles in the two systems.

Mechanisms for Ice Detection

There are three possible mechanisms for the detection of ice particles in the two devices described above (see Turner and Radke, 1973, for a more detailed discussion):

- The rotation of the plane of polarization of the light beam, produced by the birefringent property of ice, as it passes through the ice particles
- The detection of specularly reflected light from the external faces of ice crystals
- The detection of light scattered at a preferred angle by the ice particles.

Owing to the birefringent (or double refracting) property of ice, linearly polarized light that is transmitted through ice will, generally, be rotated in such a way that although the light

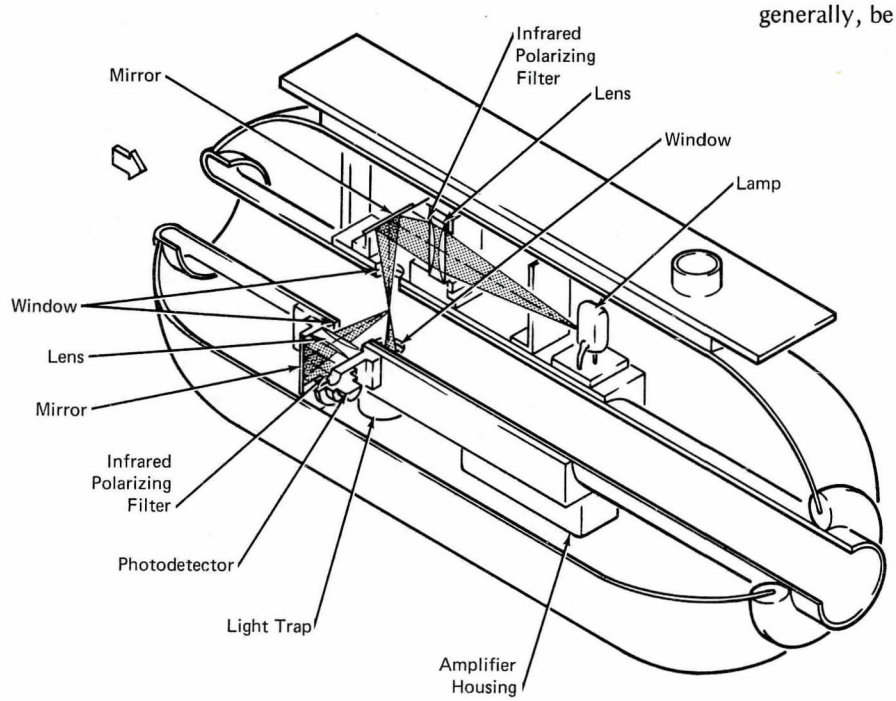

Fig. 2 Schematic diagram of the Mee Industries automatic optical ice particle counter. The pod is 45.7 cm (18 in.) long and 17.8 cm (7 in.) in diameter. The cylindrical opening in its center is 5.1 cm (2 in.) in diameter.

which leaves the crystal will still be linearly polarized, its plane of polarization will differ from that of the incident light. For example, an ice crystal 226 μm thick that is optimally oriented will rotate incident, linearly polarized light through an angle of 90°. The amount of rotation depends on both the thickness and orientation of the ice crystal.

It is clear from the geometry of the UW-IPC that the birefringent property provides a direct, first-order detection mechanism for ice particles. However, for this mechanism to be effective in the Mee-IPC, the incident light would have to be transmitted through the ice, reflected at an internal surface, and transmitted back through the ice particle. Moreover, in order for a signal to be detected, this light would have to exit at a suitable angle to enter the light sensor.

In the case of the Mee-IPC, this mechanism is almost certainly secondary in importance to specular reflections from the external faces of ice crystals. The latter mechanism suffers from the fact that, since the reflection of light from the specular face of an ice particle is a relatively discrete event, the detection of a signal will be strongly dependent on the orientation of the ice particle. Orientation is also important in the case of reflections from internal crystal faces; however, the transmission of light through the crystal will probably cause a greater divergence of the light than external reflections will. The importance of orientation will, of course, rapidly decrease with increasing size and complexity of the crystals. The detection of ice particles by reflections is not thought to be important in the UW-IPC, although it is possible for glancing reflections to occur.

The third possible mechanism for the detection of ice particles is the existence of a preferred scattering angle. Huffman and Thursby (1969) and Huffman (1970) have compared the light scattered from water drops and ice crystals. These measurements show that the difference in relative scattering function (in terms of the amount of light scattered from ice crystals) is largest at a scattering angle of about 100°. This difference is probably due to the external reflection mechanism discussed above.

The degree to which water drops are not counted when they pass through the sample ports of both instruments under discussion is of prime interest. The basic reason why water drops give signals of a much smaller magnitude than ice particles of the same size in the Mee-IPC is understandable in terms of the external reflection mechanism, since the spherical surfaces of water drops will produce much smaller signals than the specular faces of similarly sized ice particles. The reason for the rejection of water drops in the UW-IPC is more subtle. In general, when incident, linearly polarized light is scattered from a spherical water drop, it is elliptically polarized. However, the light scattered in the forward direction (0° scattered light only) and in the two principal planes is not depolarized. Thus, rejection of water drops is achieved by confining the detection to angles close to the direction of forward scattering. Further improvement is achieved by means of the sectored aperture (Fig. 1) which limits the light entering the sensor to azimuthal angles close to the principal planes of scattering. In common with the Mee-IPC, the UW-IPC will detect water drops only if they are large enough to differ appreciably from spheres.

Calibration of the Instruments

A number of calibration tests have been performed on the UW-IPC. First, wind tunnel tests have shown that there is less than 1% difference between the velocity of air through the sample port and the free-stream air velocity. In addition, extensive laboratory tests have been carried out to determine the sensitivity of the instrument to water drops. These tests have shown that water drops with diameters less than 600 μm are not detected by the instrument. Above 600 μm an increasing percentage of water drops is counted. Flight tests in fairly heavy rain have shown that while some raindrops are detected, generally the counting rate is less than 0.1 drops per liter, which is the minimum calibrated counting rate (the UW-IPC is calibrated to cover a counting rate of 0.1 to 1,000 particles per liter and has automatic true airspeed correction). The sensitivity of the instrument was maintained at a constant level for the tests described above as well as for the ice-crystal calibration tests and field observations described below.

Extensive tests of the UW-IPC have been carried out in a cold room. These tests were designed to determine the percentage of ice crystals of various types and sizes that can be detected by the counter. Clouds were created by spraying small water droplets into the cold room and then seeding the clouds with dry ice. Ice crystals grew rapidly in the seeded clouds and fell out onto the floor of the cold room. Hand-held slide replicas were used to determine the concentration, types, and sizes of the ice crystals. The ice crystals were drawn through the UW-IPC with an axial blower, but otherwise the counter was operated normally.

Figure 3 shows the results of many cold-room tests with hexagonal plate crystals. Shown in this figure is the percentage of crystals detected versus their maximum dimensions. It can be seen that when the maximum dimension of the crystal is 100 μm, about 35% of the crystals are detected. If the plot is extrapolated linearly to the point where 100% of the crystals are detected, a maximum dimension of 250 μm is obtained (it was not possible to achieve this size in the cold room because the crystals fell out before they attained it). The results of similar tests with solid hexagonal columnar ice crystals are shown in Fig. 4; the results were similar to those for hexagonal plates.

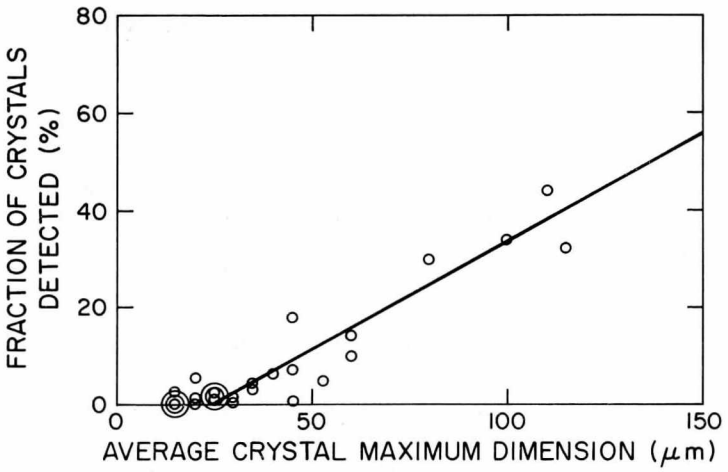

Fig. 3 Percentage of hexagonal plate ice crystals detected by the UW-IPC.

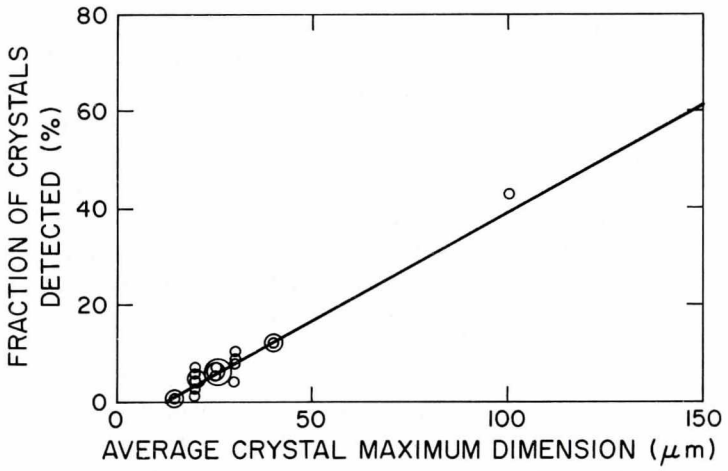

Fig. 4 Percentage of columnar ice crystals detected by the UW-IPC.

Other cold-room tests showed that the UW-IPC detects some frozen drops down to about 15 μm in diameter. Rimed ice crystals are also detected. The counter responded in the same way to lightly-to-moderately rimed ice crystals in the cold room as it did to unrimed crystals.

Laboratory calibration of the Mee-IPC has been reported by Sheets and Odencrantz (1974). The procedures followed were similar to those described above, except that the critical question of counting efficiency was not addressed. This problem is made more difficult by the fact that the counter has a front panel sensitivity adjustment. The results of Sheets and Odencrantz's calibration efforts can be summarized as follows:

- Some plates and short columns with maximum dimensions of 50 - 100 μm were detected.

- The signals generated in the counter by rimed or otherwise distorted crystals were substantially smaller than those produced by regular crystals. (This is to be expected in view of the assumed mode of detection by specular and internal reflections.)

- The use of cross-polarizing filters resulted in slight improvement in the ability of the counter to discriminate between ice and water.

- Water droplets down to 100 μm in diameter were detected; however, only drops larger than 1 mm in diameter produced signals comparable to those produced by 50 - 100 μm ice crystals.

In addition, flight tests of the Mee-IPC have shown that it can be operated to exclude most water drops occurring in light rain (Sax and Willis, 1974). However, heavy rain frequently produced counting rates equivalent to a few ice particles per liter. (The Mee-IPC does not provide a direct readout of ice particle concentration, but counts for fixed time periods or continuously. The instrument operator must convert the counts obtained in this way to actual concentrations.) The flight tests also showed that the smallest ice particle detected is about 250 μm in maximum dimension.

Some Field Observations

The UW-IPC has been flown on many data-gathering flights during the past few years, including studies of cirrus clouds, weather modification experiments, and investigations of cyclonic storms in Washington State.

To illustrate the types of results obtained, we present some data obtained on 2 January 1975, during a flight in a cyclonic storm. The measurements were made in largely stratiform clouds containing some imbedded cumulus. Liquid water contents were measured with a cloud water meter from Johnson-Williams Products, Mountain View, California, and cloud droplet concentrations (from 3 to 45 μm in diameter) with a modified axially scattering spectrometer probe (Model ASSP - 100) manufactured by Particle Measuring Systems, Inc., Boulder, Colorado.

Figure 5 shows three series of measurements obtained on 2 January 1975. Figure 5(a) shows measurements obtained near Seattle at an altitude of 2.1 km, where the temperature was −3°C. No ice particles were detected in the cloud; the liquid water content remained at about 0.1 - 0.2 g/m^3; and the cloud droplet concentration remained fairly constant with a

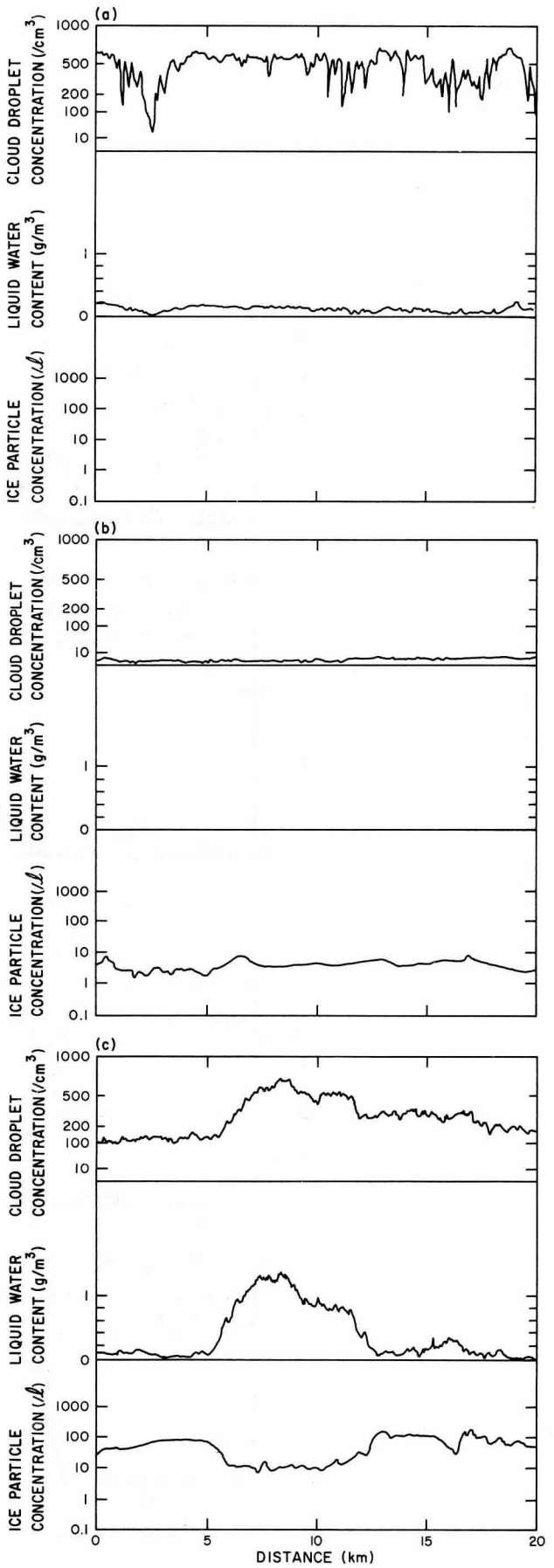

Fig. 5 Measurements of ice particle concentration (UW-IPC), cloud water content (Johnson-Williams meter), and cloud droplet concentration (Particle Measuring Systems ASSP - 100) obtained on 2 January 1975 near Seattle (a), near Olympia (b), and over Hoquiam, Washington (c).

maximum value of about 500 drops per cubic centimeter. Figure 5(b) shows measurements obtained near Olympia, Washington, at an altitude of 1.8 km where the temperature was about −4°C. There was no measurable liquid water and the droplet concentrations were very low. However, the ice particle concentrations reached peak values of ten particles per liter. Visual observations of particles impacting on a black rod showed that millimeter-sized ice particles were present. Figure 5(c) shows the measurements obtained at an altitude of 2.1 km over Hoquiam, Washington. The temperature was initially −4°C but decreased to −6°C during the traverse. The liquid water content rose to a maximum value of 1.3 g/m^3 during the penetration of a convective cell, and the droplet concentration rose to about 700 drops per cubic centimeter. The concentration of ice particles showed the opposite trend, having a maximum value of 100 particles per liter in the layer clouds and decreasing to a minimum value of about ten particles per liter in the convective cell.

The Mee-IPC has been used most extensively by the National Hurricane and Experimental Meteorology Laboratory of the National Oceanic and Atmospheric Administration. Shown in Fig. 6 are data from four sequential penetrations of a convective "bubble" rising out of a mass of tropical cumulus. The heights of penetration of the aircraft were changed successively in an attempt to remain in the rising bubble. For the first penetration these results also show that when the concentration of ice particles increases, the liquid water content decreases, and vice versa. However, in the second penetration (4 min later) these two quantities were varying together in the same manner, and by the third penetration the cloud was essentially glaciated.

Conclusions

The two automatic ice particle counters described in this article have the potential to provide, for the first time, accurate and real-time measurements of the concentrations of ice particles in clouds. The instruments are already semi-operational. However, a few cautionary remarks should be made. First, neither instrument is capable of absolute discrimination between ice and water over the entire range of sizes at which these particles occur in natural clouds. As the sensitivity of the instruments is increased in order to detect smaller ice particles, the minimum size of detected water drops

Fig. 6 Microphysical data obtained within a growing tropical cumulus bubble at 4.6 km (a), 5.2 km (b), and 5.8 km (c and d). Shown are the cloud liquid water content (Johnson-Williams meter), ice particle concentration (Mee-IPC), hydrometeor water mass, and concentration of drops >0.93 mm in diameter (foil impactor). (Courtesy of R. Sax; for a more complete discussion of these measurements, see Sax and Willis, 1974.)

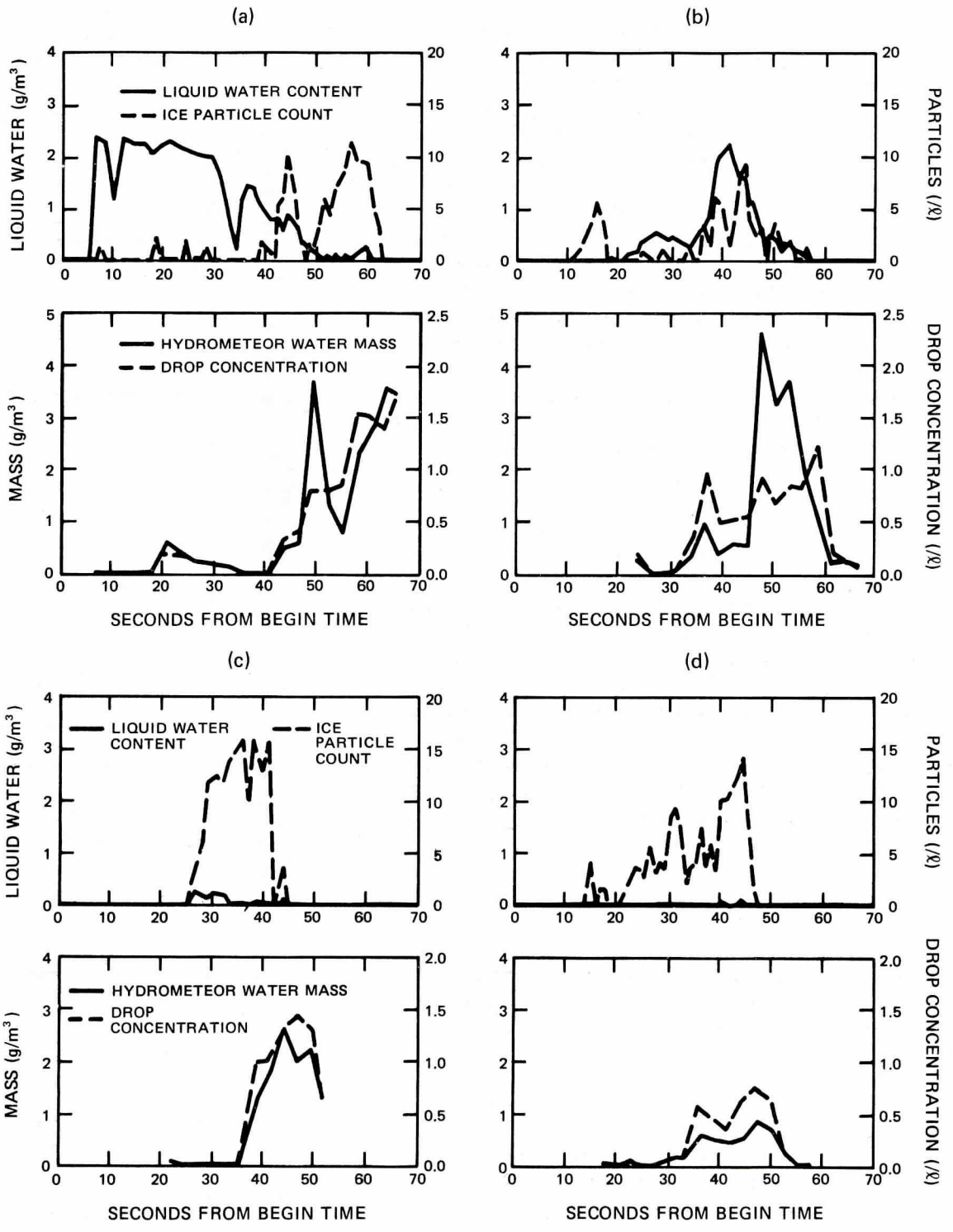

is also lowered. It is our feeling that the latest design of the UW-IPC, described in this article, is approaching the optimum in this respect. It can detect some ice particles down to about 15 μm in maximum dimension while rejecting all water drops with diameters smaller than 600 μm. Therefore, unless the cloud contains rather large precipitation-sized water drops (which can be readily determined by other means), only ice particles will be counted. Second, it should be noted that the counters do not detect all of the particles down to the minimum threshold size. Instead, as the size of the ice particles decreases the percentage that is counted decreases (e.g., the UW-IPC can detect some ice particles down to about 15 μm in maximum dimension, but the particles have to be 250 μm before they are all counted). Third, further careful calibrations of both instruments are necessary in order to establish the effects of crystal habits, riming, and aggregation on their counting efficiencies over a wide range of ice particle sizes. Finally, we recommend that, in order to ensure the compatibility of future data collected with these instruments, they be calibrated together both in the laboratory and in the field. Agreement should also be reached as to the levels of sensitivity at which they should be operated so that the minimum size of ice particles that can be detected, the counting efficiencies, and the maximum size of water drops that are rejected are known.

The preparation of this paper was supported by the Atmospheric Sciences Section of the National Science Foundation (Grant GA 40806) and Contract F19628 - 74 - C - 0066 from the Air Force Systems Command.

References

Byers, H. R., and R. R. Braham Jr., 1949: *The Thunderstorm*. U.S. Weather Bureau, Washington, D.C., 287 pp.

Huffman, P., 1970: Polarization of light scattered by ice crystals. *J. Atmos. Sci. 27*, 1207 - 1208.

———, and W. R. Thursby Jr., 1969: Light scattering by ice crystals. *J. Atmos. Sci. 26*, 1073 - 1077.

Sax, R. I., and P. T. Willis, 1974: Natural glaciation characteristics of an ensemble of Florida cumulus clouds. In Preprint Vol., Conference on Cloud Physics, held 21 - 25 October at Tucson, Ariz.; American Meteorological Society, Boston, Mass., 152 - 157.

Sheets, R. C., and F. K. Odencrantz, 1974: Response characteristics of two automatic ice particle counters. *J. Appl. Met. 13*, 148 - 155.

Turner, F. M., and L. F. Radke, 1973: The design and evaluation of an airborne optical ice particle counter. *J. Appl. Met. 12*, 1309 - 1318.

For Further Information about Equipment

Mee Ice Crystal Counter

Mee Industries, Inc.
4939 North Earle Street
Rosemead, California 91770

Cloud Water Meter

Johnson-Williams Products
Bacharach Instrument Co.
(Division of AMBAC Industries, Inc.)
2300 Leghorn Street
Mountain View, California 94040

Axially Scattering Spectrometer Probe

Particle Measuring Systems, Inc.
1855 57th Court
Boulder, Colorado 80301

Imaging Devices

Theodore W. Cannon

In order to understand clouds, the scientist makes measurements from aircraft of cloud air temperature, water vapor, air motion, electric field, and particles. Particle attributes measured include chemical composition, size, shape, concentration (number per unit volume), physical state (solid or liquid), and liquid or ice water content or both. This article concerns instruments unique in their ability to record particle shape, although size, concentration, and liquid water content may be measured as well. Such instruments are normally restricted to measurements of those cloud particles produced by condensation or sublimation of atmospheric water vapor; aerosol particles are usually too small to be detected by them.

The problem of obtaining particle shape is a difficult one. The particles generally range in size over four orders of magnitude, from tiny ice crystals and cloud droplets a few micrometers in diameter to ice particles several centimeters in diameter. Concentrations vary from a few per cubic meter for the larger precipitation particles to several thousand per cubic centimeter for cloud droplets in continental clouds—a range of nine orders of magnitude. An instrument designed to record the smaller particles will, as a rule, not sample a sufficient volume to record the larger, rarer particles in any statistically significant number. Consequently it is necessary to have more than one instrument to obtain shapes for all particle sizes. Measurements are made from aircraft flying at true airspeeds from about 40 m/s for research sailplanes to 200 m/s or higher for jet aircraft, so that the sampling time for each particle is very short. Conditions of high humidity and low temperatures can produce icing; electronic and mechanical problems compound the difficulties of obtaining these data.

Author

Theodore W. Cannon has been involved in cloud physics research at NCAR since 1966, specializing in laboratory and field measurements of atmospheric cloud particles and kinematic cloud modeling. He received a B.S. in electrical engineering from Oregon State University in 1956; after five years with General Electric Company, he returned to Oregon State to earn a Ph.D. in nuclear physics. In 1975, he was recipient of a service award from the Society of Photographic Scientists and Engineers.

A straightforward technique, used for a number of years, is to allow the particles to make an impression in thin foils or to be replicated in plastic (see the article by Spyers-Duran, this issue), but the particles are subject to splashing, shattering, freezing, and sometimes melting as they approach and encounter the foil or plastic surfaces at aircraft speeds. The trajectories of the particles are influenced by the presence of the aircraft and the collecting instrument in the airstream so that the collection efficiency (a function of particle size and airspeed) must be known in order to calculate concentrations of the particles in the cloud.

Imaging devices obtain information on particles in their natural state, as far as possible, with a minimum of disturbance to the sample by the aircraft and by the instrument. Thus the problems of the collecting devices can largely be circumvented.

The Need for Information on Particle Shapes

Imaging devices are very useful for providing information leading to an understanding of important physical processes in clouds. Some of the questions answered by using these devices are as follows:

- Are the individual cloud particles composed of water, ice, or a mixture of the two (as in wet or slushy ice)? This information, together with data on cloud temperature and air motions, indicates whether the particles are growing by droplet coalescence, an all-ice process, or both.

- In the case of ice particles, what specific growth processes are involved, e.g., accretion of supercooled droplets onto embryonic ice particles with subsequent freezing, sticking together of ice particles to form aggregates, freezing of supercooled raindrops to form ice spheres, etc.? The physical appearance of the ice particles provides understanding of these growth processes.

- Are ice crystals in the shape of needles, columns, dendritic plates, or other forms? The shapes of ice crystals give insight into the temperature and humidity conditions under which they grow from the vapor phase.

- What does the radar reflectivity from a cloud mean in terms of sizes, concentrations, and types of particles present? Radar reflectivity depends on the physical state (ice or water) and shape of individual particles and, if they are asymmetrical, on their aspect relative to the direction of propagation of the

radar pulses. Studies of hydrometeors using airborne imaging devices correlated with one or more radars observing the same region of cloud or precipitation as the aircraft will lead to further understanding of storms.

- Are automatic particle-counting and sizing instruments giving an accurate representation of the cloud being observed? By giving the scientist a "look" at the cloud, imaging devices serve as a check on the integrity of data coming from other counting and sizing instruments. Data from electronic and electro-optical devices may be influenced by electronic noise, icing, or collection efficiency problems that might otherwise go undetected if the data look reasonable. Automatic sizing instruments give the size of the projected image; the measured size depends on orientation of the particles. This orientation can often be determined with imaging instruments. The accuracy and interpretation of impressions or replicas can also be checked by comparison with images obtained using imaging devices.

We will describe three imaging devices currently in use—— the two-dimensional optical array spectrometer probe of Particle Measuring Systems (PMS), Boulder, Colorado; the NCAR particle camera; and the airborne holography system of Science Applications, Inc., El Segundo, California.

The Optical Array Spectrometer Probe

The PMS two-dimensional array spectrometer probe, developed under the direction of Robert Knollenberg (of PMS), is a unique variation of the optical array particle-sizing probe described in the article by A. Heymsfield in this issue. In the sizing probe, the particles pass through a parallel light beam from a continuously radiating laser and a shadow is cast on a linear array of light sensors (photodiodes) located in the beam. The size of each particle is determined by electronically counting the number of sensors with light extinguished below a 50% intensity threshold by the shadow. In the two-dimensional probe, the entire array of sensors is sampled at a "slice" rate proportional to the true airspeed. By use of a high-speed, front-end data storage register, each sensor can transmit up to 1,024 bits of shadow information for each particle. A series of "image slices" is recorded across the shadow to develop a true two-dimensional image.

Figure 1 illustrates the data format for a dendritic ice crystal. All together in the basic probe there are 32 sensors in the linear array, each imaging a portion of the light beam 25 μm in diameter. Because of the shadow cast by the particle, the light level falls to the threshold of detectability (50%

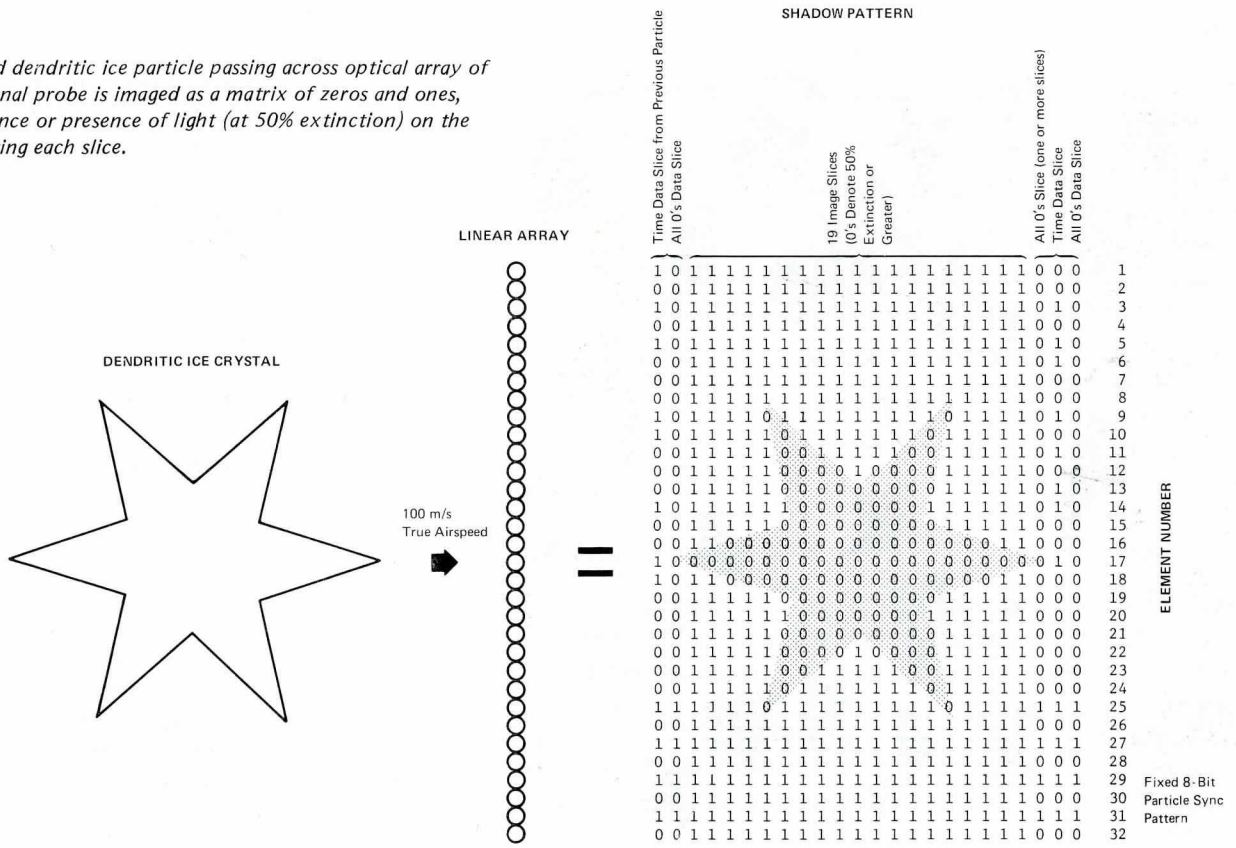

Fig. 1 Star-shaped dendritic ice particle passing across optical array of PMS two-dimensional probe is imaged as a matrix of zeros and ones, depending on absence or presence of light (at 50% extinction) on the optical sensors during each slice.

extinction) of the sensors at each point marked zero on the diagram; the points marked one denote sensors still receiving light above the threshold. At a particle speed of 100 m/s, a slice rate of 4 MHz (4×10^6 cycles per second) would result in an undistorted image, a slower rate in a compressed image, and a higher rate in an elongated image. The particle shown in Fig. 1, being approximately 475 μm wide, images across 19 slices. The images can be viewed on a cathode ray tube display during flight and stored, along with the time between passage of the particles, on magnetic tape for later computer analysis. A computer can be programmed to classify particles according to linear or areal size, and concentrations can be determined by counting the number of particles from a known volume of cloud passing through the space seen by the probe. Figure 2 shows computer-reconstructed images of several particles in cumulus cloud. The basic two-dimensional probe can be used to image particles from 25 to 800 μm in diameter, but magnifying lenses may be used to extend the range to diameters of 400 - 6,000 μm. For the basic probe the sample is about 49 ℓ/km or 4.9 ℓ/s at a true airspeed of 100 m/s. A sample volume of 784 ℓ/km or 78.4 ℓ/s is obtained with the largest (400 - 6,000 μm) size range. With the basic probe, the sample volume for particles less than 155 μm in diameter decreases with decreasing particle size.

Fig. 2 Examples of images of natural ice particles plotted by computer from two-dimensional probe data. The width of each band of images is 800 μm, corresponding to 32 sensors, each sensing a portion of the light beam 25 μm in diameter.

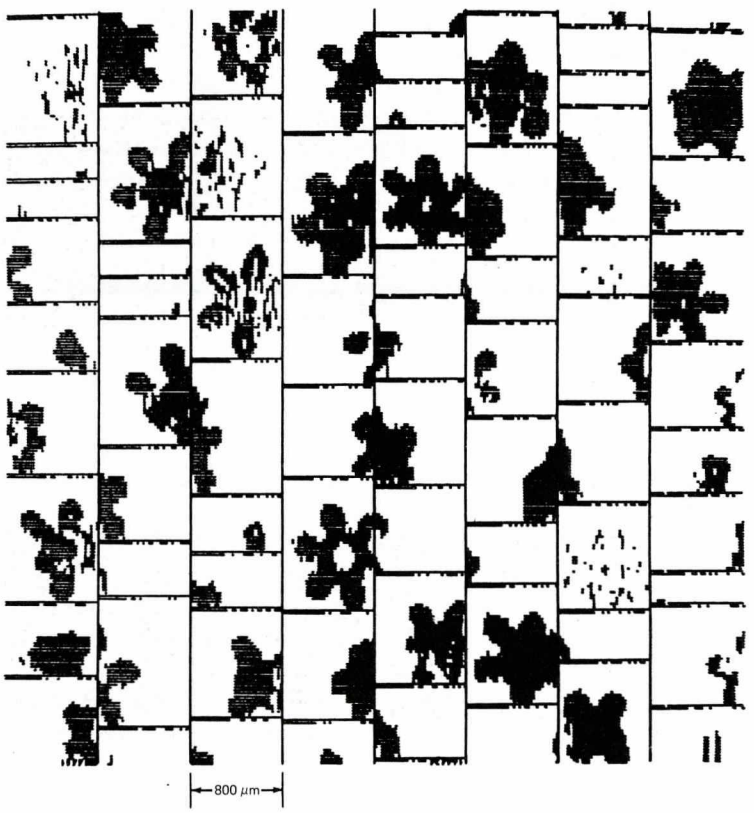

Because the images and the time between images are obtained and stored in computer-compatible (digital) form, automatic data analysis for concentration, size, and spatial distribution is straightforward, without necessity for any intermediate steps. An on-board video display allows the scientist to monitor the cloud particle content in real time and to make on-the-spot judgments on the subsequent course of the flight.

Generally, ice cannot be distinguished from water for spherical particles, since the shadow images have the same appearance for both. No internal details are recorded in the images except for regions of relatively high optical transparency, and it is sometimes difficult to interpret images as representative of known particle shapes.

The Particle Camera

By using a combination of high-speed flash lamps (about 10 μs flash duration) and a rotating mirror synchronized to the true airspeed, it is possible to stop image motion adequately to make sharp photographs of cloud particles from aircraft. A schematic diagram of a cloud particle camera developed at NCAR by the author is shown in Fig. 3. The camera is mounted on *The Explorer*, the research sailplane owned by the National Oceanic and Atmospheric Administration and operated by NCAR.

The camera is composed of two basic units. The first is a cockpit package that contains a 35 mm film transport, a film magazine (not shown), intervalometer, two xenon flash lamps, a 135 mm focal length lens, a rotating mirror with drive motor, and electronic and electro-optical components for camera control and synchronization of the shutter, rotating mirror, and lamps. The second unit is an airfoil-shaped optical housing, located 59 cm above the canopy and supported by four struts, that contains two corner reflectors and provides a flat-black background for the photographs. The camera is focused in a plane 34 cm above the top of the canopy; the sample is illuminated by crossed beams of light from the flash lamps and reflected back through the volume by the corner reflectors. This system of illumination provides front lighting necessary for the more opaque particles and at the same time provides back lighting for transparent particles and water drops.

With the present sailplane camera, photographs are taken at rates of up to two frames per second on 35 mm black-and-white recording film. Because the camera cannot be reloaded in flight, a special magazine-film combination was developed. The special magazine was developed by Robert Woltz

Associates of Newport Beach, California, for attachment to the existing electric Nikon camera film transport. Using an extra thin base (0.0025 in.) film, the magazine-film combination extends the capacity to 3,200 frames per flight, equivalent to 27 min of continuous operation at a maximum rate of two frames per second.

The camera images particles 8 μm in diameter and larger. Water particles larger than 100 μm are distinguished from ice by their characteristic signatures. Because a drop acts like a lens, forming images of the two light sources, the image of an in-focus drop is a "dot-pair" signature. Out-of-focus drops appear as overlapping disks or, for very far out-of-focus drops, as overlapping septagons (the shape of the camera aperture) (see Fig. 4). Ice particles that are too badly out of focus to show detail are imaged as irregular shapes or as a single disk (both of which are easily distinguished from the drop signature). The camera has the ability to give excellent detail for in-focus ice particle images, as shown in Fig. 5. While the majority of images are out of focus, concentration and size data can be obtained from the out-of-focus images by measuring the size and optical density of each image.

Special charts, prepared from out-of-focus photographs of particles taken in the laboratory are then used to determine the size and position of each particle at the time the photograph was taken. The method can be used without statistical corrections only when all of the ice particles have the same optical transparency and reflectivity (all graupel, all clear ice crystals, etc.). When this size-density method is used, the sample volume depends on particle size, ranging from 2.6 ± 0.5 cm^3 per photograph for particles 8 μm in diameter at a camera magnification of one up to about 1 ℓ per photograph for particles larger than about 5 mm at a camera magnification of 0.5.

The images from the camera are of generally high quality and show internal structure. By using different lenses, a wide range of particle sizes and volumes can be imaged with one camera. Data reduction is tedious, requiring manual measurements of size and optical density for each image.

The Airborne Holography System

The hologram is an interference pattern recorded on photographic film. The pattern results from coherent monochromatic light (generally from a laser) scattered by objects within the beam arriving at the photographic emulsion with different phase relationships relative to unscattered (reference) light in the beam; constructive and destructive interference results within the photosensitive emulsion. By shining laser light on the exposed and subsequently developed hologram, it is possible to reconstruct, in three dimensions, the original scene

Fig. 3 Schematic diagram of NCAR particle camera installed in research sailplane (see text for details). From Cannon (1974).

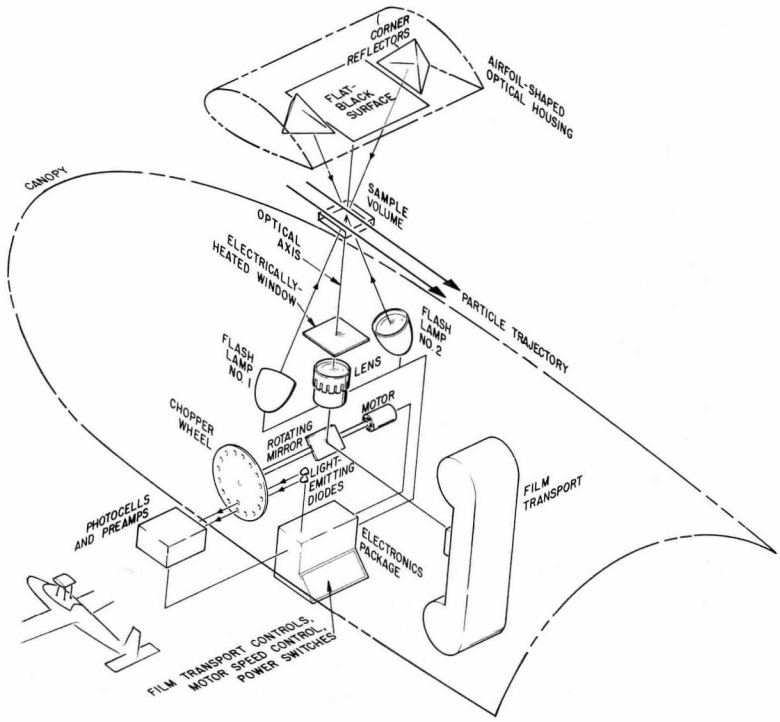

Fig. 4 Sharply focused (left), out-of-focus (middle), and far out-of-focus (right) images of raindrops in precipitation, photographed with the NCAR particle camera. (From Cannon, 1974.)

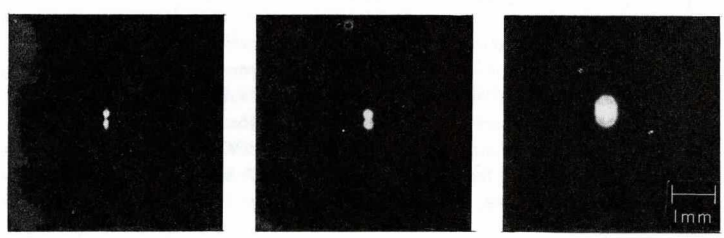

Fig. 5 Ice particle photographed with the NCAR particle camera.

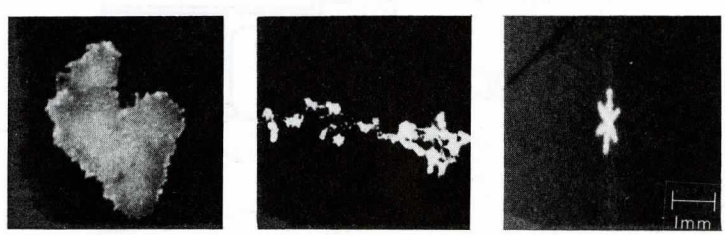

as it existed when the hologram was made. The reconstructed images come into focus within three-dimensional space in the same relative locations in which they existed when the hologram was made. They can be photographed and viewed for sizing, counting, or detailed structural information.

It is possible to make holograms of cloud particles from aircraft using a holocamera developed under the direction of James Trolinger of Science Applications, Inc. Illumination is provided by a pulsed ruby laser. Holograms of particles within a volume of approximately 300 cm^3 located between the probe tips of the holocamera (Fig. 6) are made with 10 - 15 μm resolution on 70 mm film. The technique has the advantages of stopping particle motion by the use of a very short exposure time (10 ns; i.e., 10^{-8} s) and allowing in-focus reconstruction of images of all detectable particles within the sample volume, so there are no out-of-focus images such as are obtained with the particle camera. Two reconstructed ice particle images from cirrus clouds are shown in Fig. 7.

The holocamera has been used in cirrus clouds as high as 18,300 m above sea level and at temperatures as low as −62°C. One version of this instrument is being flown on a Cessna Citation aircraft and is used by the Air Force Space and Missiles Systems Organization for weather definition.

The sampling rate is rather low; only two holograms can be made per minute. Science Applications is developing a YAG (yttrium, aluminum, garnet) laser system which will increase the sampling rate to ten holograms per second.

Fig. 6 Holocamera designed for aircraft operation. Light from pulsed ruby laser illuminates a 300 cm^3 sample volume between the two extending probes. Hologram is made on high-resolution film located in 70 mm film transport at right end of lower tube. Camera is mounted so that probes extend either out of the nose or out of the side of aircraft. (Diagram reprinted from Trolinger, 1974, p. 7, by permission of Science Applications, Inc., and the Instrument Society of America.)

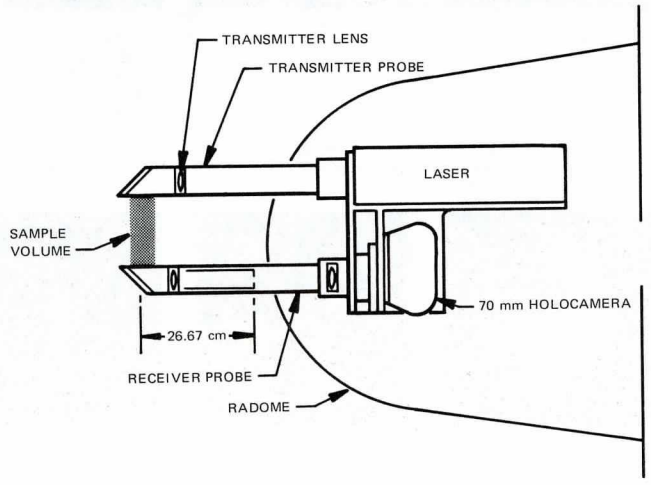

Future Improvements and Data Reduction

The imaging devices described in this article are all relatively new; the NCAR particle camera was first used in 1971, and the two-dimensional probe and holocamera in 1974. Work is under way to improve these instruments, especially in the areas of resolution of particle detail and sample volume. Improvements in resolution will enable scientists to distinguish ice from water as well as to study details in ice particles at their earliest stages of growth. A multiflash technique, higher frame rate, and larger size of film will be used on future particle cameras to obtain more images over a given flight distance.

Data reduction presents one of the rather formidable problems with imaging devices. During one flight many thousands of images may be obtained, and each one must be examined for size and shape, and for any special characteristics of interest to the scientist. In addition, the number of particles per unit volume must often be determined by size class from particle counts. Of the three instruments described, the PMS two-dimensional probe, by using an electronic imaging technique that rejects any out-of-focus images and by storing the data in computer-ready form, provides the greatest flexibility for rapid data analysis. The holocamera allows reconstruction of all images above the size threshold of detectability by use of a reconstruction system, but the procedure is tedious and several hours of manual analysis are generally required to analyze each hologram. Analysis of photographic images from the NCAR particle camera requires a great deal of manual effort, since both size and optical density must be determined for each image. There are several automatic image-analyzing computers commercially available, and in the future it will be possible to use these for data reduction for both the holocamera and the particle camera. By using one of these analyzers, size, optical image density, and shape classifications can be obtained for all images within a photograph within a few seconds, but the details of particle type, appearance, amount of aggregation, etc., must generally be decided by examination of each image by the scientist.

Fig. 7 Reconstructed holocamera images of ice particles from cirrus clouds. (By permission of Science Applications, Inc.)

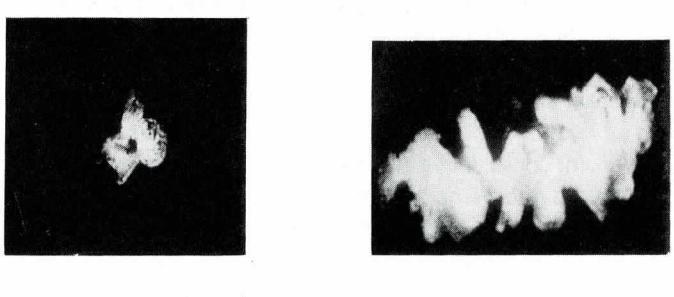

Table 1 presents the comparative advantages and limitations of the instruments described in this article. The scientist may choose among these instruments depending on need and budget, although use of more than one instrument on the same aircraft is desirable to extend the ranges of size and sample volume and for comparison over the ranges of overlapping detectable particle sizes.

References

Cannon, T. W., 1974: A camera for photography of atmospheric particles from aircraft. *Rev. Sci. Instrum. 45*, 1448 - 1455.

Trolinger, J. D., 1974: An airborne holography system for cloud particle analysis in weather studies. Paper No. 74 - 627 in *Advances in Instrumentation 29*, Proc. International Instrumentation-Automation Conference and Exhibit, held 28 - 31 October, New York, N. Y.; Instrument Society of America, Pittsburgh, Pa.

For Further Information about Equipment

Optical Array Spectrometer Probe

Particle Measuring Systems, Inc.
1855 57th Court
Boulder, Colorado 80301

Airborne Holography System

Science Applications, Inc.
101 Continental Building, Suite 310
El Segundo, California 90245

Table 1
Comparison of Existing Imaging Devices

IMAGING DEVICE	PRINCIPAL ADVANTAGES	PRINCIPAL DISADVANTAGES
PMS Two-Dimensional Optical Probe	Automatic electronic data acquisition of images and time between images with no intermediate data reduction prior to computer analysis	Shadow image showing no internal structure except regions of relatively high optical transparency
	On-board display allowing scientists to make on-the-spot decision on flight path based on particle content observed in real time	Generally cannot distinguish ice from water for spherical or near-spherical particles
	Large sample volume for given length of flight	Images sometimes difficult to interpret as representative of known particle shapes
NCAR Particle Camera	High-quality images with internal structure	Out-of-focus images requiring special consideration in data reduction
	Very wide range of particle sizes (depending on magnification used) with one instrument	Tedious data reduction
	Water drops distinguished from ice particles by characteristic signatures	
Science Applications Holocamera	Large volume in each sample	Sample rate rather low in present system
	No out-of-focus images	Tedious data reduction
	High-quality images with internal structure	
	Short exposure time obviating use of rotating mirror	

Liquid Water Content Devices

Robert E. Ruskin, Naval Research Laboratory

Measurement of ambient liquid water content (LWC) from aircraft is complicated by several factors: different sizes of drops are present in clouds, different precipitation trajectories occur around an aircraft fuselage, and collection efficiencies differ with differing projections from the aircraft and from internal to external instruments. The collection efficiency is the fraction of drops striking an obstruction as the remaining drops are diverted around it by the airflow. Unless the drops enter an instrument with isokinetic flow (no back pressure), a portion of the drops will be diverted.[1] Proportionally more small droplets than large drops are diverted around obstructions. For all sizes, a greater fraction is collected at faster speeds, at lower air densities, and on smaller obstructions.

For cross sections as large as the fuselage of a large plane, many of the drops are diverted as far away from the fuselage as a couple of meters. A droplet-counting instrument located within a meter of the fuselage may undercount or overcount by more than a factor of ten. For this reason it is generally preferable to mount instruments for LWC determination under a wing or on a boom ahead of the plane. Collection efficiency is discussed in detail by Langmuir and Blodgett (1949), and a simplified summary curve is shown in Ruskin and Scott (1974).

Two of the earliest LWC instruments were Vonnegut's capillary collector (see Mason, 1971), and the Warner and Newnham (1952) paper tape instrument, which was developed in Australia and was widely used during the 1950s. It employed a porous paper tape to which there had been applied a solution that conducts electricity when wet but not when dry. The tape moved over two fixed electrodes between which the electrical resistance was measured. Its principal limitations were that collection efficiency for small droplets was low and that at higher flight speeds and large LWC the tape softened and broke, thereby becoming inoperative for the remainder of a flight.

[1] Achieving isokinetic flow into an instrument requires that the proper amount of suction be provided (usually by the aerodynamics at the sample exit) so that during high-speed entry the droplets are neither diverted around the obstruction caused by increased pressure at the entry nor diverted into the entry by a suction.

Author

Robert E. Ruskin joined the Naval Research Laboratory (NRL) in 1942, after academic training in physics at Kansas State Teachers College and at the University of Missouri. He is a member of numerous professional and honorary societies, and his awards include listing in Who's Who in Science and Industry. *His present work at NRL involves research on marine fog and haze and their effects on electro-optical systems.*

Hot-Wire-Type LWC Instruments

The most common aircraft instrument for measuring the small-droplet portion of cloud water is the Johnson-Williams (J-W) hot-wire device manufactured by Johnson-Williams Products, Mountain View, California (Neel, 1955), which uses a hot nickel-iron wire with a known temperature coefficient of resistance (see Fig. 1). This wire is heated by a constant electric current; the resistance resulting from its temperature change is measured using a bridge circuit. In dry air the wire maintains a steady-state temperature, a result of balance between the electrical heat supplied and the heat removed by the dry airflow. However, if droplets are present in the air, they collide with the wire and cause a degree of cooling directly related to the amount of liquid water in the airstream.

Variations in airspeed, which cause variations in heat transfer, are compensated for in the electrical circuit by manual adjustment of a potentiometer, but minor variations due to fluctuations of airspeed from turbulence or cloud activity are not taken into account. The effect of ambient temperature changes is compensated for electrically by a reference hot wire in the instrument positioned parallel to the airstream so that it is affected by the airflow but not by the droplets. This reference wire forms a compensating leg of the bridge. In operation, the instrument is responsive to cloud water. However, because the reference wire gradually becomes wet in heavy precipitation, the indication tends to drift low and give a negative reading after returning to clear air. This effect is greatest when the probe is oriented so that the reference wire is at the bottom.

The J-W hot-wire device has the ability to produce a real-time electrical readout of the liquid water contained in cloud droplets, mainly in those smaller than about 20 μm in radius (Levine, 1965). The reduced reading with large drops probably is due to splattering of the drops. Though the instrument becomes saturated if the cloud water is more than about

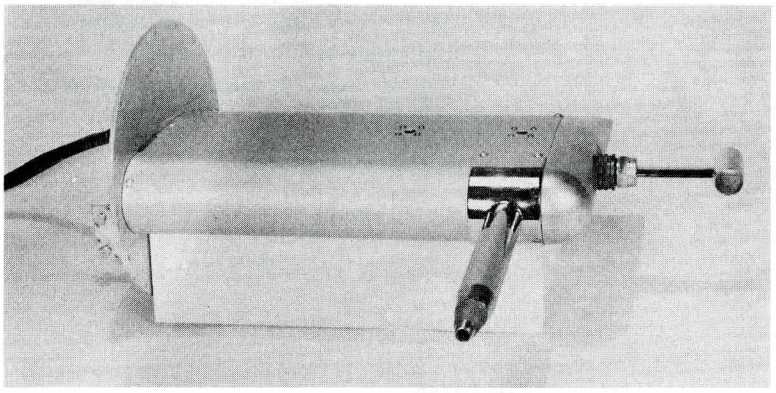

Fig. 1 The Naval Research Laboratory's pylon-mounted, evaporator Lyman-alpha instrument for total water content is now being manufactured by General Eastern Corp., Watertown, Massachusetts. A J-W, hot-wire LWC probe is mounted on the right end of the pylon.

3 g/m^3 (at an airspeed of 250 kt), it can be valuable for the detection of young, growing cells because of its discrimination against larger drops, and so it can act as a seeding criterion by indicating the presence of a usable amount of unfrozen water in small droplets.

Another instrument using wires heated by a constant current has been designed by Levine (1965). His instrument consists of two portions, called the "cloud-water instrument" and "rain-water instrument." The cloud-water instrument is a plastic yoke strung with a heated wire of similar diameter to that in the J-W instrument but longer. The rain-water instrument is a threaded ceramic cone about 5 cm in diameter wound with a similar wire. In theory, the collection efficiency characteristics and drop breakup problems that make the J-W instrument insensitive to larger drops apply only to the cloud-water instrument. The cone-shaped rain-water sensor has a collection efficiency which favors larger raindrops. This instrument system has had problems of drift during extended flights in clouds. Unlike the J-W instrument, it provides no automatic temperature compensation.

Another hot-wire instrument, which has been in use for several years in the Union of Soviet Socialist Republics, is reported to respond with equal sensitivity for all drop sizes. This instrument consists of a wire filter screen of approximately 100 cm^2 heated by high-frequency current. As with the J-W and Levine instruments, the wire temperature (and hence the resistance) is a calibrated function of LWC.

An improvement in hot-wire LWC instrumentation is based on operation in a constant-temperature mode instead of the constant-current mode. Two instruments of this type use for their LWC calibration the electric current required to maintain a constant temperature. One was designed by T. Kyle of NCAR for LWC as high as 30 g/m^3. The other, called a "nimbiometer," was designed by Merceret and Schricker (1975) at the National Hurricane Research Laboratory (NHRL), where it has undergone considerable flight use, including through hurricanes. This instrument is reported to provide a time response of a few milliseconds and to consume less current per volume sampled than either constant-current or total-evaporation types of hot-wire instruments. Its sampling area of about 0.5 cm^2 consists of about 30 cm of wire 0.177 mm in diameter. The small diameter permits a fast response, but increases the vulnerability to breakage by hail or graupel.

A limitation for most hot-wire instruments is the change in calibration because of cooling when they are operated in ice or mixed-phase precipitation or clouds. Another limitation in accuracy, particularly for fast-response, hot-wire instruments, is the cooling due to rapid fluctuations in the speed of the air passing through the probe during flight in turbulent air (which is usually the case in clouds).

Evaporation Lyman-Alpha Instruments

The problem of varied cooling under mixed-phase conditions is overcome by measuring only the vapor density resulting from total evaporation of the water, as opposed to measuring the cooling effect on the hot wires. Two instruments based on evaporation measurement employ a type of fast-response, vapor-density sensor in which water vapor causes light absorption in the spectral line of atomic hydrogen at the wavelength of 121.56 nm. This spectral line is very highly absorbed by water vapor: vapor with a dew point of 0°C causes the light to be reduced to 1/e of its dry-air value in 0.5 cm of path length. The sensor is based on the Lyman-alpha humidiometer discussed in Wexler and Ruskin (1965), in the chapters by Tillman, by Randall et al., and by Ruskin. The two instruments that use this sensor are described by Ruskin (1967) and by Kyle (1975). Although the sensor (see Fig. 2) has a response time of a few milliseconds, the overall response

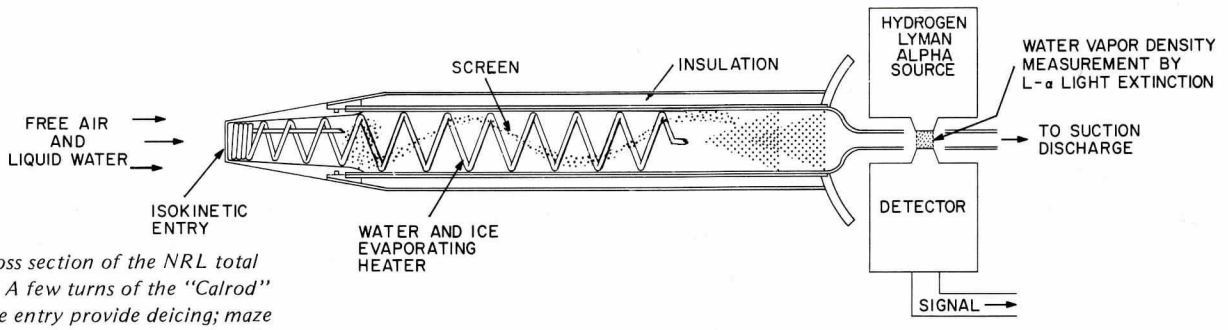

Fig. 2 Schematic cross section of the NRL total water content probe. A few turns of the "Calrod" heater brazed into the entry provide deicing; maze consisting of heater and screens evaporates cloud water in 0.01 s; Lyman-alpha detector indicates changes in resultant vapor density in a few milliseconds.

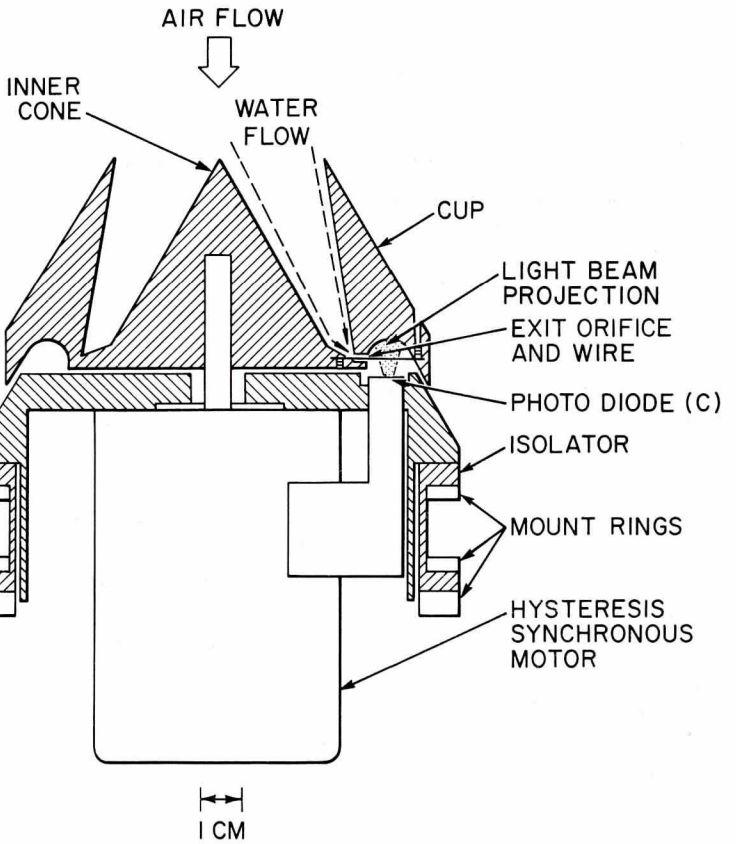

Fig. 3 Vertical cross section of the optical flowmeter, illustrating the size and relative position of components. (Courtesy of E. Brown, NCAR.)

Fig. 4 Results obtained during a comparison test comparing the optical flowmeter and a hot-wire instrument on 2 September 1970. Data shown at 46 and 51 min are from cumulus clouds with tops at 6,000 m and with rain on the exit side.

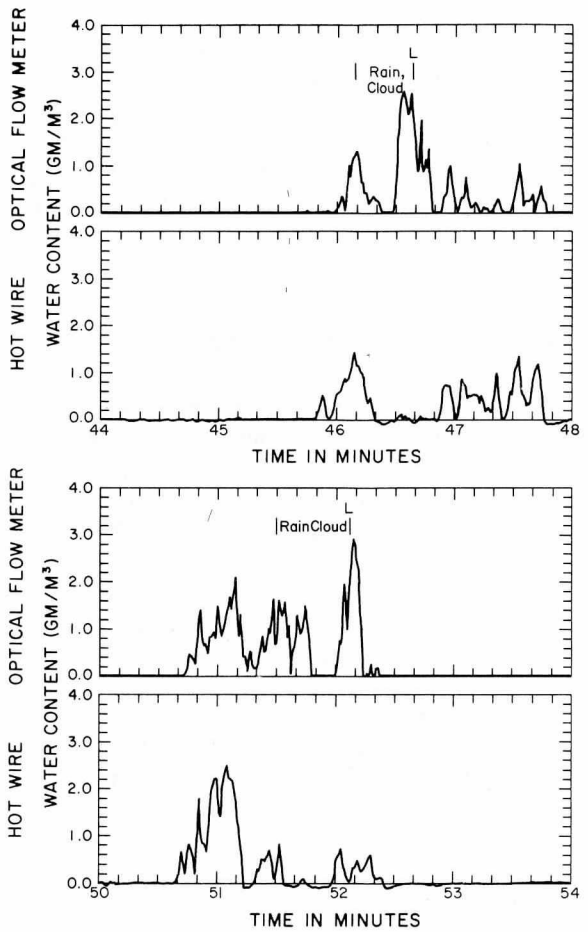

Fig. 5 Block diagram of the instrument being developed by Meteorology Research, Inc., to measure total water content.

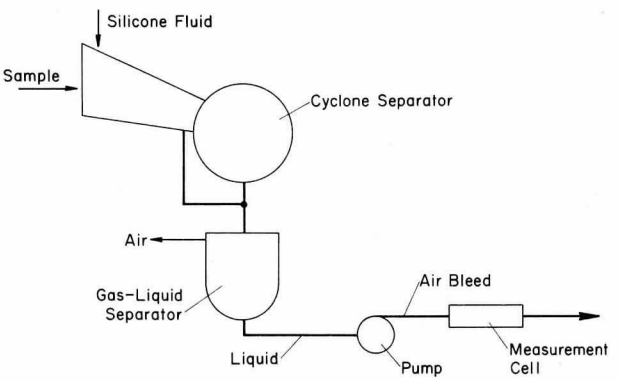

time of the instrument depends largely on the time required to bring the sample in and evaporate its water. Ruskin gives this time as a few hundredths of a second except with ice, when it becomes a few tenths. Kyle lists a response of 1 s. In both instruments the temperature of the open-mesh heating element is maintained somewhat below the boiling point of water; therefore, the water striking the heater spreads quickly over it (with a reduced surface tension) and evaporates almost instantaneously. The Kyle design has the advantage of an automatic temperature control so that LWC as high as 40 g/m^3 can be evaporated.

These evaporator instruments provide a direct measurement of the total amount of water present in all three phases (ice, liquid, and vapor). Data in this form are convenient for studies of cloud air entrainment or conservative properties. However, for LWC data it is necessary to subtract the vapor density of the air between the cloud droplets. For this purpose a thermoelectric dew-point hygrometer has been used with a water-separating sample entry, as illustrated by Ruskin and Scott (1974).

Although the Lyman-alpha sensors in the evaporator instruments can be calibrated essentially continuously while flying in clear air, still the accuracy of LWC data is limited by the combined random errors in the dew-point and Lyman-alpha instruments and by the slower (4 s) response time of the dew-point instrument. This response time limitation is obviated by the addition of a second Lyman-alpha sensor for the water-separated sample. Two new developments are expected to improve the evaporator Lyman-alpha instruments: reduction of the combined random error of two sensors by time-sharing a single sensor between the two samples (in development at the Naval Research Laboratory—NRL), and increasing the sample inlet area from 0.8 cm^2 to 10 cm^2 (in development for the U.S. Air Force at Aerospace Corporation, Los Angeles, California).

Sampling Volume Considerations

For measuring LWC in precipitation the problem of sampling volume is a major one because of the large apparent fluctuations in LWC caused by the difference in size between raindrops and cloud droplets. The LWC of a 2 mm raindrop is a million times that of a 20 μm cloud droplet and, correspondingly, there are a millionth as many raindrops as cloud droplets per unit volume for the same LWC. To provide statistical validity for rain comparable to that obtained in the same flight distance from a 1 mm^2 sampling area for cloud droplets, an area of 1,000 cm^2 is required. For further discussion of the sampling problem see Ruskin and Scott (1974).

Centrifugal Separator Types

A move toward proper sampling area is achieved in the optical flowmeter of Brown (1971, 1973) at NCAR (Fig. 3). In this instrument the sampling area is 10 cm^2. The collection efficiency for cloud droplets is smaller than for raindrops because little air passes through to carry the smaller droplets. For this reason it may measure less cloud water than was present. Raindrops are collected and centrifuged to the outer wall of a cup or bowl as it spins on its horizontal axis. The centrifugal force drives the water through a small hole in which is mounted a 0.2 mm silvered wire. The wire-water surface tension and aerodynamic drag cause the formation of a web of water. The width of this web as measured by a light source and photodiode detector provides information on the water flow rate, hence LWC. On the developmental models deicing is not available. A comparison of flight data from this instrument and a J-W hot-wire type is shown in Fig. 4. The optical flowmeter, which is more sensitive to raindrops, shows large amounts of rain water which the hot-wire instrument misses. Near the cloud edges the hot-wire instrument shows more LWC, probably because the smaller droplet sizes favor that instrument.

A promising instrument, now under development at Meteorology Research, Inc., Altadena, California, is called the "cyclone separator." This instrument improves the usually inadequate sampling volume by incorporating a 100 cm^2 entry. As shown schematically in Fig. 5, the sample impinges on a heated (deiced) plate which slopes down into a centrifugal separator. The plate is continually covered with a liquid in which the water drops become imbedded and flow into the cyclone separator where the air is expelled from the liquid sample. The liquid is then pumped to a detector cell where the fraction of water in the carrier liquid is measured by changes in capacitance resulting from changes between the high dielectric constant of the water and a lower value for the carrier liquid. This instrument can be quite accurate at LWC values as low as 0.01 g/m^3 and with drop sizes from the largest rain down to 5 or 10 μm in radius. In the first models a limitation was the instrument's slow resolving time of about 6 s plus an additional 6 s of constant delay time.

Each of the LWC instruments has advantages and limitations. Some are better for young clouds, others for precipitation. Some have fast response, others good sampling volumes. Some operate in ice or mixed phase; others do not. Therefore the researcher must consider the priorities for his particular LWC measurements and choose his instruments carefully. Whichever instrument is chosen, it will require some "living with" before meaningful and reliable data can be expected, even after it has been carefully mounted in an aerodynamically correct location on the aircraft.

References

Brown, E. N., 1971: *A Prototype Optical Flowmeter for the Measurement of Liquid Water Content.* NCAR Technical Note EDD - 61, NCAR, Boulder, Colo., 25 pp.

———, 1973: A flowmeter to measure cloud liquid water. *Atmos. Technol. 1*, 49 - 51.

Kyle, T. G., 1975: The measurement of water content by an evaporator. *J. Appl. Met. 14*, 327 - 332.

Langmuir, I., and K. B. Blodgett, 1949: *Mathematical Investigation of Water Droplet Trajectories.* Final Report under Army Contract W - 33 - 038 - ac - 9151, Report No. RL - 225 from the General Electric Company, 46 pp.

Levine, J., 1965: *The Dynamics of Cumulus Convection in the Trades, a Combined Observation and Theoretical Study.* Ph.D. thesis, Dept. of Meteorology, Woods Hole Oceanographic Institution, Woods Hole, Mass., 129 pp.

Mason, B. J., 1971: *The Physics of Clouds.* Clarendon Press, Oxford, 675 pp.

Merceret, F. J., and T. L. Schricker, 1975: A new hot-wire liquid cloud water meter. *J. Appl. Met. 14*, 319 - 326.

Neel, C. B., 1955: *A Heated-Wire Liquid-Water-Content Instrument and Results on Initial Flight Tests in Icing Conditions.* National Advisory Committee for Aeronautics Research Memo RMA54123, 33 pp.

Ruskin, R. E., 1967: Measurements of water-ice budget changes at −5C in AgI-seeded tropical cumulus. *J. Appl. Met. 6*, 72 - 81.

———, and W. D. Scott, 1974: Weather modification instruments and their use. Chapter 4 in *Weather and Climate Modification* (W. N. Hess, Ed.), John Wiley and Sons, Inc., New York, 136 - 205.

Warner, J., and T. D. Newnham, 1952: A new method of measurement of cloud-water content. *Q. J. R. Met. Soc. 78*, 46.

Wexler, A., and R. E. Ruskin (Eds.), 1965: *Humidity and Moisture. Vol. I, Principles and Methods of Measuring Humidity in Gases.* Reinhold Pub. Corp., New York, 704 pp.

For Further Information about Equipment

J-W Hot-Wire Instrument

Johnson-Williams Products
Bacharach Instrument Co.
(Division of AMBAC Industries, Inc.)
2300 Leghorn Street
Mountain View, California 94040

Cyclone Separator

Meteorology Research, Inc.
464 West Woodbury Road
Altadena, California 91001

NRL Lyman-Alpha Instrument

General Eastern Corp.
36 Maple Street
Watertown, Massachusetts 02172

Cloud Condensation Nucleus Counters

James E. Jiusto, State University of New York at Albany

Diffusion cloud chambers were devised almost 40 years ago for the purpose of maintaining high supersaturations and detecting nuclear particles. Langsdorf (1936) developed a thermal-gradient diffusion chamber in which heated alcohol vapor at 75°C diffused downward to a base plate refrigerated to −45°C by dry ice. The supersaturations of several hundred percent produced in this manner were sufficient to condense vapor on ions left in the wake of cosmic rays, thereby forming visible drops.

Twenty years were to pass before the diffusion chamber principle was first used to detect cloud nuclei active at supersaturations of only a few percent (Wieland, 1956). It remained for Twomey (1959, 1963) to pioneer the development of such instruments and to stimulate interest in the better understanding of cloud condensation nuclei (CCN).

CCN are those atmospheric particles having sufficient size and water affinity to act as centers for the formation of cloud drops at the slight supersaturations (<3%) characteristic of clouds. They are distinguished from smaller particles which, if they accumulate any condensation at all, will only produce minute, stable haze droplets.

The basic operating principle of a thermal-gradient diffusion chamber is illustrated in Fig. 1. Water vapor diffuses from a warm to a cold surface, each at water saturation, such that a nearly linear relationship exists between water vapor pressure and temperature. It can be seen that the saturation vapor pressure curve is exceeded at all intermediate points within the chamber, reaching a maximum supersaturation (S) approximately midway between the wet surfaces. It is customary to maintain the warm upper surface temperature (T_w) at room or ambient conditions and to cool the lower surface (T_c) to produce any desired supersaturation within limits. The greater the temperature differential, the greater the supersaturation, so that $S_{\%} \approx (T_w - T_c)^2/25$ (Sinnarwalla and Alofs, 1973).

A CCN counter consists of three major components: a diffusion chamber for producing supersaturated conditions and admitting ambient aerosols, a light beam and optics system with which to discern growing droplets in a prescribed volume, and a device for recording droplet (nucleus) concentrations. During the decade following Twomey's initial work, virtually all of the CCN counters in use represented modified versions of his apparatus. Several new designs of one or more of the basic components have appeared since 1970. Thus the cloud physicist has a variety of systems (virtually all noncommercial) to choose from, depending on the particular supersaturation range and measurement program of interest. Thermal-diffusion counters now in use may be classified as follows:

- Static-diffusion horizontal chambers
- Automatic static chambers
- Dynamic-flow (continuous) chambers
- Low-supersaturation (vertical) chambers

Static-Diffusion Horizontal Chambers

The basic Twomey-type system, illustrated in Fig. 1, has been studied and used extensively. Four[1] of the six CCN counters compared at the Second International Workshop on Condensation and Ice Nuclei at Ft. Collins, Colorado, in 1970 were of this general type; their counts agreed to within 30% (Ruskin and Kocmond, 1971).

This system generally consists of a cylindrical diffusion chamber with upper and lower water reservoirs or wet filter paper; the bottom plate is cooled to the desired temperature

Author

James E. Jiusto received a B.A. in mathematics and M.A. in administration from the State University of New York (SUNY) at Albany. Following Air Force service as a weather officer, he joined the Cornell Aeronautical Laboratory, Inc., where he was appointed head of the Atmospheric Physics Section in 1960. Along with his duties there, he managed to earn a Ph.D. in cloud physics from Pennsylvania State University. Currently with the Atmospheric Sciences Research Center, SUNY at Albany, he is engaged in studies of fog formation, Great Lakes snowstorms, nucleation phenomena, and weather modification.

[1] Noncommercial units from the Naval Research Laboratory, Calspan (formerly Cornell Aeronautical Laboratory), White Sands Missile Range, and the National Oceanic and Atmospheric Administration.

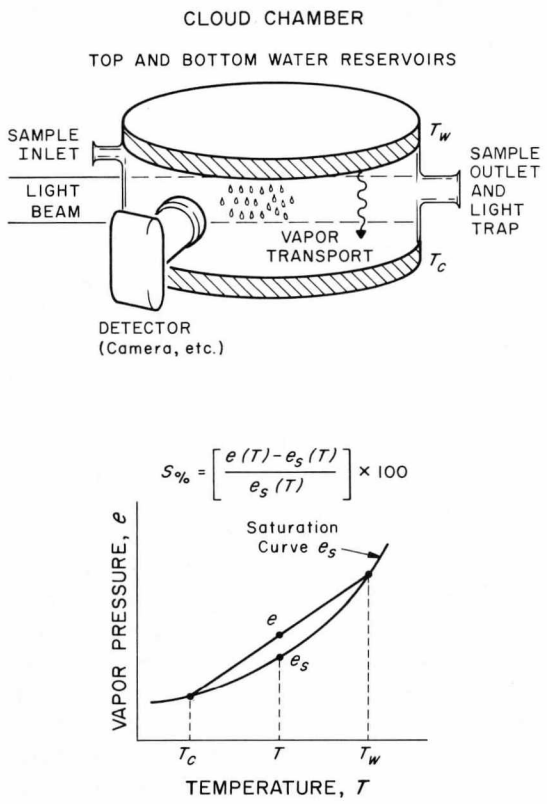

Fig. 1 Sketch of a thermal-gradient diffusion chamber for detecting cloud condensation nuclei. Temperature difference between upper and lower wet surfaces produces supersaturation, S, *as illustrated in phase diagram (bottom) and in resultant droplet growth on cloud nuclei. In the diagram,* e *represents ambient vapor pressure at about mid-level of the chamber, and* $e_S(T)$ *represents the saturation vapor pressure with respect to water at that level.*

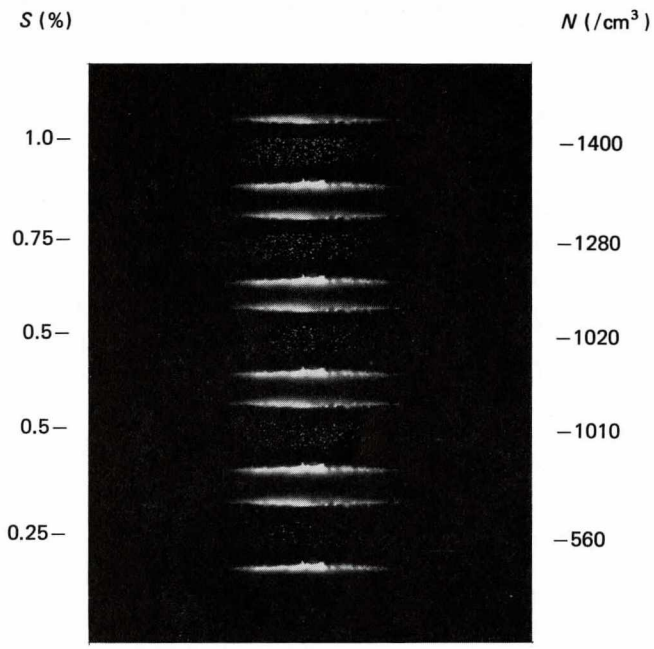

Fig. 2 Photograph of condensed drops formed in a cloud chamber from successive air samples at indicated supersaturations from 0.25 to 1.0%.

by an imbedded thermoelectric cooler. Temperatures of both plates are monitored by thermistors or thermocouples, and the temperature difference (ΔT) varied in steps over an equivalent S range of approximately 0.2 - 3%. An intense light source (e.g., a 100 - 200 W mercury arc) is collimated into a ribbon of light and the known volume is photographed at a 90° angle with a Polaroid system, 35 mm still camera, or 8 mm movie camera. The droplets, as shown in Fig. 2, are then rather laboriously counted with the help of a magnifying lens or large-screen projection, resulting in CCN spectra such as those of Fig. 3. From results such as these, certain maritime and continental aerosols can be characterized.

Several design principles must be considered in constructing a reliable diffusion chamber. Twomey (1967), Saxena and Kassner (1970), and Squires (1972) have reviewed some of the optimum characteristics of CCN counters. Table 1 summarizes certain limitations and design criteria to be considered. In essence, these guideline specifications are aimed at satisfying the following criteria:

- *Providing adequate droplet growth time at $S \geqslant 0.1$ or 0.2%.* Chamber height, h, must be restricted because the time for an air sample to equilibrate to chamber conditions is proportional to h^2. Conversely, $h \ll 1$ cm enhances drop fall-out and complicates illumination optics.

- *Minimizing wall effects.* An aspect ratio $(d/h) \geqslant 5$, where d is the diameter, generally assures that warmer walls will neither perturb the temperature and the desired S fields toward the center of the chamber, nor introduce substantial convection currents. Gagin and Terliuc (1968) further minimize such effects by using metal for the conducting walls in contrast to the Lucite or glass customarily used.

- *Avoiding large, transient supersaturations.* Because the molecular diffusion of water vapor is about 20% greater than that of heat, the introduction of relatively cold, moist air into the chamber can theoretically produce spurious high S transients (Saxena, Burford, and Kassner, 1970; Fitzgerald, 1970). Intake air at about the temperature of the top warm plate is recommended. While experiments by Radke and Hegg (1971) do not confirm these transients in their chamber (perhaps because of stronger initial eddy diffusion or complex growth

kinetics), it nevertheless would seem advisable to follow this conservative, easily achieved criterion. As the phase diagram in Fig. 1 suggests, saturated intake air colder than T_c or warmer than T_w could well produce S transients.

• *Maintaining desired supersaturations.* If excessive numbers of nuclei compete for the available water vapor, the prescribed S value will not be achieved. To avoid this, Twomey (1959) and Squires (1972) recommend diluting the sample whenever nucleus concentrations exceed about 1×10^3 nuclei per cubic centimeter at $S = 1\%$.

• *Minimizing line losses and successive sample contamination.* As indicated in the table, modest tube lengths, the avoidance of sharp bends, and adequate chamber flushing will assure that representative ambient samples are contained within the diffusion chamber.

Details of the CCN counters of this type tested at the Ft. Collins workshop can be found elsewhere (Grant, 1971). The Calspan instrument (Kocmond, 1971), in use since late 1964, has demonstrated its reliability at several comparison workshops. One of its distinctive features is the Polaroid camera (ASA film speed of 3,000) and oscilloscope mount, which enables a range of S samples to be recorded on a single film (similar to that of Fig. 2). Light from a 200 W mercury-arc source is collimated by lenses and slits to a ribbon approximately 0.2 cm deep, 0.5 cm high, and several centimeters long.

The Naval Research Laboratory unit (Ruskin and Dinger, 1971), very similar in several respects to Twomey's instrument (Twomey, 1963), also employs a mercury light source and 90° photography. However, an 8 mm movie camera is used to obtain a time sequence of frames, from which the maximum droplet concentration is ascertained. An innovation is the simultaneous viewing of droplet formation with a video camera; immediate playback and subsequent (video recorder) stop-frame counting are provided. Like some others (see, e.g., Bonner and Low, 1971), this system incorporates a preconditioning chamber for sample equilibration before injection into the chamber. When used at altitude in an aircraft, this feature is quite valuable.

Automatic Static Chambers

Photographic recording of droplets, while proven quite reliable, presents tedious data analysis problems. It tends to inhibit studies of CCN variations over fine time and space scales. Recent attempts to overcome this limitation have resorted to estimating droplet concentrations by means of light-scattering methods—either from a large volume of scatterers or from discrete drops individually counted.

The volume scattering approach is employed in a University of Washington CCN counter (Radke, 1971; Radke and Hobbs, 1969). Because light is scattered by drops in proportion to the squares of their sizes, it is essential to this method that the

Fig. 3 Typical spectra of concentrations of CCN vs supersaturation. Data can often be approximated by power functions of the form $N = cS^k$, *where* c *and* k *are constants for a given aerosol. The dashed portion of the line for oceanside at Hilo, Hawaii, represents extrapolated values.*

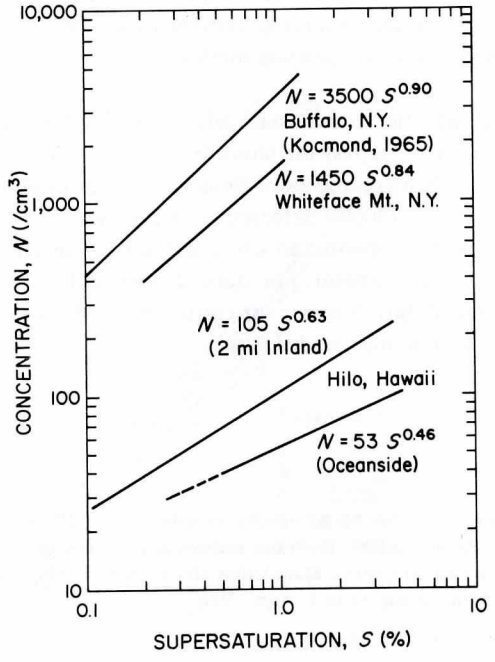

Table 1 Design Characteristics of Static Diffusion Chambers

Chamber aspect ratio (diameter to height)	≥ 5
Maximum chamber height	1 to 2 cm
Minimum reliable supersaturation	0.1 to 0.2%
Typical maximum supersaturation	1 to 3%
Maximum droplet concentration	$1 \text{ to } 2 \times 10^3/\text{cm}^3$
Intake sample air temperature	Top plate T_w
Intake sample airflow, F	
(a) Type	Nonturbulent
(b) Chamber flushings	≥ 4 to 5
(c) Tube length, L, vs flow	$F\ (\text{cm}^3/\text{s}) \geq \frac{L\ (\text{cm})}{10}$
Minimum drop size detected	$r \approx 1\ \mu\text{m}$

drops be of reasonably uniform and known size for concentration determinations. Standard calculations of droplet growth, beginning with a broad range of particle sizes and chemical composition, show that at $S \geqslant 1\%$, a cloud rapidly becomes monodisperse (Jiusto, 1967). At lower supersaturations, drop spectrum broadening increases but may well be at acceptable accuracy levels down to approximately 0.2% S, as stated for this unit. A xenon flash tube illuminates a large volume of the chamber when the cloud has become reasonably monodisperse. A laser beam at a 20° forward-scattering angle helps determine drop spread and the first Mie peak. At this point, the scattering coefficient, k_s, and mean size, r, of the drops are known, so that the cloud's scattered light, b, measured with a phototube, yields droplet concentration, N, by the following relation:

$$N = b/(k_s \pi r^2) \qquad (1)$$

This instrument compared favorably with the other CCN counters examined at the Ft. Collins workshop. (A commercial version of the Radke counter is Model 1521, manufactured by Meteorology Research, Inc., Altadena, California.)

Another light-scattering instrument is manufactured by Mee Industries, Inc., of Rosemead, California (Model 130). It is compact (15 X 43 X 50 cm), portable (18 kg), and supposedly capable of unattended operation at a fixed supersaturation or semiautomatic operation over a range of $S \leqslant 4\%$. It can be operated from either alternating or direct current power sources. A thermal diffusion chamber (30 cm^3 in volume) is illuminated with a collimated beam from a low-intensity (25 W) tungsten lamp. Light scattered from the cloud is received in the forward direction by a high-sensitivity photodetector. Correspondence between the droplet concentration and total light scattered is accomplished by microscopic calibration. The cloud drops are viewed with a microscope (at the top of the instrument); their concentration is determined by means of a ruled reticle, and the scattered light analog is adjusted to correspond. Because of low lamp intensity (to minimize power needs when airborne), the drops are difficult to see until they have reached a size at which they are sedimenting. Then concentration estimates are generally possible, though less reliable. As described below, mean droplet size will vary with supersaturation, so that this calibration should be done at various S levels for acceptable accuracy, a feature not presently provided for. These limitations (low lamp power and a single overall calibration) presumably could be readily correctable. The nucleus count (per cubic centimeter) is displayed in digital form on the front panel, along with T_w and ΔT; all information can be appropriately recorded.

Another fully automatic CCN counter is that of the State University of New York (Lala and Jiusto).[2] The basic instrument has been in use since 1968 and retains some of the general features of the unit at Calspan, where it was initially designed. These include the 90° Polaroid recording camera and a modified optics system. In addition to this absolute counting method, a corresponding light-scattering method (apparently similar to Mee's) recently has been incorporated for automatic operation. A 150 W quartzline lamp and highly sensitive photodetector (at 45° forward scatter) provide ample signal of roughly 0.4 - 1.5 mV per drop. The instrument can be programmed to operate fully automatically and unattended with several options:

- Air samples every 1 min to 1 h or more
- Chamber operation at four sequential supersaturations (e.g., 0.25, 0.5, 0.75, and 1% S) for every designated sampling interval, or at one fixed S
- Digital display and recording of N, T_w, and ΔT

Measurements indicate that the mean drop size at peak cloud concentration (prior to fallout) increases from approximately $r = 1$ μm to 2.5 μm as S increases from 0.25 to 1.0%. The size increase is reflected in the character of the scattered light spectrum and is appropriately calibrated via the photographic method. Thus far, the calibrations——one for each operating supersaturation level——appear consistent and stable (see Fig. 4).

A promising method for rapidly processing droplet images on photographs and negatives is with an automatic image analyzer. Preliminary tests with a Leitz instrument (Classimat Model or Texture Analyzer System, E. Leitz, Inc., Rockleigh, New Jersey) showed general agreement to within 15% of the manual photographic counting method.

A direct scheme for automatically measuring droplet concentrations is to pass the cloud through an optical counter (e.g., Climet, Royco, Southern Research Institute) in which each drop is individually detected. Using forward-scatter optics, these instruments can size and count drops greater than about 0.3 μm in diameter. For static diffusion chambers, this is not practical, but dynamic- or continuous-airflow counters can use this principle to advantage.

[2] G. Lala and J. Jiusto: An automatic recording cloud-diffusion chamber. Paper available from the authors at the Atmospheric Sciences Research Center, State University of New York, Albany; it has also been submitted to *J. Appl. Met.*

Dynamic-Flow Chambers

Continuous-flow CCN instruments apparently had their origin in Russia. Laktionov's vertical counter (1968) consists of two coaxial, cylindrical, wet tubes through which sample air passes. Droplets leaving the diffusion chamber are individually counted photoelectrically. Such chambers introduce a certain design complexity but proponents claim an advantage in physically separating the function of droplet growth at the prescribed supersaturation from that of droplet counting.

Hudson and Squires (1973) have developed a dynamic system that features a laminar air-sample flow (~1 cm^3/s) between two streams of particle-free sheath air along horizontal plates (h = 1.3 cm; traverse length and depth ≈29 cm) and individual droplet sensing with a Royco Model 225 (Royco Instruments, Inc., Menlo Park, California) optical counter just downwind of the chamber. The system has the advantages of a high sampling rate and an ability to size drops (haze discrimination); moreover, the authors claim that the problems associated with static chambers are lessened with this instrument.

Another dynamic chamber of horizontal parallel-plate design has been developed (Fukuta and Saxena, 1974; Fukuta, Saxena, and Gorove, 1974) which simultaneously produces air streams of varying supersaturations. The plates are 122 cm long, 30.5 cm wide, and 1.1 cm apart. Heat is conducted across the upper plate, down a conducting wall, and back through the bottom plate to a nonconducting wall. Varying vertical temperature gradients are thus produced across the chamber and, combined with moisture surfaces (filter paper) of different widths, a range of S from ~0.17 to 4% and different droplet growth times can be achieved. A Climet Model 0294 - 1 optical counter (Climet Instruments Co., Redlands, California) rides on a platform at the downstream exit of the chamber, perpendicular to the airflow; a complete scan of droplet concentrations over the S range is accomplished in 15 s. Careful control of sample flow rate versus S must be maintained to prevent droplet fallout; alternately, the sheath air surrounding the air sample entering an optical counter must not be allowed to heat up and evaporate droplets.

Fig. 4 Scattered light signal vs CCN concentration. The sample volume was ~0.1 cm^3.

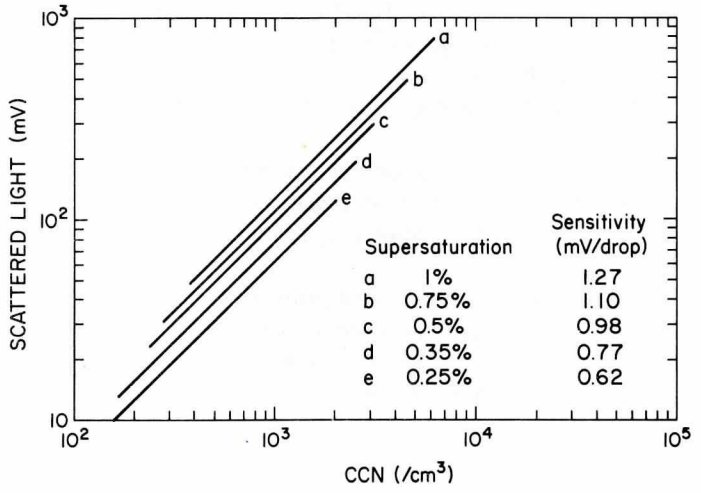

It is not yet evident that these dynamic CCN counters provide substantially greater accuracy or reliability than simpler static-diffusion chambers. Until comparison data are available, one cannot judge. Their strength appears to be the automatic droplet-counting feature, which is gained at the expense of added complexity in the control of sample flow and temperature fields.

Lower Supersaturation Chambers

Most information to date on cloud nuclei has been acquired at $S > 0.1$ or 0.2%. Yet it is known that many clouds or portions of clouds have supersaturations below this threshold. Two problems arise in detecting active cloud nuclei at low S: the growth rate of drops and fallout is much slower prior to detection; and the drops must be allowed to grow large enough to be distinguished from haze. To help circumvent these limitations, tall vertical chambers with continuous (dynamic) flow are being developed.

Sinnarwalla and Alofs (1973) have constructed a tube 100 cm high with a plate separation of 1 cm. The growth time is approximately eight times that of a conventional chamber. Such configurations and time scales introduce problems of convection and phoretic (vapor and thermal diffusion) forces that can deflect drops toward the colder wall surface. These effects reportedly are accounted for in this system, however, and the resultant drops are optically counted with a phototube and laser beam.

In unique fashion, Hudson and Squires (1974) merely tilt their horizontal dynamic counter (previously described) on end to achieve a 40 cm fall distance. Operating the counter alternately in the horizontal and vertical modes, they report concentration agreement to 1% across the overlapping range of about 0.3 to 0.7% S.

Perhaps the most ingenious and simplest approach——and the one potentially yielding the lowest values of S——has been advanced by Laktionov (1972) and reviewed in the literature by Alofs and Podzimek (1974). Laktionov derived a simple

relationship between critical supersaturation, S^*, and the size of droplets at 100% relative humidity that have condensed on hygroscopic nuclei:

$$S^* \simeq 0.04/r_{100} \quad (2)$$

Thus the equilibrium radius of a nucleus at saturation is related to critical supersaturation independently of nucleus solubility. (Completely nonhygroscopic or hydrophobic nuclei would yield a different S^*, but these particles are generally less common.) In short, simply by fitting a wet tube of appropriate length to a commercial optical counter, a low-supersaturation CCN instrument presumably is obtained. For example, a Royco 225 counter with five size thresholds from radii of 0.25 to 7.5 μm would conceivably count hygroscopic nuclei at supersaturations from approximately 0.168% down to 0.005%. Experimental verification of the concept is not yet available.

Summary

CCN counters incorporate a number of interesting physical and instrumental principles. When they are properly designed, the end product provides, over prescribed limits, quite acceptable accuracy and reliability.

A rich variety of innovations in CCN counters has appeared in recent years, the most notable features perhaps being more rapid processing of nucleus concentration data, automatic operation of certain instruments, continuous air sample flow, fine-time-scale acquisition of more reliable data, and extension of the supersaturation range to well below 0.2% S.

Twomey-type static-diffusion chambers generally have proven themselves in comparison workshops and in corresponding cloud-variable measurements. This type of chamber, updated with appropriate light-scattering methods for automatic drop sensing, offers a means for unattended counter operation. Low S counters require quite different configurations, which now appear obtainable.

As a cloud physics tool, the CCN counter has yielded considerable information on droplet growth and nucleation processes in clouds. The correlation between CCN spectra and initial drop size distributions in clouds has been demonstrated by several investigators. Insights into the size, composition, and global distribution of effective cloud nuclei have also been obtained. With the improved apparatus and techniques mentioned, it can be anticipated that knowledge of aerosol and cloud physics processes will increase substantially.

References

Alofs, D., and J. Podzimek, 1974: A review of Laktionov's isothermal cloud nucleus counter. *J. Appl. Met. 13*, 511 - 512.

Bonner, R., and R. Low, 1971: Condensation nuclei counter, Model ECOM-ASL 001. In *Second International Workshop on Condensation and Ice Nuclei* (L. Grant, Ed.), August 1970, Colorado State University, Ft. Collins, Colo., 44.

Fitzgerald, J., 1970: Non-steady state supersaturations in thermal diffusion chambers. *J. Atmos. Sci. 27*, 70 - 72.

Fukuta, N., and V. Saxena, 1974: *Cloud Condensation Nucleus Spectrometer.* Annual Report, Contract No. N00019 - 73 - C - 0176, Denver Research Institute, University of Denver.

———, ———, and A. Gorove, 1974: CCN Spectrometer II: Measurements on the natural aerosol. In Preprint Vol., Conference on Cloud Physics, held 21 - 24 October at Tucson, Ariz.; American Meteorological Society, Boston, Mass., 361 - 366.

Gagin, A., and B. Terliuc, 1968: A modified Wieland-Twomey thermal-diffusion cloud nuclei counter. *J. Rech. Atmos. 3*, 73 - 77.

Grant, L. (Ed.), 1971: *Second International Workshop on Condensation and Ice Nuclei*, August 1970, Colorado State University, Ft. Collins, Colo., 149 pp.

Hudson, J., and P. Squires, 1973: Evaluation of a recording continuous cloud nucleus counter. *J. Appl. Met. 12*, 175 - 183.

———, and ———, 1974: Evaluation of a vertical continuous cloud chamber. In Preprint Vol., Conference on Cloud Physics, held 21 - 24 October at Tucson, Ariz.; American Meteorological Society, Boston, Mass., 368 - 369.

Jiusto, J., 1967: *Nucleation Factors in the Development of Clouds.* Ph.D. dissertation, Department of Meteorology, Pennsylvania State University, 124 pp.

Kocmond, W. C., 1965: Investigation of warm fog properties and fog modification concepts. In *Second Annual Report*, Report No. RM - 1788 - P - 9, Cornell Aeronautical Laboratory, Buffalo, N.Y., 36 - 47.

———, 1971: Cornell Aeronautical Lab. (Calspan) thermal diffusion chamber. In *Second International Workshop on Condensation and Ice Nuclei* (L. Grant, Ed.), August 1970, Colorado State University, Ft. Collins, Colo., 40 - 41.

Laktionov, A., 1968: Photoelectric measurements of condensation cloud nuclei. *J. Rech. Atmos. 3*, 63 - 70.

———, 1972: Isothermal method for the determination of cloud condensation nuclei concentrations. *Izv. Akad. Nauk. SSSR, Fiz. Atmos. Okeana 8*, 672 - 677.

Langsdorf, A., 1936: A continuously sensitive cloud chamber. *Phys. Rev. 49*, 422.

Radke, L., 1971: An improved automatic cloud condensation nucleus counter. In *Second International Workshop on Condensation and Ice Nuclei* (L. Grant, Ed.), August 1970, Colorado State University, Ft. Collins, Colo., 41 - 42.

———, and D. Hegg, 1971: Experimental observations on "Non-steady-state supersaturations in thermal diffusion chambers." *J. Appl. Met. 10*, 340 - 341.

———, and P. Hobbs, 1969: An automatic CCN counter. *J. Appl. Met. 8*, 105 - 109.

Ruskin, R., and J. Dinger, 1971: Description of NRL CCN equipment. In *Second International Workshop on Condensation and Ice Nuclei* (L. Grant, Ed.), August 1970, Colorado State University, Ft. Collins, Colo., 43 - 44.

———, and W. Kocmond, 1971: Summary of CN investigations at the 1970 International Workshop. In *Second International Workshop on Condensation and Ice Nuclei* (L. Grant, Ed.), August 1970, Colorado State University, Ft. Collins, Colo., 92 - 97.

Saxena, V., and J. Kassner, 1970: Thermal-diffusion chambers as cloud-nuclei counters. In *Precipitation Scavenging*, AEC Symposium Series 22, 217 - 238.

———, J. Burford, and J. Kassner, 1970: Operation of a thermal diffusion chamber for measurements on CCN. *J. Atmos. Sci. 27*, 73 - 80.

Sinnarwalla, A., and D. Alofs, 1973: A cloud nucleus counter with long available growth time. *J. Appl. Met. 12*, 831 - 835.

Squires, P., 1972: Diffusion chambers for the measurement of cloud nuclei. *J. Rech. Atmos. 6*, 565 - 572.

Twomey, S., 1959: The nuclei of natural cloud formation, I. *Geofis. Pura Appl. 43*, 227 - 242.

———, 1963: Measurements of natural cloud nuclei. *J. Rech. Atmos. 1*, 101 - 105.

———, 1967: Remarks on the photographic counting of cloud nuclei. *J. Rech. Atmos. 3*, 85 - 90.

Wieland, W., 1956: Die Wasserdampfkondensation an natürlichem Aerosol bei geringen Übersattigungen. *Z. Angew. Math. Phys. 7*, 428 - 459.

Instrumentation for the Detection of Ice Nuclei

G. Garland Lala, SUNY at Albany

The importance of the ice phase in the formation of precipitation at high and middle latitudes has long been accepted by cloud physicists. The role of ice nuclei in the initiation of the ice phase in clouds has been well established, but the relationship of the concentration of ice nuclei to the concentration of ice crystals in clouds has remained elusive. This is owed in part to the inadequacy of our techniques for measuring ice nucleus concentrations and in part to the complicated nature of ice multiplication processes, whereby ice crystals increase in number by interacting with crystals and droplets in the cloud environment. The discrepancy among various ice nucleus counters was clearly demonstrated at the Second International Workshop on Condensation and Ice Nuclei, where the typical spread in the measurements was 100:1, with extremes of 10,000:1 (Bigg, 1971). The treatment given here will not attempt to explain these differences, but rather will concentrate on the principle of operation of various instruments and the relationship of their results to ice nucleation mechanisms.

Ice Nucleation Mechanisms

Four processes may be considered as possible mechanisms for ice phase nucleation in the atmosphere: deposition (sublimation), immersion freezing, contact freezing, and homogeneous freezing. Deposition nucleation does not require the presence of water droplets for activation. This is usually considered as the direct formation of ice on a nucleus from the vapor (Fletcher, 1962). A related process, called sorption nucleation, involves adsorption of water molecules onto a nucleus, followed by freezing. As referred to here, deposition nucleation will include both of these processes since they are indistinguishable in most ice nucleus detectors.

Author

G. Garland Lala, a research associate at the Atmospheric Sciences Research Center of the State University of New York (SUNY) at Albany, received a B.S. from Massachusetts Institute of Technology in 1967, and M.S. and Ph.D. degrees from SUNY at Albany in 1970 and 1972, respectively. His research interests center on the study and measurement of cloud condensation and ice nuclei, as well as numerical modeling of the formation of radiation fog.

Freezing nucleation (heterogeneous initiation of the liquid-solid phase transition) may occur either by a nucleus making contact with a drop or by a nucleus immersed in a drop. A distinction is made between two types of freezing nucleation because experimental laboratory evidence has shown contact nucleation to be more effective than immersion nucleation. In nature, contact nucleation can occur by the collection of a dry particle through any of several scavenging mechanisms. Immersion of a particle may occur in the same manner, depending on the nature of the particle and the circumstances of collection, or through condensation on a particle. If the condensation takes place on a mixed nucleus (partially soluble) that contains an ice nucleus, freezing nucleation will be complicated by the freezing point depression due to the presence of a dissolved salt.

Homogeneous freezing occurs through the random formation of an embryo in the liquid phase. This mechanism occurs primarily in cirriform clouds and cumulus anvils, since the nucleation rate for homogeneous freezing becomes important only at temperatures approaching -40°C. Ice nucleus detectors are rarely, if ever, operated at temperatures this low; thus homogeneous freezing can be excluded from practical consideration.

Ice Nucleus Counters: Minimum Requirements

Most ice nucleus counters operate by bringing an air or aerosol sample into an environment that simulates, as nearly as possible, conditions found in supercooled clouds. Some of the particles in the sample act as nuclei; the resulting ice crystals grow to a detectable size and are counted by some method. Thus the results of nucleation events (ice crystals) are counted, not the events themselves. The performance of an ice nucleus detector is very sensitive both to how well it simulates supercooled cloud conditions and to how well it is able to maintain these conditions reproducibly. Individual ice nucleus detectors differ primarily in the way the simulated environment is produced and in the way the resulting crystals are counted.

The significant variables in simulating a cloud environment are temperature, humidity, droplet size and concentration, and time available for nucleation to occur. Instruments using different methods do not produce the same conditions, which undoubtedly accounts for most of the variations among ice nucleus counters. Because of these differences in operating conditions, care must be exercised in extending the results to processes in clouds.

Estimates of the volume of sample required can be obtained from examination of crystal concentrations measured in

clouds and of data from the various instruments. The extremes of cloud crystal concentrations range from 100 crystals per cubic meter to values approaching 10^6 crystals per cubic meter. This sets a lower limit on sample volume of $10^{-2}m^3$ and at the same time requires the counting scheme to handle up to 10^4 ice crystals in the sample volume. Such a high concentration is rarely observed in ice nucleus detector sampling from the atmosphere. A more realistic value of the maximum count to be expected from a 0.01 m^3 sample is on the order of 10^3. The measured temperature spectrum of ice nuclei (Fig. 1) shows an increase of a factor of ten for each 4° of supercooling. For an instrument designed to operate over the range of temperature from −15 to −30°C, this corresponds to a range of concentration of 10^3 or more. Thus, an ice nucleus counter must use a minimum of 0.01 m^3 of sample air and be able to provide accurate counts for concentrations up to 10^4 crystals in this volume.

To place ice nucleus counts in perspective relative to the total aerosol count, consider a single ice nucleus at −15°C. This particle is outnumbered by Aitken nuclei by a factor of 10^7 to 10^9 and by cloud condensation nuclei by a factor of 10^6 to 10^7. Thus, in terms of the total aerosol concentration, ice nuclei are present only in trace concentrations.

Several types of ice nucleus counters are used routinely to determine ice nucleus concentrations. These instruments use different methods to model the cloud environment and different schemes for counting ice crystals. The following discussion will present an overview of the more common instruments and provide a rough interpretation of their characteristics in terms of nucleation mechanisms.

Chambers: Mixing, Diffusion, Cloud-Settling

- *Mixing chambers* are cold boxes of large volume in which clouds are maintained by adding moisture from a droplet generator or by evaporation from a warm water reservoir. The air sample to be studied is introduced into the chamber where it mixes with the supercooled cloud, resulting in the formation of ice crystals. Crystal concentrations are determined by visually counting the number of ice crystals in an illuminated volume or by collecting crystals in a supercooled sugar solution by sedimentation. The sugar solution provides a medium for the growth of ice crystals to millimeter sizes in less than a minute.

Temperature and humidity control in mixing chambers is not very good. In regions where the sample is introduced, the humidity is generally less than water saturation, but high supersaturations may occur in the region near the moisture source. Visual counting in a small illuminated volume can also contribute large errors, especially at low crystal concentrations. Use of the supercooled sugar solution can also lead to errors if care is not taken to prevent frost formation on the chamber walls. Frost crystals that break off and fall into the sugar solution are indistinguishable from crystals formed in the cloud.

- The operation of *diffusion chambers* is similar to that of mixing chambers. In the diffusion chamber, the air sample is cooled to the prescribed temperature and then humidified by allowing water vapor from a warm reservoir to diffuse into the sample volume, resulting in a supercooled cloud. Ice crystal concentrations are determined by counting in an illuminated volume or by collection with a supercooled sugar solution. Temperature control with diffusion chambers is better than with mixing chambers, but the humidity varies from high supersaturations near the moisture source to slight saturation far from the moisture source.

- The *cloud-settling chamber* is similar to the diffusion chamber, but the humidity control is better. The chamber designed by Ohtake (1971) consists of an isothermal cold box capped by a Plexiglas cylinder which supports a warm moisture source (Fig. 2). The unique feature of this chamber is that condensation occurs at near room temperature within the Plexiglas section and the resulting droplets settle into the cold

Fig. 1 Typical natural ice nucleus temperature spectrum exhibiting an exponential form.

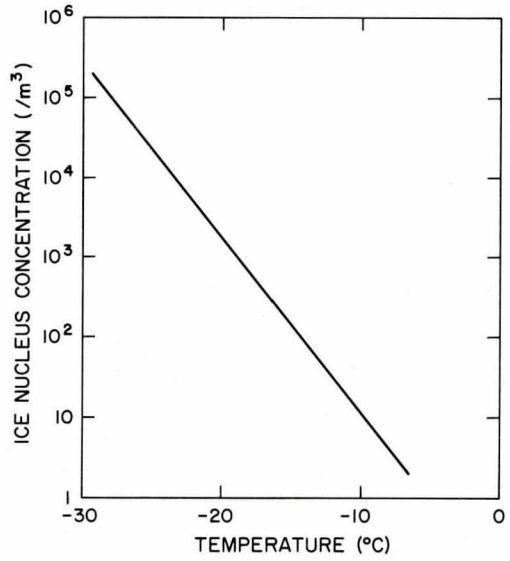

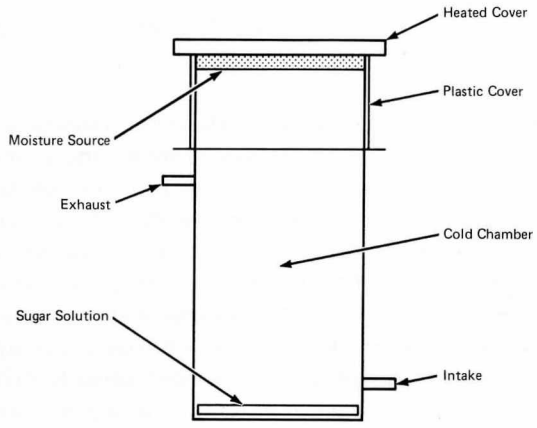

Fig. 2 Cloud-settling chamber.

Fig. 3 NCAR acoustic counter.

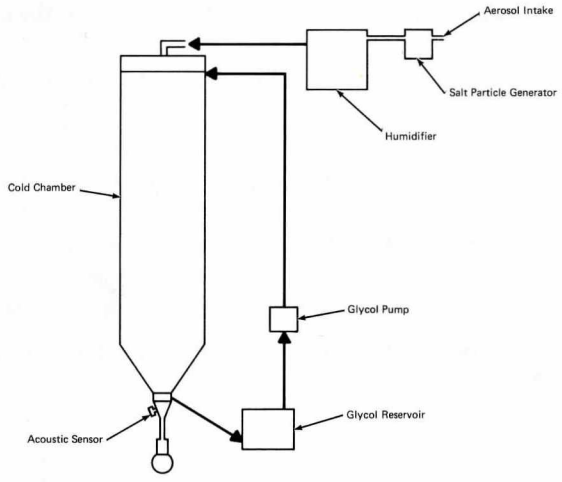

section of the chamber, avoiding the large transient supersaturations which can occur when warm saturated air is mixed with very cold air. The mean drop size can be controlled by the temperature of the humidifier, with a typical mean diameter of 10 μm corresponding to a supersaturation of about 1%. The operation of this chamber is the same as for a diffusion chamber, and the crystals are detected by means of a supercooled sugar solution.

The Colorado State University (CSU) isothermal cloud chamber (Slusher, Katz, and Grant, 1971) is a unique combination of both the diffusion and cloud-settling principles. This instrument is a large, cylindrical chamber with a working volume of 1.4 m^3 whose temperature can be regulated within 0.1°C. Moisture—in the form of droplets produced by an ultrasonic nebulizer—is continuously introduced into the center of the chamber and distributed throughout the volume. Aerosol samples are introduced by a syringe through a small opening in the side of the chamber. The number of ice crystals forming in the chamber is determined by observing sedimentation onto microscope slides near the bottom of the chamber. This detection method limits the apparatus to use for high concentrations such as those one would expect from artificial nuclei.

All of these chambers can activate nuclei by deposition and immersion freezing, but the available time (on the order of 3 - 5 min) is generally too short for any appreciable contribution by contact freezing. The cloud-settling chamber and the CSU isothermal chamber are possible exceptions: the large droplet concentration in the former and the long time available in the latter make it possible to activate a measurable fraction of the contact nuclei. Deposition nucleation is probably inhibited in chambers with high transient supersaturations because on most nuclei condensation will occur first. Interpretation of the counts from mixing and diffusion chambers is quite complicated because of the lack of control over the temperature and humidity, but the situation is better with the cloud-settling chamber, where these conditions are controlled and reproducible. The performance of the cloud-settling chamber at the Second International Workshop showed it to be one of the more consistent instruments, giving reasonable results (Bigg, 1971).

NCAR Acoustical Counter

The NCAR acoustical counter is essentially a continuous-mixing chamber (Fig. 3). Operation consists of adding condensation nuclei and water vapor to the sample followed by cooling (by mixing and conduction of heat to the walls of the cold chamber), resulting in the formation of a supercooled cloud. At the bottom of the chamber, the sample is drawn through an acoustical detector in which the air and particles are accelerated and then rapidly decelerated, resulting in an audible click for particles greater than 20 μm in diameter. The acoustical signal is detected by a microphone and counted electronically. Successful operation requires that the ice crystals exceed the acoustical threshold size while the cloud droplets remain smaller and pass through the sensor undetected. This condition is insured by adding sufficient salt nuclei to keep the drop size below the threshold value.

Frost formation is prevented by maintaining a constant flow of glycol down the chamber walls, which are covered with a porous lining to ensure even distribution. The glycol circulation is a closed system driven by a pump which carries the glycol from a reservoir to the top of the chamber where it flows down the walls into a collector and back to the reservoir.

The supersaturation produced at the point of mixing is quite high, with the result that most of the particles presumably form ice crystals by condensation followed by freezing (immersion freezing). The sample flow rate limits the residence time in the chamber to about 2 min, which is too short for any appreciable nucleation by contact nuclei that may have survived the initial high supersaturation.

One of the greatest problems of this counter is the low counting efficiency (due to the low air velocity in the chamber), which results in a considerable loss of crystals by sedimentation before they can reach the sensor. Correction factors have been determined experimentally for several types of nuclei (Langer, 1973) with a typical value of nine for atmospheric nuclei. This study showed a slight dependence of ice nucleus concentration on temperature as well as on the type of nucleant.

The capability of continuous operation is a strong asset of this instrument, making it very useful for plume tracking in cloud-seeding experiments. With careful calibration the instrument should provide consistent results, but interpretation of the counts will always be difficult because of the high supersaturation occurring at the sample inlet.

Filter Technique

The filter technique represents an entirely different approach to the problem of ice nucleus concentration measurement. Briefly, the technique consists of sampling a known volume of air by filtering, with subsequent activation of ice nuclei on the filter and growth of ice crystals in a temperature- and humidity-controlled chamber. The major advantages of the technique are that a prescribed volume of air can be sampled for processing at a later time and the conditions of processing can be carefully controlled.

The processing chambers used most recently operate on the same principle as a dew-point hygrometer. The filter is held at a constant temperature (T_f) in an ice-saturated environment at a warmer temperature (T_i). The temperature difference ($T_i - T_f$) determines the humidity over the filter. After a processing period (from 15 min to 1 h), the ice crystals that have grown on the nuclei are counted visually with the aid of a low-power microscope. A design by Stevenson (1968) uses an insulated volume in which part of the bottom surface is covered with ice and a smaller section is the colder filter support. Another design by Gagin and Aroyo (1969) uses a geometry similar to that of a thermal gradient diffusion chamber, with the top being the ice surface and the bottom the colder filter support (Fig. 4). Designs employing a flow of ice-saturated air over a colder filter have been used by Langer (1971) and by Bigg and Stevenson (1970).

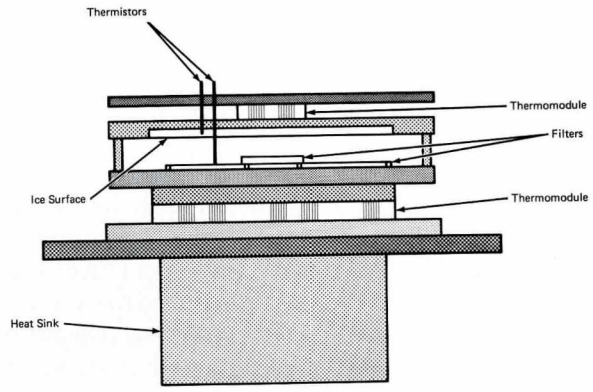

Fig. 4 Filter processing chamber.

The modes of nucleation possible in the filter technique are probably limited to deposition and condensation on mixed nuclei followed by freezing. Competition among the growing particles would in most cases restrict the maximum achievable humidity to an amount less than saturation, preventing the formation of droplets necessary for other modes of nucleation. Huffman (1973) used the filter technique at subsaturated conditions and found that the spectrum of deposition nuclei could be expressed as

$$N = C\, Si^{\alpha}$$

where N is the number of nuclei, Si is the supersaturation over ice, and C and α are constants. In the range of Si from 8 to 22%, the range of α for natural aerosol was from three to eight; for silver iodide the range was about the same but varied somewhat with the method of preparation.

The choice of a chamber height is quite important in the design of a processing chamber. Work in our laboratory and experiments at the International Workshop on Ice Nuclei (Laramie, Wyoming, 1975) have shown that decreasing the

chamber height from 1 to 0.25 cm increases the crystal count by a factor of about four. Analysis of the data indicates that crystal counts increase exponentially with decreasing chamber height. The reason is that reduction of the chamber height increases the humidity over the filter by increasing the available moisture flux and results in the activation of additional nuclei.

The major deficiency of the filter method is the lack of correlation of nucleus concentration with sample volume. This effect was analyzed by Mossop and Thorndike (1966) and attributed to lower humidities in areas around hygroscopic nuclei. A numerical model of a filter processing chamber by Lala and Jiusto (1972) also indicated this effect and showed that growing ice crystals also act to reduce the average humidity over the filter. The results of the model indicate that it may not be possible to achieve water saturation in a processing chamber because of the competition of crystals and hygroscopic particles for the available water vapor. Vali and Huffman (1973) analyzed the volume effect experimentally and theoretically and showed that a correction could be derived on the basis of the number of cloud and ice nuclei in the sample. Further work is needed to substantiate the validity of this correction and show its applicability to other processing chambers that use a different geometry.

A chamber using a flowing stream of air was devised by Langer (1971) in an attempt to increase the available water vapor and reduce the magnitude of the volume effect. At the present time the author is not aware of any comparative studies which show this to be true.

Another aspect of filter processing that can lead to errors is the filter preparation technique. To ensure good contact of the filter with the supporting substrate, some sort of bonding agent is required. Stevenson (1968) and Gagin and Aroyo (1969) have used petroleum jelly for this purpose, while others have used a variety of thick oils. Preparation with the petroleum jelly consists of placing the filter on a smooth surface of petroleum jelly and heating to a temperature of about 45°C, allowing the softened petroleum jelly to fill the filter pores without flooding the upper surface of the filter. Some practice is required to prepare filters reproducibly. Heating the filter and the nuclei may alter the behavior of the ice nuclei, but there is no experimental evidence for this.

The choice of filter type is also important for the success of the technique. Tests at the recent workshop indicate that the standard Millipore filters are significant sinks for water vapor. Higher counts were obtained from Sartorius filters of both the standard and hydrophobic type, without an increase in background counts. Hydrophobic Sartorius filters gave counts about twice those of Millipore filters. Thus, to achieve a realistic count, it is important to choose a filter which does not interfere with the processing.

The filter method is potentially one of the best methods for measuring ice nucleus concentrations under controlled conditions. If improvements in the design of the processing chambers can overcome the volume effect and achieve reliable humidities over the filter, the method may well become the standard for measuring ice nuclei activated by immersion freezing and deposition.

Drop-Freezing Spectrometer

The instruments discussed above are all used to analyze the ice nucleus content of the air samples, whereas the drop-freezing spectrometer is used to analyze the ice nucleus

Table 1
General Characteristics of Ice Nucleus Counters

COUNTER	CLOUD	HUMIDITY	TEMPERATURE CONTROL	NUCLEATION MECHANISMS			TIME (s)
				Immersion Freezing	Contact Freezing	Deposition	
Mixing chamber	Yes	Subsaturation to slight supersaturation	Fair	Yes	No	Yes	200
Diffusion chamber	Yes	Slight subsaturation to supersaturation	Fair	Yes	No	Yes	200
Drop settling chamber	Yes	Slight supersaturation	Good	Yes	No	Yes	200
NCAR acoustical counter	Yes	High supersaturation	Good	Yes	No	No	~150
Filter method	No	Subsaturation to possible small supersaturation	Excellent	Yes	Yes	Yes	900 - 5,600
Drop spectrometer	No		Excellent	Yes	No	No	

content of liquid water. The ice nucleus spectrum of a liquid sample can be used to deduce the ice nucleus concentration in precipitation, thus providing an indication of the number of nuclei that have been incorporated into precipitation by cloud processes. The technique can also be used to study suspensions of soil particles in liquids to give an indication of the number of potential nuclei in soils.

The freezing nucleus spectrum is measured by placing a number of droplets on a temperature-controlled surface and determining the number of droplets that freeze within a given temperature interval as the temperature is lowered. Vali and Stansbury (1966) have indicated that the temperature spectrum of ice nuclei in the sample can be determined from these data. An automatic system to control the cooling, to monitor the temperature, and to record freezing events has been devised and is described in detail by Vali and Knowlton (1971).

The drop-freezing technique offers a convenient way of studying the temperature spectrum of freezing nuclei in liquid suspensions. However, because other modes of nucleation occur in clouds, it must be used in conjunction with other techniques if complete information on ice nuclei in the atmosphere is to be deduced.

A modification of the drop-freezing system for the measurement of contact nuclei has been reported by Vali (1974). In this system, a captive population of droplets is held in a supercooled state while the aerosol is electrostatically deposited on them. The ratio of contact nuclei can be deduced by thawing and refreezing the drops. This technique produces higher counts than other types of ice nucleus counters, but the concentrations are still lower than would be necessary to explain crystal concentrations in clouds.

Summary

It is very difficult to compare ice nucleus counters except in the most general terms because of variations in their operating conditions and because of the large spread in their results. Even instruments of the same design can show significant variations. A summary of the general characteristics of the ice nucleus counters described here is presented in Table 1. For a more detailed comparison of the results of many ice nucleus counters, the reader is referred to the report of the Second International Workshop on Condensation and Ice Nuclei (Grant, 1971).

Ice nucleus counters all share the common objective of simulating the cloud environment in which ice nucleation occurs. The physical principles of operation and instrument configuration vary widely and all can, to some degree, simulate some of the important aspects of the supercooled cloud environment. The wide variation of nucleus counts from different instruments is an indication not so much of inaccuracy of the instrument as of the sensitivity of ice nucleation processes to environmental conditions. What is required is a clearer understanding of the influence of environmental conditions on each mechanism of ice nucleation. This undoubtedly will further the understanding of ice processes in clouds and facilitate the interpretation of ice nucleus counts in terms of nucleation mechanisms. It is not likely that any one ice nucleus counter will be able to provide concentration measurements appropriate to all nucleus types and cloud conditions. Rather, several instruments with differing operating principles will be required to assess the importance of individual nucleation mechanisms under carefully prescribed conditions.

References

Bigg, E. K., 1971: Report on the ice nucleus workshop. In *Second International Workshop on Condensation and Ice Nuclei* (L. Grant, Ed.), August 1970. Colorado State University, Ft. Collins, Colo., 97 - 105.

———, and C. M. Stevenson, 1970: Comparison of ice nuclei in different parts of the world. *J. Rech. Atmos. 4*, 41 - 58.

Fletcher, N. H., 1962: *The Physics of Rainclouds.* Cambridge University Press, 210 pp.

Gagin, A., and M. Aroyo, 1969: A thermal diffusion chamber for the measurement of ice nucleus concentrations. *J. Rech. Atmos. 4*, 115 - 122.

Grant, L. (Ed.), 1971: *Second International Workshop on Condensation and Ice Nuclei*, August 1970. Colorado State University, Ft. Collins, Colo., 149 pp.

Huffman, P. J., 1973: Supersaturation spectra of AgI and natural ice nuclei. *J. Appl. Met. 12*, 1080 - 1082.

Lala, G. G., and J. E. Jiusto, 1972: Numerical estimates of humidity in a membrane filter ice nucleus chamber. *J. Appl. Met. 11*, 674 - 683.

Langer, G., 1971: NCAR ice nucleus analyzer. In *Second International Workshop on Condensation and Ice Nuclei* (L. Grant, Ed.), August 1970. Colorado State University, Ft. Collins, Colo., 55 - 56.

———, 1973: Evaluation of NCAR ice nucleus counter. Part I: Basic operation. *J. Atmos. Sci. 12*, 1000 - 1011.

Mossop, S. C., and N. S. C. Thorndike, 1966: The use of membrane filters in measurements of ice nucleus concentrations. I. Effect of sampled air volume. *J. Appl. Met. 5*, 474 - 480.

Ohtake, T., 1971: Cloud-settling chamber for ice nuclei count. In *Second International Workshop on Condensation and Ice Nuclei* (L. Grant, Ed.), August 1970. Colorado State University, Ft. Collins, Colo., 58 - 60.

Slusher, T., U. Katz, and L. Grant, 1971: CSU isothermal cloud chamber. In *Second International Workshop on Condensation and Ice Nuclei* (L. Grant, Ed.), August 1970. Colorado State University, Ft. Collins, Colo., 60 - 61.

Stevenson, C. M., 1968: An improved Millipore filter technique for measuring the concentration of freezing nuclei in the atmosphere. *Q. J. R. Met. Soc. 94*, 35 - 43.

Vali, G., 1974: Contact ice nucleation by natural and artificial aerosols. In Preprint Vol., Conference on Cloud Physics, held 21 - 25 October at Tucson, Ariz.; American Meteorological Society, Boston, Mass., 34 - 37.

———, and P. J. Huffman, 1973: The effect of vapor depletion on ice nucleus measurements with membrane filters. *J. Appl. Met. 12*, 1018 - 1024.

———, and D. Knowlton, 1971: An automated drop freezer system for determining the freezing nucleus content of water. In *Second International Workshop on Condensation and Ice Nuclei* (L. Grant, Ed.), August 1970. Colorado State University, Ft. Collins, Colo., 75 - 79.

———, and E. J. Stansbury, 1966: Time-dependent characteristics of the heterogeneous nucleation of ice. *Can. J. Phys. 44*, 477 - 502.

NUMBER 8 – SPRING 1976

A Review of Recently Developed Instrumentation to Measure Electric Fields inside Clouds

W. David Rust, National Oceanic and Atmospheric Administration

The reliable measurement of electric fields inside clouds is recognized as fundamental to attempts to describe quantitatively the electrical conditions that exist inside clouds, including the location, polarity, and magnitude of charge centers and the regions where maximum fields are most likely to occur. Some attempts were made in the early 1900s to use balloons to measure electric fields aloft (summarized in Chalmers, 1967), but most of the early measurements were obtained when clouds engulfed measuring sites, which were frequently located atop mountains. It is particularly important, however, to measure electric fields away from the boundary effects of the earth.

The measurement of electric fields inside clouds is difficult. The apparatus and its transporting vehicle distort the quantity being measured; the high humidity and precipitation generally encountered may cause instrumental problems, such as leakage across high-impedance insulation. The charging of the instrument by precipitation or other means may produce a field that is often difficult to separate from the external field. Moreover, charged precipitation striking and splashing from the instrument can cause severe noise problems, and corona discharge from the instrument in the presence of high electric fields may generate a space charge that can alter the local electric field enough to vitiate a measurement.

This article discusses several of the relatively new instruments developed to measure electric fields aloft within clouds, including rocket-, balloon-, and aircraft-borne devices. Omitted from this discussion are instruments that use radioactive probes as the sensing elements. Although this technique is useful in some instances if used with care, its reliability in making measurements inside highly electrified clouds has been questioned by several investigators. The use of radioactive probes has been described in detail by Vonnegut, Moore, and Mallahan (1961); Chalmers (1967); Lane-Smith (1974); and others.

Instrumented Rockets

Rockets carrying electric-field measuring devices through clouds can produce nearly instantaneous profiles of the measured components of the electric field along their flight trajectories. It is difficult, however, to obtain measurements horizontally through a cloud with rockets launched from the ground. In addition, there are only a few locations within the continental United States where airspace restrictions permit the firing of adequately large rockets. In spite of their limitations, rockets are useful vehicles, and two different techniques using instrumented rockets are described here.

One rocket-borne electric field meter has been developed by Winn and Moore (1971) for measuring the component of the electric field perpendicular to the longitudinal axis of the rocket. The rocket type used is the military Mark 40, Model 1, which has a solid-fuel motor; the body of the rocket is 70 mm in diameter and about 1.5 m long when equipped with the electric-field measuring nose. The rockets are generally launched from Langmuir Laboratory, which is located on a mountain ridge (at an elevation of 3.2 km) in central New Mexico; they attain altitudes of about 7 or 8.5 km, depending on the launch technique used.

Author

W. David Rust conducts research on thunderstorm electrification and lightning suppression for the Atmospheric Physics and Chemistry Laboratory of the National Oceanic and Atmospheric Administration. He graduated from Southwestern University and pursued further studies in physics at New Mexico Institute of Mining and Technology, earning his Ph.D. in 1973. As a recipient of a National Research Council postdoctoral resident associateship for two years, he studied the use of balloon- and aircraft-borne instruments for measuring electrical parameters of clouds. During the Viking II mission to Mars, his work included the use of real-time atmospheric electricity measurements to protect rockets from the dangers of triggered lightning.

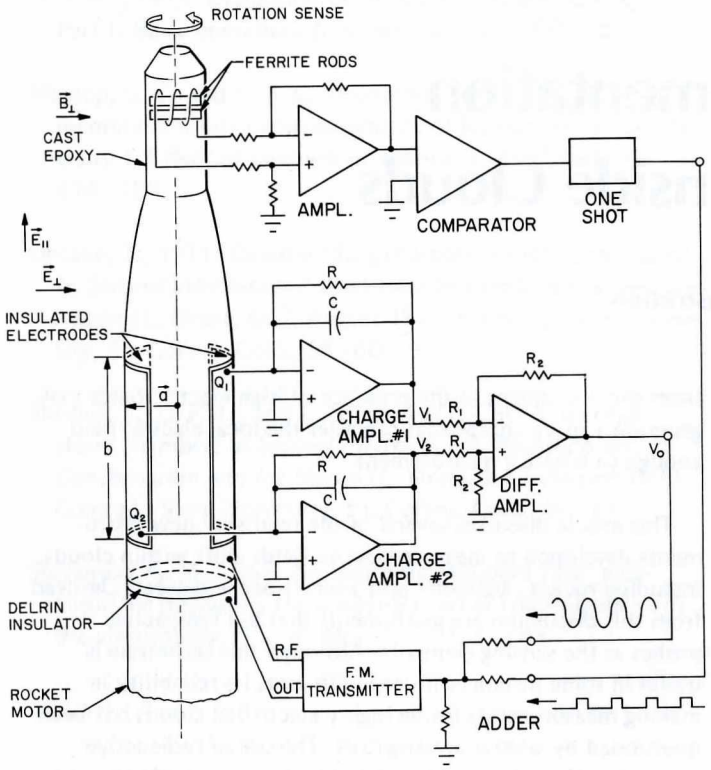

Fig. 1 Schematic of instrumented rocket payload for measuring the electric field component perpendicular to the rocket body. (Winn and Moore, 1971.)

The instrument is shown schematically in Fig. 1. The sensing electrodes are placed on the dielectric nose portion of the rocket and covered with shrinkable Teflon to increase the onset threshold of the corona. The rocket, which is generally launched nearly vertically, is made to spin about its axis by the use of canted fins. As the rocket rotates, equal and opposite charges are induced upon the sensing plates by the perpendicular component of the field. The plates are connected to charge amplifiers so that their output voltage is independent of the rocket spin rate. Subtraction of the signals from each plate using a differential input amplifier allows a determination of the external field normal to the rocket's longitudinal axis.

The direction of this perpendicular component of the field relative to the earth's magnetic field is determined by comparing the phase of a signal from a rotating coil and that from the field sensors. (Both the coil and the field sensors are fixed within the epoxy nose of the rocket.) The electric field and direction data are telemetered back to a ground receiving station by using the electric-field signal to modulate directly the oscillator of an FM transmitter.

Since the rocket-borne sensor must rotate in an external field to obtain a measure of that field, direct calibration of the device by placing it in known electric fields is difficult and has not been done. This is not a serious disadvantage since the calibration obtained from the characteristics of the electronic circuitry and the cylindrical geometry of the rocket is straightforward and reasonably accurate. In addition, the rotating coil, which senses the earth's magnetic field, is used to produce, once during each revolution, a calibration pulse whose magnitude can be compared with the signal produced by the electric field. This technique provides an in-flight system calibration.

As Winn and Moore (1971) state, care must always be exercised when making measurements of electric fields within clouds and caution used in interpreting the data. They discuss two possible sources of error in their instrument: charge on the device and corona discharge from the rocket. For the first, any charge that is distributed on the rocket body results in a direct current (dc) offset of the sinusoidal signal that is produced by the external field. There is thus no difficulty in separating the field produced by charge on the rocket from the actual external field.

Frier (1972) has warned of possible vitiation of the measurements if corona is produced at the front of the rocket. Winn and Moore (1972) argued that even in the unlikely event of corona from the dielectric nose ahead of the sensors, the field thus caused could always be distinguished from the external field unless the corona produced a sinusoidally varying space charge around the sensors. The more likely place for corona to occur, they contend, is at the fins, with the only result normally being spike-type noise on the telemetry record. This is shown on several of their recordings and is easily distinguishable from signals due to the external field.

Winn, Schwede, and Moore (1974) report on the maximum fields they have observed inside thunderclouds over New Mexico. They commonly measured field components with magnitudes of about 50 kV/m perpendicular to the rocket. The maximum measurement they quote as reliable is approximately 160 kV/m; they report two higher values, 400 kV/m and 1 MV/m, whose reliability they question.

A second type of rocket-borne instrument for the measurement of the vertical electric field was described by Ruhnke (1971). The electric field is determined by measuring the corona current that flows from a sharply pointed conductor mounted on the nose. This current is related to the field in a

nonlinear fashion, but a high-ohm resistor used in series with the pointed tip makes the current approximately a linear function of the electric field. The current is then converted into pulses that are used to modulate a 403 MHz transmitter. Some test flights have been made, and the data obtained from a penetration through the edge of one thunderstorm have been presented (Ruhnke, 1971).

Although the device can be calibrated directly by placing it in known electric fields, there appear to be several drawbacks to the instrument in its present configuration. Fields less than those necessary to initiate corona at the tip cannot be measured. This is, of course, a problem only if measurement of low fields is desired. Currents due to any charge transfer to the point by particle impaction cannot be distinguished from those caused by the external field, and the polarity of the field cannot be determined. Because of the design of the telemetry oscillator circuitry, the telemetering capability apparently works well only in fields up to about 40 kV/m; this problem conceivably could be overcome with appropriate circuit changes.

Dropsonde Field Mill

Evans (1969a) developed a rotating-differential electric-field mill that he suspended beneath a parachute and dropped from an aircraft flying over thunderclouds. The instrument consists essentially of two vertical, cylindrical input electrodes that are alternately shielded from and exposed to the external electric field by means of a windowed cylinder that is rotated with a small motor. The inputs are connected differentially to an electrometer. The output of the electrometer is synchronously rectified and then telemetered to a receiving station. The electronics allow measurements to be made over a range of 100 V/m to 250 kV/m. Evans noted, however, that his laboratory calibrations indicate that corona will be present above 50 kV/m, which could result in large errors in the measurements of fields above this value.

Evans (1969a) described the data obtained when several of these field meters were dropped through thunderstorms. He stated that the fields observed, which did not exceed about 40 kV/m, were substantially lower than generally had been assumed to exist within thunderstorms.

Evans' measurements were questioned by Vonnegut (1969). Since the device is not electrically symmetrical about any horizontal plane, Vonnegut suggested that it was susceptible to errors due to charge on the housing. Additionally, he said that problems might be caused by the release of point discharge ions, particularly from a "symmetry" rod placed vertically beneath the instrument. Evans (1969b) argued that the differential input of the instrument allowed a check on instrument charging; he added that the instrument had been tested both theoretically and experimentally in the laboratory.

Balloon-Borne Instruments

The use of balloons to make measurements of electric fields within clouds is advantageous in that the creation of space charge by high-speed impaction with cloud and precipitation particles is not a problem. The use of captive balloons offers the additional advantage of easy retrieval of the instrumentation. Unfortunately, even when one is using a dielectric tether line material, such as fiber glass, there must always be some question about the validity of the electric field measurements, since tether lines span potential differences in thunderstorms that may reach several million volts. Accordingly, when the flying line becomes wet, some current must flow, and this may alter the electric field in the vicinity of the instrument. Free balloons, on the other hand, do not have this limitation. A free balloon system will tend to follow the potential of the environment, and so the ground tether contamination problem is inherently eliminated. Probably the most serious drawbacks to the use of free balloons is that control of their position or flight path and retrieval of the instrumentation at the end of a flight are often quite difficult.

Numerous types of field-measuring devices have been developed for use with both free and tethered balloons. Several attempts to measure electric fields within clouds were made with meteorological radiosondes that were modified with radioactive probes or corona points. The reader is referred to Moore, Vonnegut, and Botka (1958) and Chalmers (1967) for details of these instruments. During the past decade several balloon-borne field mill systems have been developed to make electric field measurements inside clouds. Two of these, which have actually been used to obtain data within thunderstorms, are reported here.

One instrument, a field meter that was designed for use with tethered balloons by C. B. Moore (and reported by Clark, 1971), consists of two field mills recessed within a smooth, spherical aluminum housing 0.3 m in diameter. The field mills are mounted so that one faces outward horizontally and the other downward vertically. The spherical shape of the housing and the gently rounded mounting ports for the mills are used to minimize point discharge problems. Clark fitted his field meter with an internal tape recorder for data recording in his efforts to determine the maximum fields within thunderstorms.

The field meter has subsequently been modified by adding a 1,680 MHz transmitter (Rust and Moore, 1974). This allows real-time display of the data as they are transmitted by FM-FM

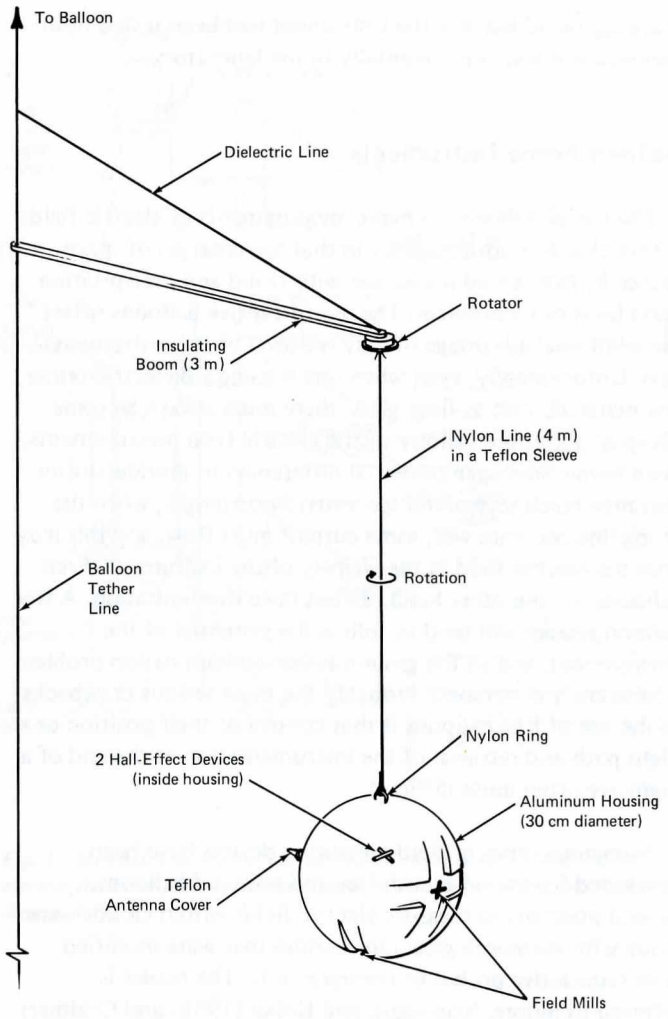

Fig. 2 Arrangement of spherically housed field mills for determining the electric field vector aloft. (Rust and Moore, 1974.)

telemetry and received at a ground station. The quarter-wave transmitting antenna stub is approximately 39 mm long and is encased in a rounded Teflon housing; the antenna protrudes through the sphere at a point diametrically opposite the horizontally facing field mill, as may be seen in Fig. 2.

Although the basic design of field mills has been reported by Chalmers (1967) and others, a brief description of those used in this balloon-borne field meter is presented here. The sensing element of the field mill consists of a stationary, flat stator having four vanes above which is placed a grounded rotor of the same configuration. The stator is alternately exposed to and shielded from the external field as the motor-driven rotor spins, and a periodic charge is thus induced on the stator by the external field. Use of a charge amplifier connected directly to the stator makes the measurement of the field independent of rotor spin rate.

The polarity of the electric field is determined by comparing the phase angle between the position of the rotor and the time-varying charge on the stator. The position of the rotor is determined with a reference signal generated by a phototransistor mounted between two segments of the stator and looking outward at the ambient light through the vanes of the rotor. Phase-sensitive demodulation of the reference and input signals allows a determination of both the magnitude and polarity of the electric field.

The maximum fields that can be reliably measured are determined by how deeply the mills are recessed into the spherical housing. In Clark's work, the field meter was calibrated to fields of about 2 MV/m. Rust and Moore used the instrument primarily for the study of initial cloud electrification and the early stages of thunderstorm development, and they placed the field mills so that 25 kV/m was the maximum that could be measured. The calibration was done by applying known potentials directly to the spherical housing, thus producing radial electric fields, and by placing the field meter between parallel plate electrodes across which known potential differences were imposed. Both calibration techniques show the instrument to be linear within its intended range.

In use, the field meter was suspended from a motor-driven, rotating bearing by a Teflon-insulated, nylon line equipped with rain diverters. It revolved about its vertical axis at about 10 rpm. The instrument was attached at least 30 m below the balloon in an effort to minimize any electrical perturbations caused by the balloon.

The data from both mills are used to determine the charge on the instrument and the horizontal and vertical components of the electric field. The output from the horizontal mill consists of a sinusoidal wave from the external horizontal field and a dc voltage offset from any charge on the instrument. The vertical, downward-facing mill provides a measure of the vertical component of the field plus the field from charge on the instrument.

Two Hall-effect semiconductors mounted at right angles within the sphere allow a determination of the instrument's orientation relative to the earth's magnetic field. From the combined outputs of all sensors, the electric field vector outside the instrument can be reconstructed and determinations made of any charge on the instrument as a function of time.

Another type of balloon-borne field meter has been developed by W. P. Winn (see Winn and Byerley, 1974) for use beneath small, free balloons (Fig. 3). The instrument is designed to measure the horizontal component of the electric field during vertical traverses of a thunderstorm as it ascends below the balloon and then descends beneath a parachute after it has been released from the rising balloon by a pressure-activated squib. The instrument is attached with nylon monofilament line about 20 m below the balloon and the parachute. Figure 4 is a simplified schematic of this field meter. The two hollow copper spheres placed horizontally opposite each other serve as the housing for the electronics, the transmitting antenna, and the field sensors. In flight the motion of the air past coated balsa wood propeller blades located 1 m above the sensors causes the instrument to rotate about its vertical axis at approximately 60 rpm. The charge induced on the rotating spheres by the external field produces a sinusoidal output from which the horizontal component of the electric field is determined. Any charge that is acquired by the sensors themselves can also be determined since the charge produces a dc voltage that results in an offset of the sinusoidal output.

The field meter can be calibrated in a parallel-plate electrode system; it is also calibrated internally during flight by the cyclic application of 0 V and 2 V pulses. Winn and Byerley (1974) have reported observations with this instrument of horizontal electric fields as high as 100 kV/m within thunderstorms.

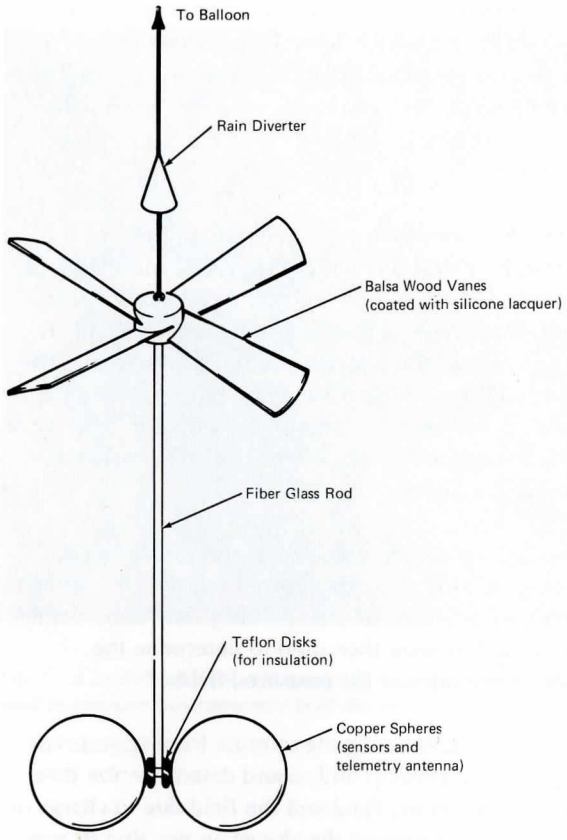

Fig. 3 Sketch of the field meter designed to measure the horizontal electric field by ascending below a balloon and then descending on a parachute. (After Winn and Byerley, 1974.)

Fig. 4 Simplified schematic diagram of the field meter for measuring the horizontal components of electric field aloft. (Winn and Byerley, 1974.)

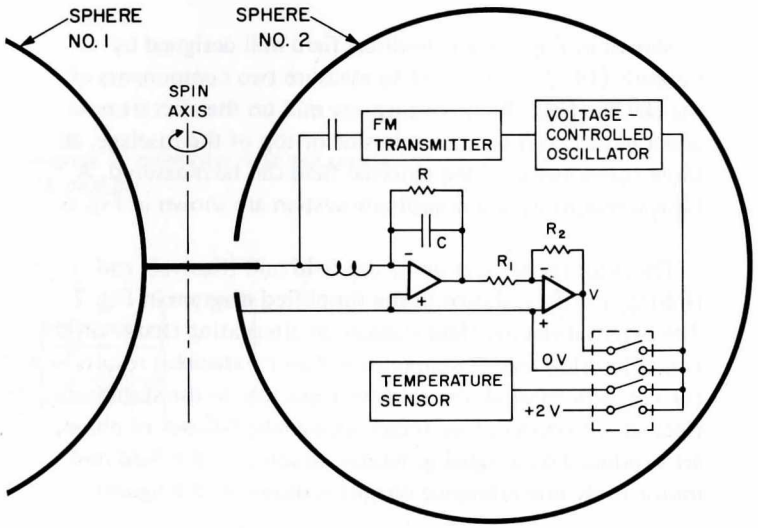

Aircraft Instrumentation

The use of aircraft to make measurements of electric fields within clouds and thunderstorms makes easier the control of when and where the data are obtained than is possible with balloons or rockets. Aircraft also make it simple to obtain measurements horizontally through clouds, with several traverses usually possible in a relatively short time compared with the storm's development. Disadvantages of using aircraft include the problem of creating local space charge due to high-speed impaction with cloud or precipitation particles; corona from relatively sharp edges such as propellers and wingtips; charge on the aircraft as a result of impaction, corona, or engine exhaust; and possible hazards to those on board during penetration of thunderstorms.

If reliable measurements are to be made using aircraft, care must be exercised to design and install a field mill system so that it can be calibrated and so that the effects of charge on the aircraft may be determined directly from the measurements or compensated for by either electronic or mechanical techniques.

There are two types of field mill systems that are generally used on aircraft to obtain more than one component of the electric field aloft: those using several single-component mills, coupled to give field components that are orthogonal in the aircraft coordinate system, and those using field mills that determine two orthogonal components of the field with a single instrument.

One system that uses four single-component field mills is that developed by Fitzgerald and Byers (1962) and used on a C - 130 aircraft. They mounted one mill facing outward on each wingtip; the remaining two were mounted fore and aft along the underside of the fuselage and faced downward. The field mills were of the standard induction type and used the flat stator-rotor configuration described previously; polarity of the field was determined by phase-sensitive rectification of input and reference signals.

Calibration of the system was done theoretically by approximating the aircraft as an ellipsoid and then experimentally determining estimates of the necessary field enhancement factors. These factors were then used to determine the approximate magnitudes of the measured fields.

By electronically combining the outputs from appropriate mills, Fitzgerald and Byers (1962) could determine the three components of the electric field and the field due to charge on the aircraft. The magnitude of the charge on the aircraft was then calculated from the field due to the charge and the capacitance of the aircraft, again approximating the aircraft as an ellipsoid.

Numerous cloud penetrations were made with the C - 130 and also with a similarly instrumented F - 100F jet aircraft. Fitzgerald (1965) reports fields well above 200 kV/m within active thunderstorms, with magnitudes near 50 kV/m apparently fairly common.

Shown in Fig. 5 is a cylindrical field mill designed by Kasemir (1972) that is used to measure two components of the electric field. By mounting one mill on the aircraft nose and a second mill on the underside or top of the fuselage, all three components of the external field can be measured. A typical mounting and coordinate system are shown in Fig. 6.

The most recent version of the field mill (Kasemir and Holitza, 1972) is shown in the simplified diagram in Fig. 7. The external electric field induces an alternating charge on the two cylindrical sensor segments as they rotate. This results in a current flow through the rotating capacitor to the stationary electronic circuitry. Two reference signals, 90° out of phase, are produced by a signal generator coupled to the field mill motor (only one reference output is shown in the figure). These are used in the phase-sensitive rectification circuits so that the two components of the external field may be determined. The outputs corresponding to the field components are aligned with the geometrical axes of the aircraft by electronically phase-shifting the reference signals. After phase-sensitive rectification, the signals are filtered to give a direct current output proportional to the electric field.

The field mills themselves are calibrated in the laboratory between parallel plate electrodes. Calibration of the field mill system on the aircraft is done in two steps. First the vertical component measured on the aircraft is calibrated by using the value of the vertical fine-weather field, which is measured using a suitable field mill located at the ground. The two horizontal components are then calibrated by flying the aircraft in a series of banks, climbs, and dives whose angles relative to the vertical fine-weather field are determined. This direct calibration compensates for the distortion of the field caused by the aircraft.

The effects of charge on the aircraft are reduced to a minimum by the use of smoothly rounded metal bosses called "hump rings," which are mounted on the cylindrical housing just below the sensing elements (see Fig. 5). The procedure is to charge the aircraft in flight either by changing engine power settings (exhaust charging) or preferably by placing a probe outside the exterior of the aircraft and applying high voltage to it. It is of interest to note that aircraft have a tendency to be electrically charged. The details of aircraft charging by engine exhaust are not fully understood, but the emission of charged engine gases results in charging until a charge-limiting process causes equilibrium. The charge acquired in this manner during cruise flight conditions is significantly less than that obtained by use of the corona probe.

Application of high voltage to the probe results in corona current that flows into the air. As the airstream flowing by the aircraft carries away the corona-produced ions of one polarity, the aircraft tends to be charged to the opposite polarity. Equilibrium is reached when the charge on the aircraft causes an electric field sufficient to deflect a portion of the ions back to the aircraft skin. This generally takes only a few seconds, and at this equilibrium point, the charge on the aircraft is quite constant. The hump ring is then moved and rotated until the charging procedure causes no noticeable outputs from the field mill even on sensitive ranges. This is a slow and tedious task since the hump ring cannot be moved in flight, but the technique is reliable.

The dynamic range of the system is determined by means of range-switching circuitry located within a control panel. Full-scale ranges of approximately 50 V/m to 500 kV/m are covered in 13 steps that change full scale by factors of either 2 or 2.5. Aircraft equipped and calibrated as above have

measured electric fields as high as 280 kV/m inside thunderstorms, with values of 100 kV/m frequently observed even in relatively small thunderstorms (Holitza et al., 1974).

Concluding Remarks

Several of the field mill systems that have been discussed here are currently in use and are updated and improved on a continuing basis. There are advantages and problems in each type of system, and the use of each results in some sort of compromise. Many investigators in atmospheric electricity believe, however, that the instrumentation necessary to measure electric fields inside the cloud and thunderstorm environment has been developed to a degree sufficient to allow reasonably reliable measurements. The continuing use of these instruments is a major part of the effort to describe quantitatively the electrical growth and behavior of clouds. In addition to electric fields, the charges carried by cloud and precipitation particles, their size distributions, and other parameters of

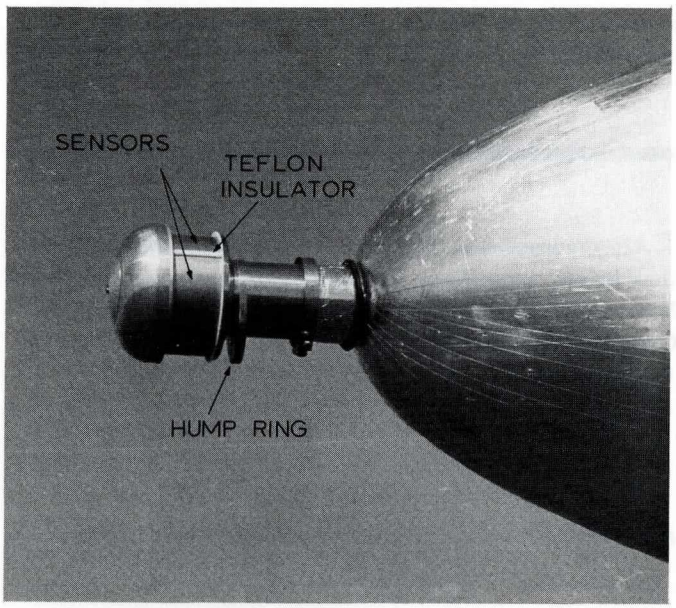

Fig. 5 A cylindrical field mill mounted on the nose of an aircraft and used to measure two components of the electric field. (Kasemir, 1972.)

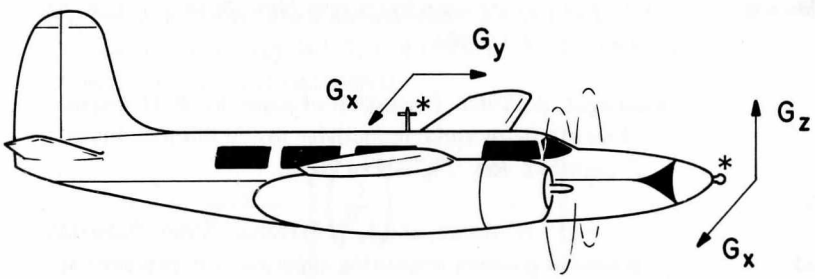

Fig. 6 Cylindrical field mills (indicated by asterisks) are located along lines of aircraft symmetry; shown is a typical coordinate system used to define the three components of the electric field, described here in terms of potential gradients, i.e., G points toward positive charge.

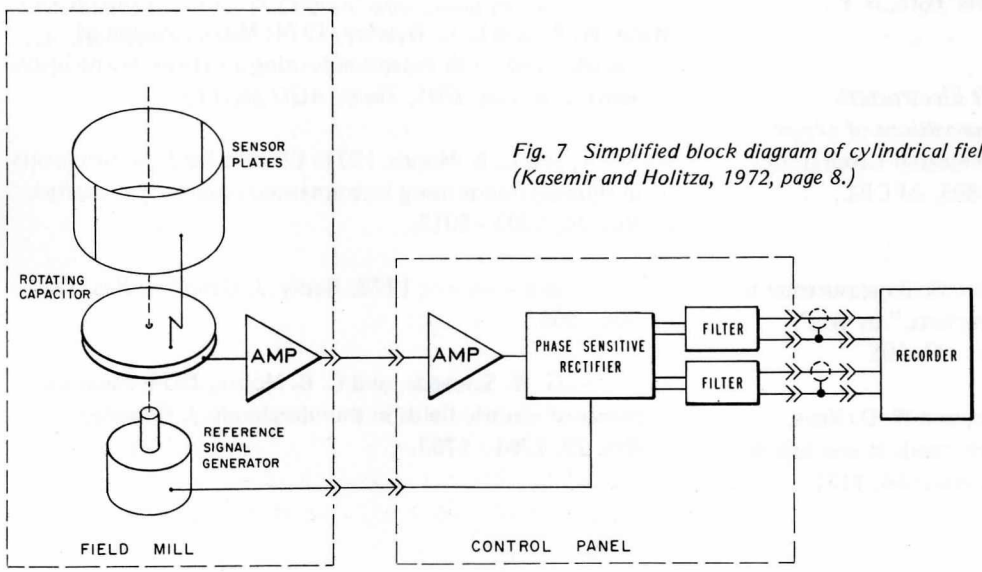

Fig. 7 Simplified block diagram of cylindrical field mill system. (Kasemir and Holitza, 1972, page 8.)

cloud physics need to be measured simultaneously near and within clouds and thunderstorms if we are to determine the interrelationships between electrical and microphysical developments.

Acknowledgments. I thank F. J. Holitza and W. P. Winn for their helpful suggestions. This work has been supported by the National Research Council (NRC) under an NRC/National Oceanic and Atmospheric Administration Resident Research Associateship.

References

Chalmers, J. A., 1967: *Atmospheric Electricity*, 2nd ed. Pergamon Press, Oxford, 515 pp.

Clark, D., 1971: *Balloon-Borne Electric Field Mills for Use in Thunderclouds*. M.S. thesis, New Mexico Institute of Mining and Technology, Socorro, N. Mex., 60 pp.

Evans, W. H., 1969a: Electric fields and conductivity in thunderclouds. *J. Geophys. Res. 74*, 939 - 948.

———, 1969b: Reply. *J. Geophys. Res. 74*, 7056 - 7057.

Fitzgerald, D. R., 1965: Measurement techniques in clouds. *Problems of Atmospheric and Space Electricity* (S. Coroniti, Ed.). Elsevier Publishing Company, New York, N.Y., 199 - 212.

———, and H. R. Byers, 1962: *Aircraft Electrostatic Measurement Instrumentation and Observations of Cloud Electrification*. Air Force Cambridge Research Laboratories Technical Report, AFCRL - TR - 62 - 805, AFCRL, Bedford, Mass.

Frier, G. D., 1972: Comments on "Electric field measurements in thunderclouds using instrumented rockets," by W. P. Winn and C. B. Moore. *J. Geophys. Res. 77*, 505.

Holitza, F. J., H. W. Kasemir, W. E. Cobb, and W. D. Rust, 1974: Aircraft measurements of electric fields in and below thunderstorms (abstract). *E⊕S, Trans. AGU 56*, 1131.

Kasemir, H. W., 1972: The cylindrical field mill. *Meteorologische Rundschau 25*, 33 - 38.

———, and F. J. Holitza, 1972: *Description and Instruction Manual for the Cylindrical Field Mill System*. NOAA Technical Memorandum, NOAA TM ERL APCL - 14, 20 pp.

Lane-Smith, D. R., 1974: Review of instrumentation for atmospheric electricity. Paper presented at Fifth International Conference on Atmospheric Electricity (sponsored by International Council of Scientific Unions and World Meteorological Organization), held 2 - 7 September at Garmisch-Partenkirchen, Germany; book publication pending.

Moore, C. B., B. Vonnegut, and A. T. Botka, 1958: Results of an experiment to determine initial precedence of organized electrification and precipitation in thunderstorms. *Recent Advances in Atmospheric Electricity* (L. G. Smith, Ed.), Pergamon Press, Elmsford, N.Y., 333 - 360.

Ruhnke, L. H., 1971: *A Rocket Borne Instrument to Measure Electric Fields inside Electrified Clouds*. NOAA Technical Report, NOAA TR ERL 206 APCL - 20, 26 pp.

Rust, W. D., and C. B. Moore, 1974: Electrical conditions near the bases of thunderclouds over New Mexico *Q. J. R. Met. Soc. 100*, 450 - 468.

Vonnegut, B., 1969: Discussion of paper by W. H. Evans, "Electric fields and conductivity inside thunderclouds." *J. Geophys. Res. 74*, 7053 - 7055.

———, C. B. Moore, and F. J. Mallahan, 1961: Adjustable potential-gradient measuring apparatus for airplane use. *J. Geophys. Res. 66*, 2393 - 2397.

Winn, W. P., and L. G. Byerley, 1974: Measurements of electric fields in thunderclouds using a balloon-borne instrument (abstract). *E⊕S, Trans. AGU 56*, 1131.

———, and C. B. Moore, 1971: Electric field measurements in thunderclouds using instrumented rockets. *J. Geophys. Res. 76*, 5003 - 5017.

———, and ———, 1972: Reply. *J. Geophys. Res. 77*, 506 - 508.

———, G. W. Schwede, and C. B. Moore, 1974: Measurements of electric fields in thunderclouds. *J. Geophys. Res. 79*, 1761 - 1767.

Contributions from our readers are printed in this "Short Reports" section. Further information on these subjects should be obtained from the contributors rather than from the editor. Short reports (maximum 750 words) may deal with new techniques for atmospheric measurements and data processing, evaluation of existing instrumentation, analysis of unfilled needs for systems and techniques, and other topics related to the technology of atmospheric measurement. Art should be held to a minimum and should be submitted in camera-ready form. We also welcome letters to the editor commenting on materials published in *Atmospheric Technology*. Our intent is to encourage responsive and critical reading of the publication's contents and a sharing of opinions among readers. Articles may be sent to the Managing Editor of *Atmospheric Technology*, Publications Office, NCAR.

Correction

Equation (1) of the Short Report by E. N. Brown, "Aircraft Static Pressure Errors: Their Measurement and Influence," *Atmospheric Technology* No. 7, Fall 1975, p. 89, was printed incorrectly. The correct equation is

$$M_t = \frac{2}{\gamma - 1}\left[\left(\frac{P_t}{P_s}\right)^{\frac{\gamma - 1}{\gamma}} - 1\right]$$

Our thanks to reader P. Church, who called the error to our attention.